

Utah State University

DigitalCommons@USU

All Graduate Theses and Dissertations

Graduate Studies

12-2008

Hydrological Characterization of A Riparian Vegetation Zone Using High Resolution Multi-Spectral Airborne Imagery

Osama Zaki Akasheh
Utah State University

Follow this and additional works at: <https://digitalcommons.usu.edu/etd>

 Part of the [Environmental Sciences Commons](#)

Recommended Citation

Akasheh, Osama Zaki, "Hydrological Characterization of A Riparian Vegetation Zone Using High Resolution Multi-Spectral Airborne Imagery" (2008). *All Graduate Theses and Dissertations*. 172.
<https://digitalcommons.usu.edu/etd/172>

This Dissertation is brought to you for free and open access by the Graduate Studies at DigitalCommons@USU. It has been accepted for inclusion in All Graduate Theses and Dissertations by an authorized administrator of DigitalCommons@USU. For more information, please contact digitalcommons@usu.edu.



12-1-2008

Hydrological Characterization of A Riparian Vegetation Zone Using High Resolution Multi-Spectral Airborne Imagery

Osama Zaki Akasheh
Utah State University

Recommended Citation

Akasheh, Osama Zaki, "Hydrological Characterization of A Riparian Vegetation Zone Using High Resolution Multi-Spectral Airborne Imagery" (2008). *All Graduate Theses and Dissertations*. Paper 172.
<http://digitalcommons.usu.edu/etd/172>

This Dissertation is brought to you for free and open access by the Graduate Studies, School of at DigitalCommons@USU. It has been accepted for inclusion in All Graduate Theses and Dissertations by an authorized administrator of DigitalCommons@USU. For more information, please contact digitalcommons@usu.edu.

Take a 1 Minute Survey- <http://www.surveymonkey.com/s/BTVT6FR>



HYDROLOGICAL CHARACTERIZATION OF A RIPARIAN VEGETATION ZONE
USING HIGH RESOLUTION MULTI-SPECTRAL AIRBORNE IMAGERY

by

Osama Z. Akasheh

A dissertation submitted in partial fulfillment
of the requirements for the degree

of

DOCTOR OF PHILOSOPHY

in

Irrigation Engineering

Approved:

Dr. Christopher M. U. Neale
Major Professor

Dr. Wynn R. Walker
Committee Member

Dr. Gary P. Merkley
Committee Member

Dr. Lawrence E. Hipps
Committee Member

Dr. Roger K. Kjelgren
Committee Member

Dr. Byron R. Burnham
Dean of Graduate Studies

UTAH STATE UNIVERSITY
Logan, Utah

2008

ABSTRACT

Hydrological Characterization of a Riparian Vegetation Zone Using High Resolution
Multi-spectral Airborne Imagery

by

Osama Z. Akasheh, Doctor of Philosophy

Utah State University, 2008

Major Professor: Dr. Christopher M. U. Neale

Department: Biological and Irrigation Engineering

The Middle Rio Grande River (MRGR) is the main source of fresh water for the state of New Mexico. Located in an arid area with scarce local water resources, this has led to extensive diversions of river water to supply the high demand from municipalities and irrigated agricultural activities. The extensive water diversions over the last few decades have affected the composition of the native riparian vegetation by decreasing the area of cottonwood and coyote willow and increasing the spread of invasive species such as Tamarisk and Russian Olives, harmful to the river system, due to their high transpiration rates, which affect the river aquatic system. The need to study the river hydrological processes and their relation with its health is important to preserve the river ecosystem.

To be able to do that a detailed vegetation map was produced using a Utah State University airborne remote sensing system for 286 km of river reach. Also a groundwater model was built in ArcGIS environment which has the ability to estimate soil water potential in the root zone and above the modeled water table. The Modified Penman-

Monteith empirical equation was used in the ArcGIS environment to estimate riparian vegetation ET, taking advantage of the detailed vegetation map and spatial soil water potential layers. Vegetation water use per linear river reach was estimated to help decision makers to better manage and release the amount of water that keeps a sound river ecosystem and to support agricultural activities.

(155 pages)

ACKNOWLEDGMENTS

So many people contributed to this project that I am at a loss of where to begin and with a fear that I may leave a “thank you” unsaid. I owe a deep tribute of appreciation to so many people that made this dissertation possible and who contributed to this amazing experience.

First and foremost, I would like to express my gratitude to my advisor, Dr. Christopher M. U. Neale, for his patience and advice. His support and expertise throughout this allowed me to gain a higher proficiency in my studies.

I would like to express my deepest appreciation to my committee members, Dr. R. Walker, Dr. Gary P. Merkley, Dr. Lawrence E. Hipps, and Dr. Rojer K. Kjelgern, for all the valuable comments, views, and corrections. To Dr. Lyman S. Willardson, “I will never forget your kindness, support, help and encouragement.”

This research was funded partially by the United States Bureau of Reclamation, Albuquerque office and supported by the Utah Agricultural Experimental Station and the Remote Sensing Services Laboratory at Utah State University.

For all the valuable data I obtained from Dr. Salim Bawazir, Dr. James R. Cleverly, Dr. James R. Thibault, and Debra Callahan: “Thank you.”

I would like to thank all my colleagues in the Remote Sensing Services Lab for the help and the learning experience that I had with them. Also, special thank you to the Biological and Irrigation engineering staff: Anne Martin, Jed Moss, Linda John, and Rebeca Olsen.

I would like to thank Ali Al-Bitar for his valuable help in many aspects especially the computer programming process. Thank you for your computer expertise, more so for your irreplaceable friendship. Also, I want to thank Bassel Timani and Yasir Kaheil for their valuable help.

To all my friends who helped me through their support, encouragement, and care, I say “Thank you.” There are many times that you helped me focus or get through these difficult years. I appreciate your friendship and your belief in me through this whole process.

Osama Z. Akasheh

DEDICATION

To my Parents

Thaqla & Zaki

“Mom you are always on my mind, rest in peace”

To my lovely Sisters and Brothers

Maha, Rania, Emad, and Bassim

CONTENTS

ABSTRACT	II
ACKNOWLEDGMENTS.....	IV
DEDICATION	VI
LIST OF TABLES	IX
LIST OF FIGURES.....	X
CHAPTER	
1. GENERAL INTRODUCTION.....	1
PROBLEM STATEMENT	2
SIGNIFICANCE OF RESEARCH.....	3
RESEARCH QUESTION.....	4
RESEARCH OBJECTIVES	5
REFERENCES.....	5
2. DETAILED MAPPING OF RIPARIAN VEGETATION IN THE MIDDLE RIO GRANDE RIVER USING HIGH RESOLUTION MULTI-SPECTRAL AIRBORNE REMOTE SENSING.....	7
ABSTRACT.....	7
INTRODUCTION	8
METHODOLOGY.....	11
IMAGE ACQUISITION AND PROCESSING.....	12
GROUND TRUTH DATA COLLECTION	14
IMAGE CLASSIFICATION PROCEDURE	15
CLASSIFICATION ACCURACY ASSESSMENT	17
RESULTS AND DISCUSSION	18
VEGETATION DISTRIBUTION ANALYSIS	20
IN-STREAM ANALYSIS.....	21
CONCLUSIONS AND RECOMMENDATIONS	28
REFERENCES.....	29
3. MODELING GROUNDWATER AND EVAPOTRANSPIRATION IN THE MIDDLE RIO GRANDE RIVER RIPARIAN CORRIDOR.....	35
ABSTRACT.....	35
INTRODUCTION	36
BACKGROUND	37
Riparian Vegetation	37
Use of Airborne Remote Sensing to Estimate	40
Riparian Vegetation ET	40
Modified Penman Monteith Method and.....	43
Stomatal Conductance Model.....	43
Groundwater Modeling.....	44

METHODOLOGY.....	45
Study Area	45
Water Table Modeling.....	47
Drain and River Water Levels	52
Water Flux and Transmissivity.....	53
Depth to Water Table.....	55
Soil Moisture Profile above the Saturated Zone.....	56
Evapotranspiration Estimation.....	57
Penman-Monteith Method	59
Stomatal Conductance Models	62
Canopy Minus Air Temperature (Tc-Ta) ET.....	64
Estimation Method.....	64
RESULTS AND DISCUSSION	66
ArcGIS Groundwater Table Model	66
General Description	66
ArcGIS Evapotranspiration Model General	67
Description.....	67
Groundwater Model Interface and Inputs.....	68
Evapotranspiration Model Interface and Inputs.....	72
GROUNDWATER MODEL OUTPUT	75
Groundwater Surface Creation in ArcGIS.....	75
Depth to Water Table Estimation	79
Water Table Variation in Space and Time.....	82
Model Validation	84
Stream Flow vs. Water Table and River.....	86
Water Level.....	86
EVAPOTRANSPIRATION MODEL OUTPUTS	96
Evapotranspiration of Riparian Vegetation	96
Spatial Evapotranspiration Mapping	97
Canopy Resistance.....	115
Water Potential Output	116
Water Flux Output	117
Riparian Vegetation Water Use along the River	120
SUMMARY.....	121
CONCLUSIONS AND RECOMMENDATIONS.....	123
REFERENCES.....	124
4. GENERAL CONCLUSIONS AND RECOMMENDATIONS.....	129
APPENDICES.....	131
CURRICULUM VITAE	140

LIST OF TABLES

Table	Page
2.1 Contingency table showing classification errors of omission and commission for the four major vegetation classes along the Middle Rio Grande River.....	19
2.2 Main riparian vegetation surface class areas along the middle Rio Grande in hectares per linear km of river resulting from the image classification, per 1:24,000 USGS quadrangle listed from upstream (Albuquerque) to downstream (Paraje).....	23
2.3 In-stream class area distribution for Middle Rio Grande River, in hectares per linear Kilometer of river, obtained from the classified airborne images. The asterisk (*) superscript indicates the presence of a diversion dam within that quad sheet and the number in parenthesis () indicates the number of drain inflows to the river within that quad sheet.....	26
3.1 Well location and names used in the validation.....	85
3.2 Well names and location of river flow gages and distance from each other.....	88
3.3 Total water used by major riparian vegetation in (m ³ /day/km).....	122

LIST OF FIGURES

Figure	Page
2.1 River section covered with imagery from the USU airborne system in 2001 and ground truthing data point locations along the river. Background map provided by the New Mexico Department of Tourism (2007)	12
2.2 Three-band mosaic (left) and corresponding classified image (right) with final classification scheme of a section of the Middle Rio Grande in the Abeytas area, along with full image resolution detail	22
2.3 A section of the river in the Albuquerque area where Cottonwood is the predominant vegetation class (dark green color) along with the attribute table	24
2.4 Water diversion at Isleta showing an increased amount of exposed sand downstream from the diversion dam and decreased water surface area	25
2.5 Mean daily stream flow at four different locations along the Middle Rio Grande during the month of July 2001 (United States Geological Survey, http://www.usgs.gov)	27
3.1 Analyzed river section of the MRGR, showing the location of river flow gages and flux towers.....	46
3.2 Dupuit-Forchheimer scheme and equation with no recharge	51
3.3 Dupuit-Forchheimer scheme and equation with recharge	51
3.4 Multi-spectral image of a section of the Rio Grande river showing possible flux directions.....	55
3.5 Soil moisture distribution above the saturated zone under hydrostatic equilibrium where ψ is matric suction, ϕ is total head and θ is the soil moisture content.....	57
3.6 Eddy covariance flux Tower with a 3D-sonic anemometer, a krypton hygrometer, a net radiometer, and other meteorological equipment	59
3.7 Groundwater model interface.....	70
3.8 Example of the water table model input data base table.....	71
3.9 Boundary conditions (red circles), water table wells (yellow triangle) locations and groundwater model initial output (red squares) in Bosque del Apache area.....	71
3.10 Evapotranspiration model interface	73
3.11 Interface for selecting land use classes for ET estimation (pops up when clicking on the select bottom adjacent to “land use code window”) (select the class by checking the small box).....	74

3.12	Example of the ET module input data base table.....	74
3.13	Water table raster layer created in ArcGIS for Feb. 22, 2003 at 12 pm.....	76
3.14	Water Flux (m/hr) including downstream flux in Bosque Del Apache area, Feb. 22, 2003 at 12 pm.....	77
3.15	Water table cross-sections along the Bosque del Apache riparian zone, February 22, 2003	78
3.16	Depth to water table at the Bosque del Apache, Feb 1, 2003	79
3.17	USGS 10-meter resolution DEM of the Bosque del Apache area	81
3.18	Depth to water table layer (meters) on Feb 22, 2003 at Bosque del Apache.....	81
3.19	Water table elevation for a modeled cross-section in the Albuquerque area.....	82
3.20	Depth to water table for a cross-section in Albuquerque area (zero distance at the river center)	83
3.21	Modeled water table elevation cross-section in the Belen area	83
3.22	Depth to water table cross-section in the Belen area (zero distance at the river center).....	84
3.23	Groundwater model validations at the Albuquerque and Belen areas	85
3.24	Locations of wells and gages along the Middle Rio Grande River, New Mexico.....	90
3.25	Flow rate vs. average daily water table for a 250 meter riparian section from the river center for the month of July 2001 (reference used 1490 m AMSL).....	91
3.26	Flow rate vs. river water level for the month of July 2001 for the Albuquerque area (reference used: 1490 m AMSL).....	91
3.27	Average daily water tables for 250 meter riparian section from river center vs. river water level for the month of July 2001 (reference used: 1490 m AMSL).....	92
3.28	Flow rate vs. average daily water table for 250 meter riparian section from river center for the month of July 2001 (reference used: 1455 m AMSL)	92
3.29	Flow rate vs. river water level for the month of July 2001 (reference used 1455 m AMSL)	93
3.30	Average daily water tables for 250 meter riparian section from river center vs. river water level for the month of July 2001 (reference used: 1455 m AMSL).....	93
3.31	Flow rate vs. average daily water table for 250 meter riparian section from river center for the month of July 2001 (reference used: 1365 m AMSL)	94
3.32	Flow rate vs. river water level for the month of July 2001 (reference used 1365 m AMSL)	94

3.33	Average daily water tables for 250 meter riparian section from river center vs. river water level for the month of July 2001 (reference used: 1365 m AMSL).....	95
3.34	Flow rate vs. average daily water table for 250 meter riparian section from river center for the month of July 2001 at Sevilleta (reference used: 1420 m AMSL)	95
3.35	Flow rate vs. river water level for the month of July 2001 at Sevilleta (reference used: 1420 m AMSL).....	96
3.36	Measured Tamarisk evapotranspiration on DOY 121, 168, and 242 (mm/hr)	98
3.37	Cumulative measured evapotranspiration for Tamarisk on DOY 121, 168, and 242.....	98
3.38	Net radiation (W/m ²) on DOY 121, 168, and 242.....	99
3.39	Solar radiation (W/m ²) on DOY 121, 168, and 242.....	99
3.40	Albuquerque area vegetation map.....	102
3.41	Tamarisk ET estimation locations (Red dots). The dashed box is shown in the next figure	103
3.42	Close-up of the dashed box indicated in the previous figure showing the depth to water table coverage in that area.....	104
3.43	Evapotranspiration estimates (mm/day) for the riparian vegetation (Coyote Willow, Cottonwood, and Tamarisk) in the Albuquerque section for DOY 242, 2001.....	105
3.44	Cottonwood evapotranspiration model estimates (mm/day) (using T _c -T _a method) compared to measured ET at Albuquerque. Averages of daily measured and estimated ET were 6.6 mm and 6.4 mm, respectively, with an RMSE of 0.54 mm	106
3.45	Cottonwood evapotranspiration model estimates (mm/day) (using T _c -T _a method) validation with eddy covariance ET at Belen. Averages of daily ET measured and the ET estimated were 5.7 mm and 5.3 mm, respectively, with an RMSE of 0.66 mm	106
3.46	Tamarisk evapotranspiration model estimates (mm/day) using Modified Penman-Monteith compared to eddy covariance ET in the Bosque area (South tower). Averages of daily ET measured and the ET estimated were 7.0 mm and 6.5 mm, respectively. RMSE was 0.62 mm for the year 2001.....	108
3.47	Tamarisk evapotranspiration model estimates (mm/day) using Modified Penman-Monteith compared to Eddy Covariance ET in Bosque area (North tower). Averages of daily ET measured and the ET estimated were 6.1 mm and 6.5 mm, respectively. RMSE was 0.47 mm for the year 2001.....	108
3.48	Tamarisk evapotranspiration model estimates (mm/day) by temperature differential method comparison with Eddy Covariance ET in Bosque area	

(North tower). Averages of daily ET measured and the ET estimated were 6.1 mm and 5.5 mm, respectively. RMSE was 1.8 mm for the year 2001	109
3.49 Tamarisk evapotranspiration model estimates (mm/day) using temperature differential method compared to Eddy Covariance ET in Sevilleta area. Averages of daily ET measured and the ET estimated were 5 mm and 4.7 mm, respectively. RMSE was 0.46 mm for the year 2001	109
3.50 Tamarisk evapotranspiration model estimates (mm/day) using Modified Penman-Monteith compared to Eddy Covariance ET in Sevilleta area. Averages of daily ET measured and the ET estimated were 5 mm and 6.2 mm, respectively. RMSE was 1.2 mm for the year 2001	110
3.51 Cottonwood evapotranspiration estimates and measured values (mm/day) for 16 days in Albuquerque area using Tc-Ta method	111
3.52 Cottonwood evapotranspiration estimates and measured values (mm/day) for 16 days in Belen area using Tc-Ta method.....	112
3.53 Tamarisk evapotranspiration model estimates (canopy temperature method) (mm/day) for 14 days in Sevilleta area using Tc-Ta method.....	112
3.54 Tamarisk evapotranspiration model estimates (Penman Monteith Method) (mm/day) for 14 days in Bosque area (south tower).....	113
3.55 Tamarisk evapotranspiration model estimates (Penman Monteith Method) (mm/day) for 12 days in Bosque area (north tower).....	113
3.56 A section from Bosque del Apache area vegetation map	114
3.57 Canopy resistance for Tamarisk at the Bosque del Apache estimated using the Ball-Berry Model	115
3.58 Vapor pressure deficits (Pa).....	116
3.59 Soil water potential in Bosque del Apache	118
3.60 Soil water potential along a cross-section in Bosque del Apache Feb 1st 2003 (DOY 121)	118
3.61 Water flux across the riparian zone between the river and the drain on DOY 121.....	119
3.62 Water flux across the riparian zone between the river and the drain on DOY 168.....	119
3.63 Water flux across the riparian zone between the river and the drain on DOY 242.....	120

CHAPTER 1

GENERAL INTRODUCTION

Rivers around the earth have been the cradles for all major civilizations. For example, the Mesopotamian civilization along the Tigris and Euphrates, the Egyptian civilization along the Nile, the Harrapan civilization along the Indus valley, and the Chinese civilization along Yangtze Rivers, are examples of major civilizations supported by rivers. The link between civilization and rivers is that rivers have traditionally been the main source of water for household use, cultivation of crops, raising livestock, and transport of people and materials.

The Middle Rio Grande River flows through an arid area and is the main source of water for the people of central New Mexico. Currently, approximately 40% of New Mexico's population lives in the Middle Rio Grande River (MRGR) valley and depends on the river for their water supply and sustenance. According to Bartolino (1997), the MRGR is a "critical basin" owing to the fact that its riparian system and the groundwater in the basin support both rapid economic and population growth.

A river system and its riparian zone are both open ecosystems dynamically linked to each other along the river laterally and vertically by hydrological and geomorphic processes (Ward, 1989). Both the hydrologic and geomorphic processes act as primary ecosystem drivers where chemical and biological factors act as secondary response variables (Tabacchi et al., 1998). The surface soil layer (root zone) controls water movement and retention which in turn controls the main water supply for riparian vegetation especially during dry periods when groundwater and river levels are low.

Interaction between river discharge and groundwater has a large influence on water use by vegetation at all stages (Tabacchi et al., 1998). Therefore, riparian vegetation is considered an important indicator of hydrological and geomorphic events (Nilsson, 1987).

PROBLEM STATEMENT

The relatively large amount of water diverted from MRGR for immediate human use (namely domestic, industry, and agriculture) affect both the groundwater table depth in the immediate river surroundings, the riparian vegetation water needs as well as the river ecosystem water needs. The state of New Mexico is in the process of developing better strategies for managing water resources in the MRGR basin. Of specific interest in this context is the need to estimate how much water is being used by the riparian zone vegetation, and to what extent this affects groundwater depth. Currently, little is known about the interaction between groundwater and riparian vegetation water use (Tabacchi et al., 1998).

In estimating the riparian vegetation water use, it is not enough to simply estimate the ET for the different vegetation types involved. The area covered by each type of vegetation along the river must also be known in order to convert the ET value for each vegetation type to the total water use. This can be achieved by multiplying the individual area estimates with the ET value.

The major types of riparian vegetation along the MRGR include the Tamarisk (*Tamarix ramosissima*) and the native vegetation (e.g. Cottonwood (*Populus deltoids*)) (see Chapter 2). How much water the Tamarisk uses as compared to other native

vegetation types is unknown. The major concern with the Tamarisk is that it is deemed harmful to the river system; its roots can go very deep, and in dry conditions it lowers the water table beyond the reach of any other vegetation, thus guaranteeing its survival. In addition, as a defensive measure, Tamarisk brings up the salts from the root zone and accumulates them on the soil surface to prevent any growth around it. This is one of the reasons why Tamarisk spreads fast along the river, outcompeting the native species.

Attempts have been made to use remote sensing (RS) and Geographical Information System (GIS) to estimate the water consumption of riparian vegetation as an input variable in the riparian zone hydrologic response function (Rango et al., 1983; Savabi et al., 1995). They generally gave poor estimates and inaccurate riparian zone hydrologic accounting. A major factor contributing to these poor estimates was the use of low resolution remote-sensing data that tends to cover large areas, and for which no meaningful vegetation delineation can be made (Muller et al., 1993).

To complete the connectivity between groundwater and riparian vegetation, and for better estimates of ET, depth to water table representative of the entire riparian zone is needed. While point measurements can be used, these may not be representative of the entire riparian zone water table depth or its spatial variability. Such an estimate of water table depth representative of the entire riparian zone can be achieved using an appropriate groundwater model and iterative scheme.

SIGNIFICANCE OF RESEARCH

Riparian vegetation is a major component of riparian zone hydrology, which in turn is fundamental to understanding riparian zone dynamics (Gurnell, 1995; Hughes et

al., 1997; Large, 1997). Therefore it is important that the water consumption of riparian vegetation is properly and accurately estimated and correctly coupled to the groundwater response.

Understanding how high resolution remote sensing data could be used to improve estimation of riparian vegetation evapotranspiration, and the coupled groundwater response is important in water resources management, and is crucial for improving knowledge of riparian zone dynamics. In addition, such high-resolution RS and GIS data could be used to produce high-resolution maps for improved regional water resource management (Goodrich et al., 2000; Shen et al., 2004). Mapping and estimating the water use by each vegetation type might lead to a better water resources management in the Middle Rio Grande River Basin.

RESEARCH QUESTION

Since MRGR flows in an arid area, and has water distribution problems among the competing interests, this research will address the following questions:

- (1) What is the water use by the major vegetation types in the riparian zone and can remote sensing be used to obtain evapotranspiration of riparian species?
- (2) What is the relationship between the riparian vegetation aggregate water use and the underlying water table depth?
- (3) Can the effect of the surrounding arid conditions on the riparian vegetation ET be taken into account?

RESEARCH OBJECTIVES

The major objectives of this study are as follows:

- (1) To produce a high-resolution riparian vegetation map for the MRGR based on airborne multi-spectral remote sensing.
- (2) To develop a model for estimating depth to water table and couple it with an evapotranspiration model
- (3) To combine the remotely sensed vegetation information and the groundwater/ET models to estimate spatial distribution of ET for the main riparian vegetation along reaches of the MRGR.
- (4) Validate the model results with measured evapotranspiration using eddy covariance flux towers

REFERENCES

- Bartolino, J. R., 1997. Middle Rio Grande Basin Study: U.S. Geological Survey Fact Sheet FS-034-97, pp. 1-4.
- Goodrich, D. C., Chehbouni, A., Goff, B., 2000. The semi-arid land-surface-atmosphere (SALSA) program: special issue preface paper. *Agricultural and Forest Meteorology*, 105, 3–20.
- Gurnell, A. M., 1995. Vegetation along river corridors: hydrogeomorphological interactions. In: Gurnell, A.M., Petts, G.E. (Eds.), *Changing River Channels*. Wiley, Chichester, pp. 237–260.
- Hughes, F. M. R., Richards, K. S., El-Hames, A. S., Harris, T., Peiry, J. L., Pautou, G., Girel, J., 1997. Investigations into hydrological influences on the establishment of riparian tree species. In: Large, A.R.G. (Ed.), *Floodplain Rivers: Hydrological Processes and Ecological Significance*. British Hydrological Society Occasional Paper 8, 17–29.
- Large, A. R. G., 1997. Linking floodplain hydrology and ecology – the scientific basis for management. In Large, A.R.G. (Ed.), *Floodplain Rivers: Hydrological Processes and Ecological Significance*. British Hydrological Society Occasional Paper 8, 1–5.

- Muller, E., Decamps, H., Dobson, M. K., 1993. Contribution of space remote sensing to river studies. *Freshwater Biology* 29, 301-312.
- Nilsson, C., 1987. Distribution of stream-edge vegetation along a gradient of current velocity. *Journal of Ecology* 75, 513-522.
- Rango, A., Feldman, A., George, T. S., Ragan, R. M., 1983. Effective use of Landsat data in hydrologic models. *Water Resource Bulletin* 19, 165-174.
- Savabi, M. R., Flanagan, B. H., Engel, B. A., 1995. Application of WEPP and GIS-GRASS to a small watershed in Indiana. *Journal of Soil and Water Conservation* 50, 477-483.
- Shen, Y., Kondoh, A., Tang, C., Xiao, J., Oki, T., Kanae, S., 2004. Development and application of a remote sensing model for estimating soil water status and evapotranspiration in semiarid region. Available from: <http://www.wrrc.dpri.kyoto-u.ac.jp/~aphw/APHW2004/proceedings/RCW/56-RCW-A305/56-RCW-A305_craft.pdf>.
- Tabacchi, E., Correll, D. L., Hauer, R., Pinay, G., Tabacchi, A. M., Wissmar, R. C., 1998. Development, maintenance and role of riparian vegetation in the river landscape. *Freshwater Biology* 40, 497-516.
- Ward, J. V., 1989. The four-dimensional nature of the lotic ecosystem. *Journal of the North American Benthological Society* 8, 2-8.

CHAPTER 2

DETAILED MAPPING OF RIPARIAN VEGETATION IN THE MIDDLE RIO
GRANDE RIVER USING HIGH RESOLUTION MULTI-SPECTRAL AIRBORNE
REMOTE SENSING¹

ABSTRACT

This paper describes procedures used to map riparian vegetation in the middle Rio Grande River, New Mexico. Airborne multi-spectral digital images were acquired at 0.5 m spatial resolution over the riparian corridor of the middle Rio Grande River in July 2001. The images were corrected for lens vignetting effects, lens radial distortions, rectified to a map base, mosaicked, calibrated in terms of reflectance and classified. The classification accuracy was assessed using ground truth information obtained through comprehensive field campaigns and independent ground truth information. Surface areas of vegetation classes and in-stream features were extracted from the classified imagery. A longitudinal vegetation distribution analysis was conducted to study the changes in vegetation and water surface areas along the river. This analysis showed an increase in surface areas of the invasive type of vegetation Tamarisk (*Tamarix ramosissima*) in the down stream direction corresponding to decreases in water surface areas and flow. This indicates significant impacts on the river ecosystem due to many factors. The high resolution airborne multi-spectral remote sensing proved to be a powerful tool for

¹ Coauthored by Christopher M. U. Neale, and Harikishan Jayanthi.

mapping riparian vegetation which is very hard to map using satellite imagery due to its complexity, high diversity, and spatial variability occurring at finer scales.

INTRODUCTION

Remote sensing (RS), especially the use of high resolution multi-spectral imagery, has proven to be a very objective, reliable, and useful tool in inventorying riparian and wetland areas. Gaussman et al. (1977) delineated woody plant species using reflectance measurements. Field spectral-radiometric measurements were used to separate weed, wetland, and rangeland species (Best et al., 1981; Everitt et al., 1986; Gaussman et al., 1983). Aerial inventorying of riparian and wetland vegetation classes initially consisted of using color infrared (CIR) photography (Bonner, 1981; Carneggie et al., 1983; Everitt and Deloach, 1990; Lonard et al., 1998; Tueller, 1982). The rigors involved in manual field inventorying and classification of riparian and wetland areas, the extent of time spent, and inaccessibility issues were all overcome by using RS techniques (Martin, 1988). In addition, radiometric responses in the CIR photographs facilitated textural image analysis that helped delineate detailed vegetation types (Everitt, 1998).

Resource scientists realized that airborne multi-spectral video RS systems provided information faster than photography or spectral-radiometry (Hutchinson et al., 1990; Everitt et al., 1991; Meisner and Lindstrom, 1985; Neale, 1991; Nixon et al., 1987; Vlcek and King, 1985), and at lesser costs (Nixon et al., 1992). Everitt and Nixon (1985) and Nixon et al. (1987) observed that airborne videography provided better near real time information for qualitative visual assessment of plant and soil conditions. Everitt et al. (1986, 1988), Kliman (1988), Lulla et al. (1987), Richardson et al. (1988, 1990), and

Weigand et al. (1988) used video digital count data to monitor plant growth, plant condition, and yield. As the video digital counts were uncalibrated, scene-to-scene comparisons and multi-temporal analyses were not possible owing to changing brightness conditions due to presence of clouds and change in solar zenith angle. Another disadvantage of video imagery was its relatively low resolution when compared to film (Mausel et al., 1992).

Neale (1992, 1997), Bartz et al. (1994), Redd et al. (1994), and Shoemaker et al. (1994) observed that airborne multi-spectral videography was very cost effective in mapping riparian and wetland systems. Interestingly, King and Vlcek (1990) noted that absolute radiometric calibration of aerial multi-spectral imagery was not necessary in forestry and rangeland applications, and found that this approach was very cost effective and efficient.

Airborne RS was implemented initially using aerial photographs which played an important role in early attempts in detailed vegetation mapping (Sandmann and Lertzman, 2003). On the other hand, higher spatial resolution imagery showed good results for urban applications and extracting urban related features (Benediktsson et al., 2003; Farag et al., 2001; Herold et al., 2003). Therefore, it is expected that high resolution imagery will have the ability to capture and separate different vegetation signatures and produce good results in vegetation mapping (Carleer and Wolff, 2004).

Imagery from the LANDSAT Thematic Mapper (TM) and SPOT- HRV (“Système Pour l’Observation de la Terre” – High Resolution Visible) satellite instruments have proven insufficient for differentiating vegetation types in detailed vegetation studies (Harvey and Hill, 2001; Kalliola and Syrjanen, 1991) mostly due to

spatial resolution issues. The use of these images resulted in 40% or less classification accuracy (Czaplewski and Patterson, 2003). Satellite multi-spectral imagery, by virtue of its ability to cover large areas, has also been used to map riparian vegetation (Sugumaran et al., 2004; Williams, 1992). Limitations with satellite imagery are (1) the difficulties faced in distinguishing fine, ecological divisions between certain vegetation classes, (2) the larger pixel sizes with respect to the small scale variability in some riparian systems, and (3) the inability of passive sensors (such as optical multi-spectral imagery) from both satellite and airborne platforms to effectively penetrate the canopy and monitor the understorey vegetation. Riparian vegetation classes were observed to share common heterogeneous traits and similar spectral responses while using SPOT and TM data (Williams, 1992).

It is important to mention that the term high resolution imagery can relate to spatial and spectral resolution. Spatial resolution is defined as the smallest area on the ground surface for which information is obtained in an image represented by a unit picture element or pixel, while spectral resolution represents the number of spectral bands and the band width that can be detected by the sensor or sensors in the RS system. Vegetation classification and mapping can be achieved using multi-spectral bands in the red, green and the near infrared wavelengths and high spatial resolution imagery is well suited for riparian systems in semiarid areas (Neale, 1992, 1997).

Riparian vegetation is a major component of riparian zone hydrology, which in turn is fundamental to understanding riparian zone dynamics (Gurnell, 1995; Hughes et al., 1997; Large, 1997). It is therefore important that the water consumption of the riparian vegetation is properly and accurately estimated and correctly coupled to the

groundwater response. High spatial resolution RS data could be used to produce high resolution GIS-based thematic maps for improved regional water resource management (Goodrich et al., 2000; Shen et al., 2004).

Detailed mapping of the riparian vegetation described in this paper will result in a better estimation of the water use by each vegetation type and the response of the coupled groundwater system, potentially leading to a more efficient water resources management in the Middle Rio Grande River Basin (MRGRB).

METHODOLOGY

Study Area

The study area consisted of the MRGRB that covers the area from Cochiti dam to Elephant Butte Dam, New Mexico (NM) (Figure 2.1). Forty percent of New Mexico's population lives along this 286 km long stretch of river. The river flow is controlled by Cochiti dam, which releases water for municipal use, irrigation diversions, and to keep a sound river ecosystem (ideally) by maintaining river base flows. The river floodplain is bordered by two drains on each side. These drains serve the adjacent agricultural areas by collecting irrigation runoff water. Beyond the drains there is either irrigated agriculture or arid areas with natural vegetation which occupies most of New Mexico.

The main vegetation species along the riparian corridor are Cottonwood (*Populus deltoids*), Tamarisk (*Tamarix ramosissima*), Russian Olives (*Elaeagnus angustifolia*), and Coyote Willow (*Salix exigua*).

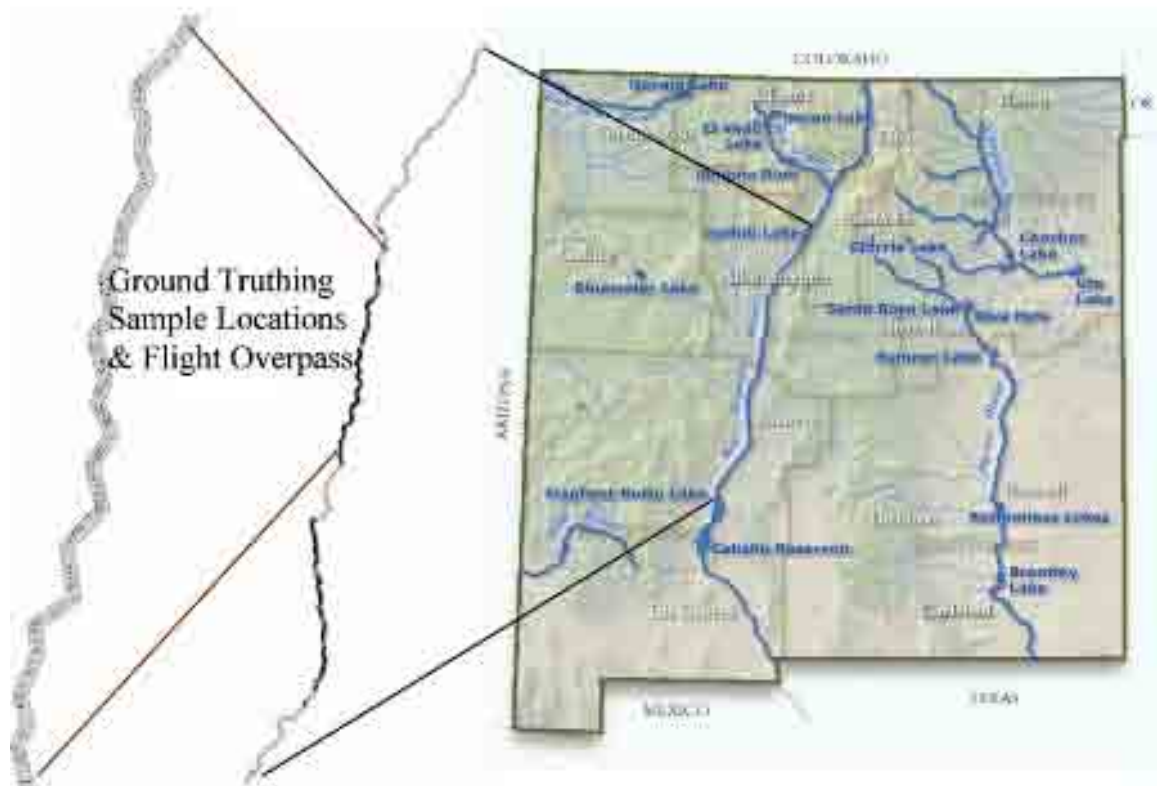


Figure 2.1 River section covered with imagery from the USU airborne system in 2001 and ground truthing data point locations along the river. Background map provided by the New Mexico Department of Tourism (2007)

IMAGE ACQUISITION AND PROCESSING

High-resolution airborne multi-spectral imagery of the middle Rio Grande from Cochiti Dam down to Elephant Butte reservoir was acquired with the USU airborne multi-spectral digital system at spatial resolution of 0.5 m. The image acquisition flights occurred on the 24, 25, and 26 of July, 2001, under mostly clear-sky conditions. Figure 2.1 also shows the sections of the river covered by the airborne imagery, as well as the approximate width of the riparian buffer, for which images were processed and analyzed.

The present generation of the USU airborne multi-spectral digital system described by Cai and Neale (1999), is a newer version of the system presented by Neale and Crowther (1994). It acquires spectral images using Kodak Megaplug 4.2i digital cameras with interference filters forming spectral bands in the green (0.545-0.555 μm), red (0.665-0.675 μm) and near-infrared (NIR) (0.790-0.810 μm) wavelengths of the electromagnetic spectrum. The digital cameras were calibrated against a radiance standard following a method described by Neale and Crowther (1994) using natural sunlight. The images were acquired at a nominal overlap of 60% along flight lines in one swath centered over the river. For the most part, the 1-km swath width was enough to cover the riparian zone on both sides of the river, including the drains that ran parallel to the river on both sides.

The individual spectral band images were geometrically corrected for radial distortions (Sundararaman and Neale, 1997), radiometrically adjusted for lens vignetting effects (Neale and Crowther, 1994) and registered into three-band images. The three-band images were rectified to 1:24000 USGS digital orthophoto quads using common control points visible in both sets of imagery. The rectified images were mosaicked into larger image strips along the flight lines representing reaches of the river. The mosaicked strips were calibrated to a reflectance standard using the USU system camera calibration and concurrent measurements of incoming solar radiation using an Exotech radiometer with similar spectral bands as the airborne system. The radiometer was placed looking down from nadir over a barium sulfate standard reflectance panel with known bi-directional properties (Chavez et al., 2005; Neale and Crowther, 1994). The panel was

located at the Albuquerque airport and the radiometer was sampled every 1 min throughout the airborne image acquisition period.

The image strips were segmented and named according to the corresponding 1:24,000 orthophoto quad sheet they covered, and numbered from north to south. For most of the USGS quad sheets in the present study, there were either two or three strips covering the river reaches in those quads.

GROUND TRUTH DATA COLLECTION

Field visits were made to many locations along the river, using laminated rectified multi-spectral images prints to aid in the identification of different surfaces. Global Positioning System (GPS) equipment was used to locate and obtain the geographic coordinates of different vegetation types and spectral signatures identified in the field and/or visible in the printed images. Polygons were drawn on the laminated maps using water-proof marker pens to characterize large monoculture vegetation extents. Efforts were made to conduct a detailed inventory of riparian and wetland classes in the selected multi-spectral prints by describing the overstorey and understorey vegetation classes to the species level. Forty map sheets, covering a total area of 40 km² (each sheet covered an area of 1 x 1 km), were inventoried in this study. Four people were involved in the field campaign, two local researchers from University of New Mexico who gave guidance and facilitated access, and two graduate students from Utah State University. The trees were fairly easy to identify at the species level in the high-resolution multi-spectral imagery, and each positive specie identification was accompanied by GPS coordinate to facilitate a revisit on the rectified digital images later.

In addition, a second ground truthing dataset were made available by the US Bureau of Reclamation, Denver office, Colorado, from a vegetation mapping project covering the floodplain from Velarde to Elephant Butte (Callahan and White, 2004). This data set added more credibility to the accuracy assessment and confirmed previously collected features.

IMAGE CLASSIFICATION PROCEDURE

The detailed ground truth information played a significant role in the development of the final classification in this study. Seventy percent of the ground truth data were used for identifying areas-of-interest (AOI) signature extraction polygons and in the generation of training signatures using ERDAS Imagine 8.5. The remaining 30% were later used in the accuracy assessment analysis.

An iterative supervised classification procedure was used in this study. Initially, the supervised seeding routines in ERDAS Imagine 8.5 were used to extract spectral signatures for the major separable riparian and wetland classes. The transformed divergence (TD) method was used to test signature separability. This method statistically compares all spectral signatures in a signature set among themselves, assigning a TD index number between 0 and 2000, where the value of 2000 indicates total separability and 0 indicates the opposite. This method is fully explained in the ERDAS Field Guide (1999). The TD lower bound value of 1700 was used, which allows for some overlap or confusion among those classes, but decreases the overall number of classes required for the classification. This could be the case for signatures seeded to represent the same vegetation class, for example, the directly sunlit vs. the shaded side of a Cottonwood

canopy. Though there is overlap and spectral confusion between the signatures of these two seeded classes allowed by the lower TD bound, they will be eventually merged together after the classification into the Cottonwood class of the final product. The TD procedure generated a separability table where each class, when compared against each other through the TD index number, helped the operator identify any confusion between signatures.

The classification process was iterative. At each iteration, the existing signature set was used to classify the image using the maximum likelihood scheme, leaving the unclassified rule option in ERDAS Imagine as “unclassified.” In this way, pixels that did not belong to any of the existing classes in the signature set were left blank, or unclassified. By comparing the resulting classified image with the calibrated three-band mosaic, new signatures were obtained to represent the larger blank or unclassified areas, adding to the signature set. The new signatures were compared against the existing signatures using the TD method and overlapping signatures were dropped. The resulting remaining signature set was then used in a new iteration of the classification. The process was repeated until the last of the unclassified pixels were in the form of “salt and pepper” pixels in the image. The final classification pass was then conducted using the maximum likelihood algorithm and all pixels in the image were assigned to known classes by changing the unclassified rule in ERDAS Imagine to “parametric rule.”

The resulting final signature file contained several dozen signatures, many representing the same type of vegetation. In this way, nuances in the signatures caused by bi-directional reflectance effects or density of the vegetation were accounted for. Finally, the classes representing the same vegetation type were recoded into one class. The

recoding process reduced the dozens of classes in the classified image into specific basic classes. After the recoding process was completed, a 3 x 3 majority filter was applied to the recoded classified image to eliminate isolated pixels. Manual recoding was performed to remove any remaining confusion and obvious misclassifications in the classified images. The classified image strips were cut to fit each corresponding 1:24,000 quadrangle sheet. The classification was conducted on imagery acquired from Albuquerque down to Elephant Butte, covering a distance of approximately 208 km along the river.

CLASSIFICATION ACCURACY ASSESSMENT

The assessment of classification accuracy consisted of determining the efficiency of extracting relevant information derived from remotely sensed imagery. It was conducted on the classified images using ground truth field data that was set aside for this purpose. The accuracy assessment was conducted on the major vegetation classes, Cottonwood, Tamarisk, Russian Olives, and Coyote Willow. Not enough ground truth data were available for other vegetation types within the system to include them in the accuracy assessment analysis. In terms of surface area and water use from the river system, they represent a very small fraction of the overall vegetated area. Likewise, there were no ground truth data for the in-stream features as the ground truth campaign was conducted several weeks after the airborne image acquisition flight, under different river flows and conditions. In addition, the in-stream analysis was not a thrust of the project at that time.

Each ground truth data point was compared to the classified vegetation type on the image, and the matching and mismatching events were recorded. In the case of mismatching events, the mismatched class was noted under the corresponding class in the contingency table in the classification column (Table 2.1). Five parameters were calculated: user's accuracy, producer's accuracy, and overall accuracy that helped in estimating the omission and commission errors. User's accuracy is a measure of reliability of classification or the probability that a sample on a map actually represents that category on the ground. It is calculated by dividing the number of samples correctly classified by the number of samples in that class. The producer's accuracy is a measure of how well a certain class is classified and is calculated as the number of samples of the ground truth class that were correctly classified divided by total number of samples of the ground truth. Commission and omission errors are the result of 100% accuracy minus the user and producer accuracy, respectively.

RESULTS AND DISCUSSION

Accuracy Assessment

Table 2.1 shows the classification contingency table for the four major vegetation classes in the river system. The ground truth data set aside for assessing classification accuracy were used for this purpose. Coyote Willow had the highest classification producer accuracy with 92% while Cottonwood had highest in user accuracy with 89%. The classification methodology identified Tamarisk and Russian Olives at 86% and 82% user accuracy and with a producer accuracy of 86% and 82%, respectively. One of the reasons for the higher accuracy for Coyote Willow and Cottonwood in the final product is

that they are easier to distinguish from other tree classes. The large shadows of Cottonwoods while smaller and almost no shadows of Coyote Willow helped identify and delineate these classes accurately in the recoding procedures. The overall accuracy for the classified image map product was assessed at 88%. The classification method used in the present study gave similar results to other classification studies using high spatial resolution airborne multi-spectral imaging (May and Neale, 1999; May et al., 2001; Neale et al., 2007).

The Kappa statistics were also calculated as an alternative method of estimating classification accuracy in order to correct for any agreement that might occur by chance.

Table 2.1 Contingency table showing classification errors of omission and commission for the four major vegetation classes along the Middle Rio Grande River

Vegetation Classification Accuracy Assessment							
	Ground Truth						
Classification	Cottonwood	Tamarisk	Coyote Willow	Russian Olive	Total # of samples	User Accuracy (%)	Error of Commission (%)
Cottonwood	42	1	1	3	47	89	11
Tamarisk	2	24	1	1	28	86	14
Coyote Willow	1	2	23		26	88	12
Russian Olive	2	1		18	21	86	14
Total # of samples	47	28	25	22	122		
Producer Accuracy (%)	89	86	92	82	Overall accuracy	88	
Error of Omission (%)	11	14	8	18			

The resulting Kappa index for this classification data set was 83%, which is lower than the overall accuracy estimated through the contingency table. Kappa usually under estimates the overall accuracy, but it is recommended for vegetation mapping projects and is commonly used by the vegetation mapping community (Congalton and Green, 1999).

The good classification results obtained in this research are attributed to the high resolution imagery used. Such results and details in the vegetation map would not be possible if low spatial resolution imagery had been used.

The vegetation map produced in this study has many foreseen uses. It is a required input for calculating the evapotranspiration and water balance along the river whether the vegetation (“crop”) coefficient method or energy balance method is used (Brower, 2004; NASA, 2007). Furthermore, it documents the vegetation pattern and vegetation status at a certain time and location.

VEGETATION DISTRIBUTION ANALYSIS

Different vegetation class areas were extracted from the final classified and recoded images for every corresponding quadrangle base map. The area values were extracted from the riparian zone, digitized as AOI polygons in the three-band image mosaics. The riparian zone and floodplain essentially corresponded to the region between the two drains that ran parallel to the river in most sections of the middle Rio Grande. Figure 2.2 shows a three-band rectified mosaic strip and corresponding classified image for a section of the river in the Abeytas area. The AOI (yellow line) class area values were extracted and presented in the attribute table which shows the class area and

corresponding color. Figure 2.2 also shows the full resolution detail of both the three-band multi-spectral and classified imagery for the area highlighted in the small rectangular box.

In Table 2.2, the main riparian vegetation class areas per linear kilometer of river and per USGS quadrangle sheet extracted from the classified imagery are shown listed from north to south along the x-axis. The most important observation is that the Cottonwood tree area within the riparian zone decreased from north to south while the area of Tamarisk trees increased. Introduced species such as Tamarisk have been observed to successfully compete with the native species such as Cottonwood and Willow. The presence of Tamarisk results in the deterioration of soil chemical and physical properties, and prevents new Cottonwood seedlings and other native species from emerging. Irrigation water diversions and the resulting decrease of in-stream flows as the river flows from north to south may be affecting the balance and capacity of the native species to resist the spread of Tamarisk (Busch and Smith, 1995). In addition, Tamarisk can cause a drop in the water-table and an increase in salinity, deteriorating water quality in benefit of Tamarisk which is salinity resistant (Brock, 1994; Busch and Smith, 1995; Loope et al., 1988).

IN-STREAM ANALYSIS

Figure 2.3 shows a northern section of the Rio Grande close to Albuquerque where Cottonwood is the dominant riparian vegetation species and a large surface water area within the river is present. Meso-scale hydraulic features such as riffles, runs and pools were classified but merged into a water surface class for the area analysis. The

water surface area parameter is estimated as an indicator of water flow volume in the river, a reasonable assumption due to the mild slopes of the river bottom, and also as a means of showing how changes occur along the Middle Rio Grande as the river flows downstream. Both meso-scale hydraulic features and vegetation classification are important for river fisheries habitat and geomorphology studies. Accuracy analysis was not conducted on the in-stream hydraulic features, as riparian vegetation was the main thrust of the study and not enough data corresponding to these features were available.

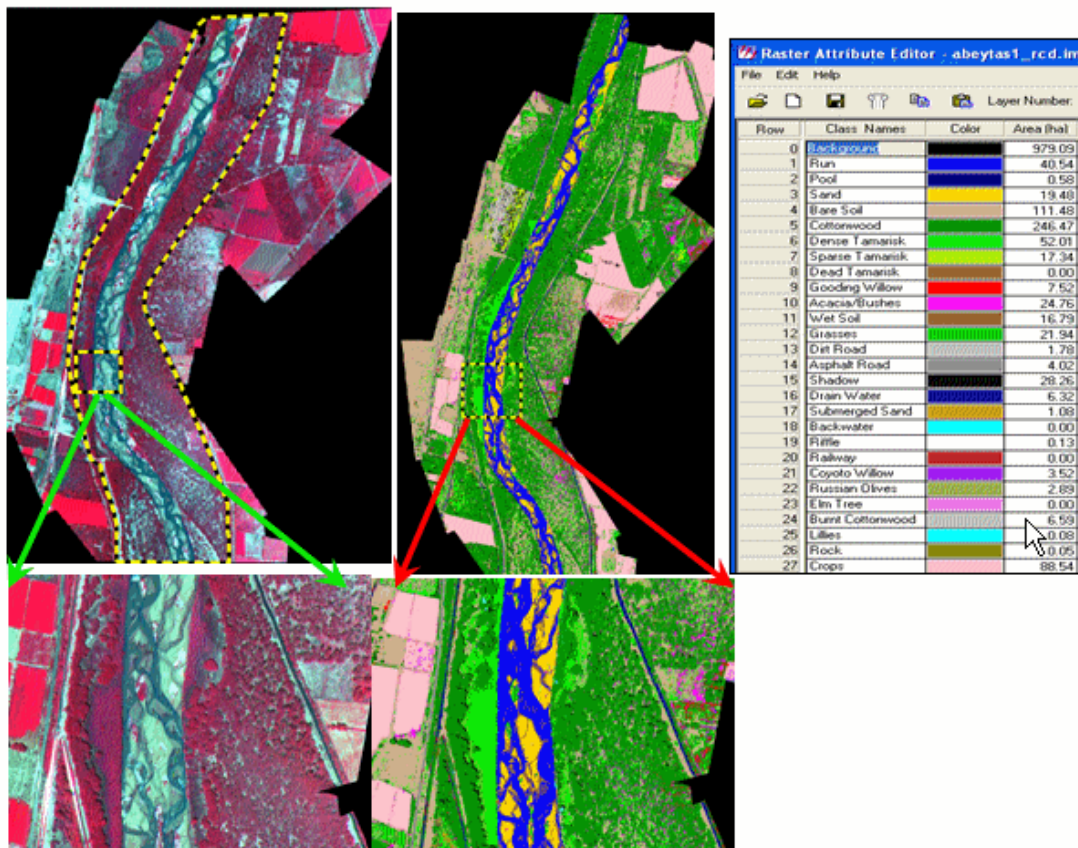


Figure 2.2 Three-band mosaic (left) and corresponding classified image (right) with final classification scheme of a section of the Middle Rio Grande in the Abeytas area, along with full image resolution detail

Table 2.2 Main riparian vegetation surface class areas along the middle Rio Grande in hectares per linear km of river resulting from the image classification, per 1:24,000 USGS quadrangle listed from upstream (Albuquerque) to downstream (Paraje)

	Cottonwood	Tamarisk	Coyote Willow	Russian Olives
Albuquerque	20.53	1.24	1.63	0.70
Isleta	25.56	5.44	6.13	1.69
Las Lunas	23.93	3.09	4.97	1.42
Tome	19.16	2.74	4.55	0.53
Turn_Veguita	18.88	6.21	2.92	1.10
Abeytas	20.08	13.42	1.38	0.33
La Joya	15.29	11.05	1.02	2.29
San Acacia	10.87	14.03	0.85	0.42
Loma De Canas	11.71	17.57	0.49	0.61
San Antonio N.	13.57	39.68	1.95	1.86
San Antonio S.	10.01	30.51	2.64	0.61
San Marcial	16.89	31.98	0.00	0.12
Paraje	15.14	15.17	0.72	0.17

However, earlier research has shown the possibility of extracting these features with relative confidence (Anderson et al., 1994; May et al., 2001; Panja et al., 1994). Some of these in-stream features can be seen in the full resolution three-band inset on the lower left side of Fig 2.2.

The image classification showed changes in vegetation distribution and water surface area as the river flows from north (Albuquerque) to the south (San Antonio). More Cottonwood and fewer Tamarisks appear in northern sections of the river while more Tamarisks and less water surface area are present in the downstream sections, south of San Antonio. Analyzing the imagery from upstream to downstream, it was clear that

water diversions had a big effect on water surface area in the river implying that water flow volumes were affected as well. Figure 2.4 shows the effect of a water diversion for irrigation purposes on the in-stream water surface area at the Isleta diversion dam, located within the Isleta quadrangle sheet. The river corridor downstream from the diversion dams has a much higher area classified as dry and wet sand and greatly reduced water surface area, compared to the upstream section.

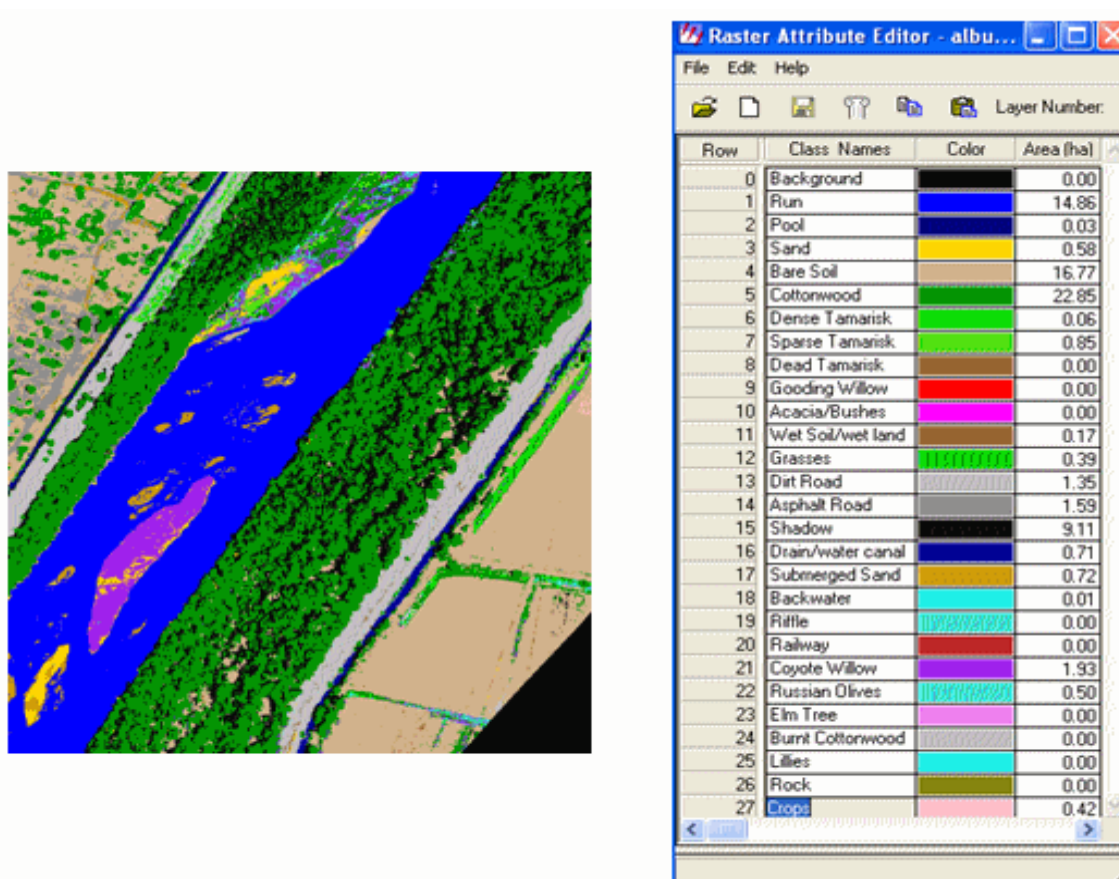


Figure 2.3 A section of the river in the Albuquerque area where Cottonwood is the predominant vegetation class (dark green color) along with the attribute table

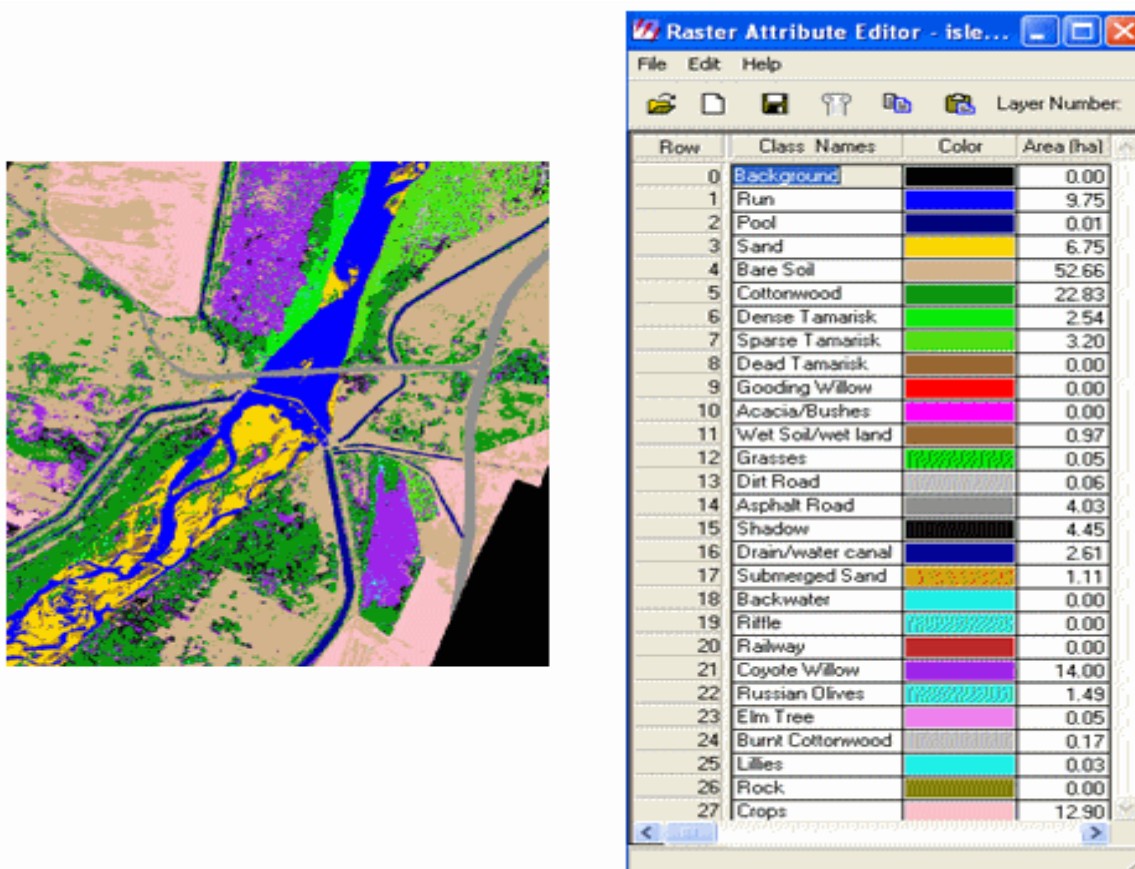


Figure 2.4 Water diversion at Isleta showing an increased amount of exposed sand downstream from the diversion dam and decreased water surface area

The consequence of diversions for irrigation and municipal use can be seen in Table 2.3, where a general decrease in total water surface area along the river from north to south can be observed. The number of the diversion dams where water is extracted from the river and drains that contribute water to the river are also indicated, per USGS quad sheet. Changes in the water surface area as well as the areas of wet and dry sand are a function of the inflows and outflows to the river in upstream reaches, including the removal of water through evapotranspiration by the riparian vegetation.

Table 2.3 In-stream class area distribution for Middle Rio Grande River, in hectares per linear Kilometer of river, obtained from the classified airborne images. The asterisk (*) superscript indicates the presence of a diversion dam within that quad sheet and the number in parenthesis () indicates the number of drain inflows to the river within that quad sheet

	Run	Pool	Back water	Riffle	Wet Soil	Sand	Submerged Sand	Surface Water Area
Albuquerque ⁽³⁾	10.68	0.08	0.02	0.00	0.25	0.73	0.73	11.51
Isleta ^{*(2)}	8.11	0.07	0.00	0.00	1.52	1.39	1.39	9.57
Las Lunas	3.92	0.09	0.34	0.00	4.90	2.01	2.01	6.37
Tome ⁽⁴⁾	2.93	0.04	0.43	0.00	2.69	1.43	1.43	4.83
Turn Veguita ⁽¹⁾	4.50	0.07	0.87	0.00	1.38	0.77	0.77	6.21
Abeytas	5.33	0.11	0.00	0.04	2.21	3.61	1.66	7.13
La Joya ⁽¹⁾	5.44	0.00	0.00	0.00	1.27	0.12	0.12	5.56
San Acacia ^{*(1)}	4.65	0.12	0.00	0.04	3.70	1.30	1.30	6.12
Loma De Canas ⁽¹⁾	3.96	0.19	0.00	0.27	1.37	2.18	2.18	6.60
San Antonio N.	5.18	0.46	0.18	0.00	0.71	1.67	1.67	7.51
San Antonio S. ⁽¹⁾	3.37	0.18	0.19	0.65	1.24	1.82	1.82	6.22
San Marcial ⁽¹⁾	2.35	0.99	0.02	0.00	1.28	0.18	0.18	3.54
Paraje	1.57	0.09	0.01	0.03	1.51	1.40	1.40	3.11

Records of mean daily river flows during the image acquisition period (24-26 July 2001) corroborate these classification results (Figure 2.5). The measurements were conducted at four gauging stations going from north (below Cochiti) to south (San Marcial) and show a significant decrease in-stream flow. The peaks might be attributed to the effects of precipitation events in the watershed. The disappearance/smoothing of the peaks at the southern gauge stations may be a combination of extensive diversions in

upstream sections and/or absorption of water in previously de-watered sections downstream from the diversions.

Rapid variations in river flows affect in-stream fishery habitats and riparian vegetation. These observations can aid policy makers in setting diversions and preserve in-stream flows to support the native riparian vegetation and river habitats.

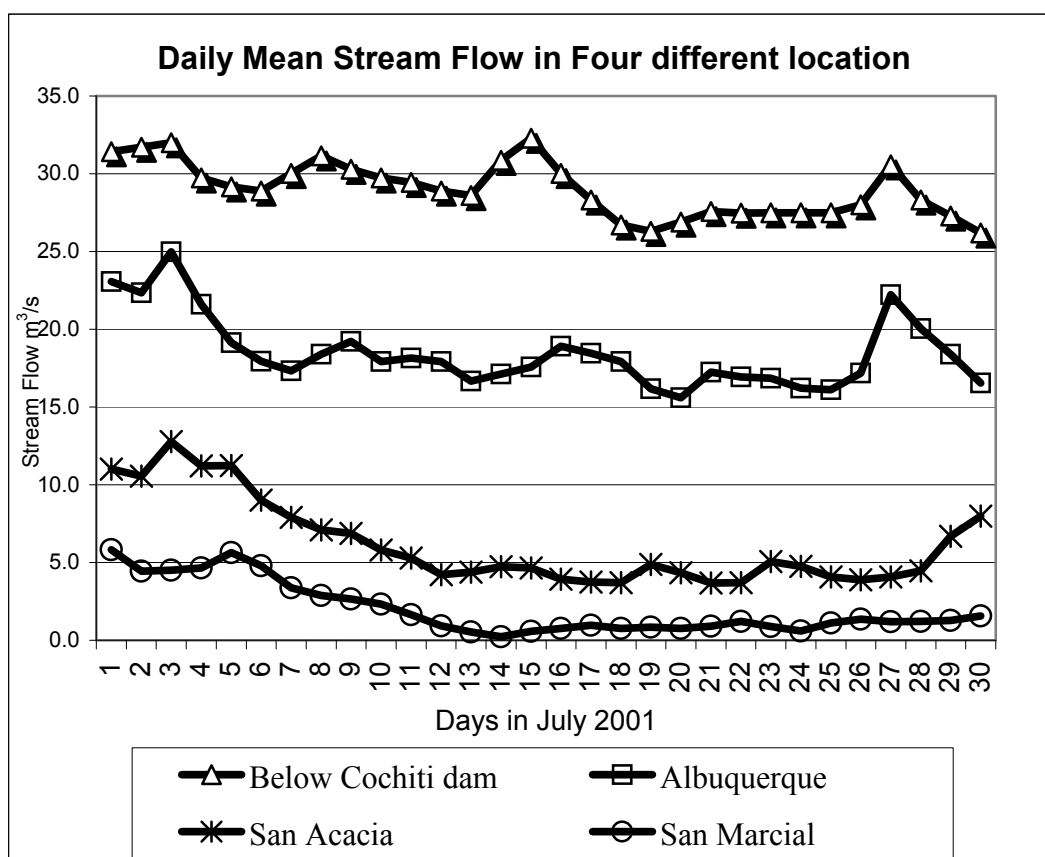


Figure 2.5 Mean daily stream flow at four different locations along the Middle Rio Grande during the month of July 2001 (United States Geological Survey, <http://www.usgs.gov>)

CONCLUSIONS AND RECOMMENDATIONS

Vegetation mapping using high resolution RS gives a broad and comprehensive indication of riparian zone health and condition along the river. In the case of the Middle Rio Grande, results show changes in vegetation distribution in which invasive vegetation is replacing native species. Vegetation distribution analysis of the classified imagery showed a decline in Cottonwood and an increase in Tamarisk in the downstream direction along with a general decrease in water surface areas and increase in exposed sand within the river corridor.

The accuracy assessment showed promising results in the use of high-resolution airborne images for mapping complicated forest structure like the riparian vegetation. Overall accuracy reached was 88% with the ability for more improvement. The high-quality vegetation map produced from this research will help in future planning by aiding decision makers in identifying problems that affect the river system and allowing for the study of vegetation interactions with the groundwater system and river as well as the surrounding areas. It will also provide a basis for the detection of changes resulting from any management plan applied to the river corridor with the aim of protecting and restoring the river ecosystem.

Future monitoring of riparian and wetland ecosystems using high-resolution airborne RS will aid in the detection of escalating problems due to water quantity and quality in the riverine habitats. High-resolution RS can aid in detecting changes in vegetation due to natural causes or control practices on introduced or invasive species such as Tamarisk. The effectiveness of new Tamarisk control methods such as using a

beetle imported from Asia could also be assessed with a future over flight of the river and similar analysis of the imagery.

REFERENCES

- Anderson, P. C., Hardy, T. B., Neale, C. M. U., 1994. Application of multispectral videography for the delineation of riverine depths and meso-scale hydraulic features. In: Proceedings of the 14th Biennial Workshop on Color Aerial Photography and Videography for Resource Monitoring. American Society for Photogrammetry and Remote Sensing, 25–29 May 1993, Logan, UT.
- Bartz, K. L., Kirschner, J. L., Ramsey, R. D., Neale, C. M. U., 1994. Delineating riparian cover types using multi-spectral airborne videography. In: Proceedings of the 14th Biennial Workshop on Color Aerial Photography and Videography for Resource Monitoring. American Society for Photogrammetry and Remote Sensing, 25–29 May 1993, Logan, UT.
- Benediktsson, J. A., Pesaresi, M., Amason, K., 2003. Classification and feature extraction for remote sensing images from urban areas based on morphological transformations. *IEEE Transactions on Geoscience and Remote Sensing* 41, 1940–1949.
- Best, R. G., Wehda, M. E., Linder, R. L., 1981. Spectral reflectance of hydrophytes. *Remote Sensing of Environment* 11, 27–35.
- Bonner, K. G., 1981. Riparian vegetation mapping in northeastern California using high altitude color infrared aerial photography. In: Proceedings of 8th Biennial Workshop on Color Aerial Photography in Plant Sciences. American Society of Photogrammetry and Remote Sensing, 21–23 April 1981, Falls Church, VA.
- Brock, J. H., 1994. *Tamarix* sp. (salt cedar), an invasive exotic woody plant in arid and semi-arid riparian habitats of western USA. In: De Waal, L.C., Child, L.E., Wade, M., Brock, J.H. (Eds.), *Ecology and Management of Invasive Riverside Plants*. Wiley, New York, pp. 27–44.
- Brower, A., 2004. ET toolbox evaporation toolbox for the Middle Rio Grande—a water resources decision support tool. Final Draft, Bureau of Reclamation. US Department of Interior, Denver, CO, 154pp.
- Busch, D. E., Smith, S. D., 1995. Mechanisms associated with decline of woody species in riparian ecosystems of the southwestern US. *Ecological Monographs* 65, 347–370.
- Cai, B., Neale, C. M. U., 1999. A method for constructing 3-dimensional models from airborne imagery. In: Proceedings of the 17th Biennial Workshop on Color Photography and Videography in Resource Assessment. American Society for Photogrammetry and Remote Sensing, 5–7 May 1999, Reno, NV.
- Callahan, D., White L., 2004. Vegetation mapping of the Rio Grande floodplain from Velarde to Elephant Butte. US Bureau of Reclamation Report, Denver Technical Service Center, 6pp.

- Carleer, A. P., Wolff, E., 2004. Exploitation of very high resolution satellite data for tree species identification. *Photogrammetric Engineering and Remote Sensing* 70, 135–140.
- Carneggie, D. M., Schruppf, B. J., Mouat, D. M., 1983. Rangeland applications. In: Colwell, R.N. (Ed.), *Manual of Remote Sensing*. American Society for Photogrammetry and Remote Sensing 2, pp. 2325–2363.
- Chavez, J. L., Neale, C. M. U., Hipps, L. E., Prueger, J. H., Kustas, W. P., 2005. Comparing aircraft-based remotely sensed energy balance fluxes with eddy covariance tower data using heat flux source area functions. *Journal of Hydrometeorology* 6, 923–940.
- Congalton, R. G., Green, K., 1999. *Assessing the Accuracy of Remotely Sensed Data: Principles and Practices*, first ed. Lewis Publishers, CRC Press Inc., Florida.
- Czaplewski, R. L., Patterson, P. L., 2003. Classification accuracy for stratification with remotely sensed data. *Forest Science* 49, 402–408.
- ERDAS, 1999. *ERDAS Field Guide*, fifth ed. ERDAS Inc., Georgia.
- Everitt, B. L., 1998. Chronology of the spread of Tamarisk in the central Rio Grande. *Wetlands* 18, 658–668.
- Everitt, J. H., Deloach, C. J., 1990. Remote sensing of Chinese Tamarisk and associated vegetation. *Weed Science* 38, 273–278.
- Everitt, J. H., Nixon, P. R., 1985. Video imagery: a new remote sensing tool for range management. *Photogrammetric Engineering and Remote Sensing* 51, 675–679.
- Everitt, J. H., Richardson, A. J., Nixon, P. R., 1986. Canopy reflectance characteristics of succulent and nonsucculent plant species. *Photogrammetric Engineering and Remote Sensing* 52, 1891–1897.
- Everitt, J. H., Escobar, D. E., Villarreal, R., 1988. Evaluation of single band video and video based indices for grassland phytomass assessment. *Photogrammetric Engineering and Remote Sensing* 54, 1177–1180.
- Everitt, J. H., Escobar, D. E., Noreiga, J., 1991. A high resolution multispectral video system. *GeoCarto International* 6, 45–51.
- Farag, F., Neale, C. M. U., Kjelgren, R., 2001. Using remote sensing and GIS to analyze irrigated urban landscape water demand. In: *Proceedings of the 18th Biennial Workshop on Color Photography & Videography in Resource Assessment*. American Society for Photogrammetry and Remote Sensing, 16–18 May 2001, University of Massachusetts, Amherst, USA.
- Gaussman, H. W., Everitt, J. H., Gebermann, A. H., Bowen, R. L., 1977. Canopy reflectance and film image relations among three south Texas rangeland plants. *Journal of Range Management* 31, 449–450.
- Gaussman, H. W., Escobar, D. E., Bowen, R. L., 1983. A video system to demonstrate interactions of near infrared radiation with plant leaves. *Remote Sensing of Environment* 13, 363–366.

- Goodrich, D. C., Chehbouni, A., Goff, B., et al., 2000. The semi-arid land–surface–atmosphere (SALSA) program: special issue preface paper. *Agricultural and Forest Meteorology* 105, 3–20.
- Gurnell, A. M., 1995. Vegetation along river corridors: hydrogeomorphological interactions. In: Gurnell, A.M., Petts, G.E. (Eds.), *Changing River channels*. Wiley, New York, pp. 237–260.
- Harvey, K. R., Hill, G. J. E., 2001. Vegetation mapping of a tropical freshwater swamp in the northern territory, Australia: a comparison of aerial photography, Landsat TM and SPOT satellite imagery. *International Journal of Remote Sensing* 22, 2911–2925.
- Herold, M., Gardner, M. E., Roberts, D. A., 2003. Spectral resolution requirements for mapping urban areas. *IEEE Transactions on Geoscience and Remote Sensing* 41, 1907–1919.
- Hughes, F. M. R., Richards, K. S., El-Hames, A. S., Harris, T., Peiry, J. L., Pautou, G., Girel, J., 1997. Investigations into hydrological influences on the establishment of riparian tree species. In: Large, A.R.G. (Ed.), *Floodplain Rivers: Hydrological Processes and Ecological Significance*. British Hydrological Society Occasional Paper 8, pp. 17–29.
- Hutchinson, C. F., Schowengerdt, R. A., Baker, L. R., 1990. A two-channel multiplex video remote sensing system. *Photogrammetric Engineering and Remote Sensing* 56, 1125–1128.
- Kalliola, R., Syrjanen, K., 1991. To what extent are vegetation types visible in satellite imagery? *Annales Botanici Fennici* 28, 45–57.
- King, D. J., Vlcek, J., 1990. Development of a multi-spectral video system and its application in forestry. *Canadian Journal of Remote Sensing* 16, 15–22.
- Kliman, D. H., 1988. Detection of seasonal vegetation change with video remote sensing. In: *Proceedings of First Workshop on Videography*. American Society for photogrammetry and Remote Sensing, Terra Haute, IN.
- Large, A. R. G., 1997. Linking floodplain hydrology and ecology—the scientific basis for management. In: Large, A.R.G. (Ed.), *Floodplain Rivers: Hydrological Processes and Ecological Significance*. British Hydrological Society Occasional Paper 8, pp. 1–5.
- Lonard, R. I., Judd, F. W., Everitt, J. H., Escobar, D. E., Davis, M. R., Crawford, M. M., Desai, M. D., 1998. Evaluation of color infrared photography for distinguishing annual changes in riparian forest vegetation of the lower Rio Grande in Texas. In: *Proceedings of the 1st Conference of Geospatial Information in Agriculture and Forestry*. ERIM, University of Michigan, Ann Arbor, MI.
- Loope, L. L., Sanchez, P. G., Tarr, P. W., Loope, W. L., Anderson, R. L., 1988. Biological invasions of arid land nature reserves. *Biological Conservation* 44, 95–118.
- Lulla, K., Mausel, P., Skelton, D., Kramber, W., 1987. An evaluation of video band based vegetation indices. In: *Proceedings of 11th Biennial Workshop on Color Aerial Photography and Videography*. American Society for Photogrammetry and Remote Sensing, Weslaco, TX.

- Martin, M. E., 1988. Determining forest species composition using high spectral resolution remote sensing data. *Remote Sensing of Environment* 65, 249–254.
- Mausel, P. W., Everitt, J. H., Escobar, D. E., King, D. J., 1992. Airborne videography: current status and future perspectives. *Photogrammetry and Remote Sensing* 58 (8), 1189–1195.
- May, C., Neale, C. M. U., 1999. Mapping resources in the Escalante river corridor using airborne multispectral imagery. In: *Proceedings of the 17th Biennial Workshop on Color Photography and Videography in Resource Assessment*. American Society for Photogrammetry and Remote Sensing, 5–7 May 1999, Reno, NV.
- May, C. J., Neale, C. M. U., Henderson, N., 2001. Mapping riparian resources in semi-arid watersheds using airborne multispectral imagery. In: *Proceedings of the Remote Sensing and Hydrology 2000 Symposium*. IAHS Publication No. 267, pp. 539–541.
- Meisner, D. E., Lindstorm, O. M., 1985. Design and operation of a color infrared aerial video system. *Photogrammetry Engineering and Remote Sensing* 51, 555–560.
- NASA, 2007. Evaluation report for AWARDS ET toolbox and river ware decision support tools. Available from: <http://wmp.gsfc.nasa.gov/reports/EvalRpt_RiverwareAwards.doc>.
- Neale, C. M. U., 1991. An airborne multispectral video/radiometer remote sensing system for agricultural and environmental monitoring. In: *Automated Agriculture for the 21st Century, Proceedings of the International Conference*, ASAE, December 1991.
- Neale, C. M. U., 1992. An airborne multi-spectral video/radiometer remote sensing system for natural resource monitoring. In: *Proceedings of 13th Biennial Workshop on Color Aerial Photography and Videography in Plant Sciences*. American Society for Photogrammetry and Remote Sensing, 6–9 May 1991, Orlando, FL.
- Neale, C. M. U., 1997. Classification and mapping of riparian systems using airborne multispectral videography. *Restoration Ecology* 5, 103–112.
- Neale, C. M. U., Crowther, B. G., 1994. An airborne multi-spectral video/radiometer remote sensing system: development and calibration. *Remote Sensing of Environment* 49, 187–194.
- Neale, C. M. U., Wenger, D., Jayanthi, H., Farag, F., 2007. Mapping and monitoring wetlands using airborne multispectral imagery. In: *Remote Sensing for Environmental Monitoring and Change Detection*. IAHS Publication No. 316, pp. 100–109.
- Nixon, P. R., Escobar, D. E., Menges, R. M., 1987. A multi video false color imaging system for remote sensing applications. In: *Proceedings of 11th Biennial Workshop on Color Aerial Photography and Videography in Plant Sciences*. American Society of Photogrammetry and Remote Sensing, Falls Church, VA.

- Nixon, P. R., Escobar, D. E., Menges, R. M., 1992. Use of multi-spectral video/radiometer remote sensing system for natural resource monitoring. In: Proceedings of 13th Biennial Workshop on Color Aerial Photography and Videography in Plant Sciences. American Society for Photogrammetry and Remote Sensing, 6–9 May 1991, Orlando, FL.
- Panja, K., Hardy, T. B., Neale, C. M. U., 1994. Comparison of meso-scale hydraulic features at different discharges in a turbid river system using multispectral videography. In: Proceedings of the 14th Biennial Workshop on Color Aerial Photography and Videography for Resource Monitoring. American Society for Photogrammetry and Remote Sensing, 25–29 May 1993, Logan, UT.
- Redd, T., Neale, C. M. U., Hardy, T. B., 1994. Use of airborne multispectral videography for the classification and delineation of riparian vegetation. In: Proceedings of the 14th Biennial Workshop on Color Aerial Photography and Videography for Resource Monitoring. American Society for Photogrammetry and Remote Sensing, 25–29 May 1993, Logan, UT.
- Richardson, A. J., Heilman, M. D., Escobar, D. E., Everitt, J. H., 1988. Nitrogen and tillage treatment effects of sorghum as measured by aerial video and handheld ground reflectance. In: Proceedings of First Workshop on Videography. American Society for Photogrammetry and Remote Sensing, Terra Haute, IN.
- Richardson, A. J., Heilman, M. D., Escobar, D. E., 1990. Estimating grain sorghum yield from video and reflectance based PVI measurements at peak canopy development. *Journal of Imaging Technology* 16, 104–109.
- Sandmann, H., Lertzman, K. P., 2003. Combining high-resolution aerial photography with gradient-directed transects to guide field sampling and forest mapping in mountainous terrain. *Forest Science* 49, 429–443.
- Shen, Y., Kondoh, A., Tang, C., Xiao, J., Oki, T., Kanae, S., 2004. Development and application of a remote sensing model for estimating soil water status and evapotranspiration in semiarid region. Available from: <http://www.wrrc.dpri.kyoto-u.ac.jp/~aphw/APHW2004/proceedings/RCW/56-RCW-A305/56-RCW-A305_craft.pdf>.
- Shoemaker, J., Hardy, T. B., Neale, C. M. U., 1994. Jurisdictional delineation of wetlands with multipsectral aerial videography. In: Proceedings of the 14th Biennial Workshop on Color Aerial Photography and Videography for Resource Monitoring. American Society for Photogrammetry and Remote Sensing, 25–29 May 1993, Logan, UT.
- Sugumaran, R., Meyer, J. C., Davis, M., 2004. A web-based environmental decision support system (WEDSS) for environmental planning and watershed management. *Journal of Geographical Systems* 6, 307–322.
- Sundararaman S., Neale C. M. U., 1997. Geometric calibration of the USU videography system. In: Proceedings of the 16th Biennial Workshop on Color Photography and Videography in Resource Assessment. American Society for Photogrammetry and Remote Sensing, 29 April–1 May 1997, Weslaco, TX.
- Tueller, P. T., 1982. Remote sensing for range management. In: Johannsen, J., Sanders, L. (Eds.), *Remote Sensing for Range Management*. Soil Conservation Society of America, Ankeny, IA, pp. 125–140.

- Vlcek, J., King, D., 1985. Development and use of a 4-camera video system for resource surveys. In: Proceedings of 19th International Symposium on Remote Sensing of Environment. Environmental Research Institute of Michigan, University of Michigan, Ann Arbor, MI.
- Weigand, C. L., Scott Jr., A. W., Escobar, D. E., 1988. Comparison of multi-spectral videography and color infrared photography versus crop yield. In: Proceedings of First Workshop on Videography. American Society for Photogrammetry and Remote Sensing, Terra Haute, IN.
- Williams, J. A., 1992. Vegetation classification using Landsat TM and SPOT-HRV imagery in mountainous terrain, Kananaskis Country, S.W. Alberta''. Alberta Recreation and Parks, Kananaskis Country Operations Branch, Environmental Management, Canmore, Alberta. Available from: <[http://www.ucalgary.ca/uofc/faculties/SS/GEOG/Virtual/Remote Sensing/williamsrsveg.html](http://www.ucalgary.ca/uofc/faculties/SS/GEOG/Virtual/Remote%20Sensing/williamsrsveg.html)>.

CHAPTER 3

MODELING GROUNDWATER AND EVAPOTRANSPIRATION IN THE MIDDLE
RIO GRANDE RIVER RIPARIAN CORRIDOR

ABSTRACT

The Middle Rio Grande River, New Mexico is the focus of this research due to the complex interactions between in-stream flows, riparian vegetation and multiple diversions for competing interests. The connection between the river flow and the water table with the riparian vegetation evapotranspiration (ET) was studied. The Dupuit equation was implemented to model the water table surface using water table readings from observations wells in the riparian zone. The model output is used to estimate the depth to the water table and the soil water potential above the saturated zone, used later in the ET estimation. Two evapotranspiration methods were applied on the two major types of riparian vegetation; Tamarisk (*Tamarix ramosissima*) and the native vegetation Cottonwood (*Populus deltoids*). The Tamarisk evapotranspiration was estimated using two methods; (1) the modified Penman-Monteith (PM) in conjunction with Ball-Berry stomatal conductance model and (2) the canopy temperature minus air temperature method. The Cottonwood ET was estimated using the canopy temperature method only.

The outputs from both methods were compared with the measured ET using the eddy covariance method adjusted for energy balance closure. The modeled spatially-distributed ET estimates using the modified PM method were in good agreement with the measured Tamarisk ET, while the canopy temperature method showed good agreement only in a sparse Tamarisk canopy and for Cottonwood.

INTRODUCTION

The Middle Rio Grande River (MRGR) is the main source of fresh water for the state of New Mexico. As it flows through an arid area with scarce local water resources, it has been extensively diverted to supply the high demand from municipalities and irrigated agriculture. Over the last few decades, these diversions have affected the composition of the native riparian vegetation by decreasing the area of Cottonwood and Coyote Willow and increasing the spread of invasive species such as Tamarisk and Russian Olives, harmful to the river system, due to their high transpiration rates and extensive presence. There is need to study the river hydrological processes and their relationship with ecosystem health. The water table within the riparian zone is intrinsically connected to the flows in the river. Large withdrawals of water by Tamarisk affect the surface flows, which coupled with the large diversions for irrigation result in a complicated river management problem.

Previous evapotranspiration (ET) studies have focused mostly on crops for either human or animal stock consumption. Riparian vegetation has received less attention due to its perceived lower economic value and the difficulties in making ET measurements because it is often present in narrow strips and is heterogeneous. In order to preserve the riparian vegetation resource it is very important to estimate its evapotranspiration and understand its interaction with water tables and river flows. This will allow for better management of the storage dams and releases and the distribution of water among different uses.

Previous studies have shown that evapotranspiration in the MRGR is affected by the advection process where dry hot air from surrounding arid areas replaces the air

above the riparian canopy. Dry, hot air increases the saturated vapor deficit above the riparian canopy and leads to increased evapotranspiration. It is essential to take into consideration all energy components affecting evapotranspiration in order to get the most accurate estimate.

In this chapter, the methodology used to spatially model the evapotranspiration and the water table depth and water fluxes within the riparian zone of the Middle Rio Grande River is described and tested. A modified Penman-Monteith approach with a coupling factor suggested by Hattori (2004) is used to estimate the evapotranspiration of the riparian vegetation. Water table readings are used as input and to check the groundwater model. Evapotranspiration by the riparian vegetation is included in the soil moisture and groundwater flux balance. The model developed in Visual Basic runs as an application in the ArcGIS environment utilizing different spatial layers including digital elevation model, soils and riparian vegetation maps, the latter obtained from the classification of airborne high resolution multi-spectral imagery presented in the previous chapter. The model was applied to different sections of the MRGR where water table and ET measurements were available.

BACKGROUND

Riparian Vegetation

Riparian vegetation is defined by the National Research Council (1992) as “the corridor of hydrophytes vegetation growing on the banks of streams and rivers, and having an annual evapotranspiration level that influences surface and groundwater hydrology.” Biologically, riparian vegetation species are integral parts of river and stream

ecosystems, and are intimately related with the sustenance of biodiversity found in such ecosystems. Studies have shown that riparian vegetation reduces solar heating of river water through shading which has a large effect on fish and birds populations (Brown and Krygier, 1970). Riparian ecosystems occupy less than 1% of north and western parts of the north-American continental landscape, yet they provide habitat for far more species of birds than all other vegetation types combined (Knopf et al., 1988). One important function of riparian vegetation is to slow down stream flows and promote sedimentation and deposition of suspended particles contributing to the control of soil erosion along rivers and stabilization of stream banks (Chescheir et al., 1991; Tabacchi et al., 1998).

Riparian vegetation forms an important boundary/interface between open surface water and groundwater. Interestingly, until the twentieth century, there was no differentiation between riparian and wetlands vegetation systems.

It is very fundamental and important to understand riparian zone vegetation dynamics from a hydrology point of view (Brinson, 1990). There is little information available on the consequences of subsurface flow (groundwater) on riparian vegetation and its dynamics (Tabacchi et al., 1998). Vegetation is an essential part of corridors along rivers, and calls for detailed research on the linkages between plant species distributions, river flow, erosion, water table levels and soil moisture dynamics (Gurnell, 1995; Hughes et al., 1997; Large, 1997).

Preliminary studies have indicated that the spread of Tamarisk in Middle Rio Grande River has driven the water table to low levels because of its high water use, and its ability to sustain high ET rates due to a deep rooting system (Brotherson et al., 1984;

Cleverly et al., 1997). The direct effect of Tamarisk on the riparian water table can be seen between day and night time water table measurements (Cleverly et al., 1997).

Previous studies and research activities have considered riparian vegetation as a source of energy and matter for the aquatic ecosystem (Peterjohn and Correll, 1984). Investigations revealed the role of riparian vegetation in removing and retaining particulates on the land surface, in addition to the role of riparian vegetation as regulators of diffuse subsurface pollution (Peterjohn and Correll, 1984). It has also been suggested that the relationship between rivers and riparian vegetation should be given more attention, especially following the alterations caused by human activities (Poff et al., 1997).

In terrestrial energy balance terms, riparian vegetation helps reduce solar heating of river water by shading (Brown and Krygier, 1970), resulting in cooling of river waters (Sinokrot and Stefan, 1993), and a reduction in stream water loss through evaporation. Consequently more water is available for immediate use as well as contributing to sustaining groundwater. In addition, riparian vegetation through the evapotranspiration process has also a cooling effect on river water (Sinokrot and Stefan, 1993). However, phreatophytes such as Tamarisk can extract large amounts of groundwater from the system decreasing the flows within the river channel. In the MRGR, riparian vegetation ET is usually energy limited in the morning and governed by saturated deficit and stomatal resistance in the afternoon when advection occurs. Hattori (2004) observed that these factors had to be taken into consideration in order to obtain good estimates of ET.

The link between riparian vegetation, wetland vegetation, evapotranspiration, river flows, and groundwater is very complex and not well understood. The knowledge

regarding these relationships is essential to protect the biodiversity, and to better manage, and conserve scarce water resources. Therefore, to maintain a sustainable river ecosystem, all its components – catchments, river hydrology and hydraulics, wetland and riparian regimes, groundwater must be considered in an integrated manner (Ward, 1989).

Conventional methods of estimating depletion of water from riparian hydrologic systems through ET processes are severely affected by complexity of vegetation regimes (understorey vs. overstorey), diversity (species differences) and associated inaccessibility within the differences in measurement scales (leaf level vs. stand level) over variable soil-vegetation. Eddy covariance and Bowen Ratio flux towers have been suggested as the most accurate methods of measuring ET at scales ranging between 0.1 to 1 km (Rana and Katerji, 2000). The best previous measurements of riparian vegetation ET were obtained using Bowen ratio energy balance measurements over Tamarisk stands in lower Colorado River and in New Mexico (DeLoach et al., 2000). Nichols et al. (2004) listed different methods to estimate potential evaporation from riparian vegetation combined with a factor that accounts for moderating effect on flux by the canopy.

Wylie et al. (2003) observed that extrapolating aerodynamic data from flux tower foot prints to larger landscape units could lead to bias in regional ET estimates. They recommended the use of remote sensing and other ancillary data to develop algorithms for extrapolating site-specific tower data to similar land cover types at regional scales.

Use of Airborne Remote Sensing to Estimate Riparian Vegetation ET

Nagler et al. (2005) gave an ecophysiological justification for a remote sensing based ET model for riparian vegetation in western US riparian corridors. Normalized Difference Vegetation Index (NDVI) and Enhanced Vegetation Index (EVI) (Huete et al.,

2002) were computed from time composites of MODIS imagery over the Middle Rio Grande River in New Mexico. EVI was reported to be more closely related with ET than NDVI and this was attributed to the saturation of the latter with high leaf area index (LAI) values of the riparian vegetation. The authors observed that a multivariate regression for predicting ET from EVI and air temperature (T_a) had an $r^2=0.82$ across sites, species and years. It was reported that estimated riparian ET was considerably lower than ET estimated by indirect, water balance methods.

SEBAL (Bastiaanssen et al., 2005) and METRIC (Allen et al., 2007) belong to integrated class of modeling-observation merged procedures for estimating landscape ET from satellite sensors. These methods index sensible heat flux from land surfaces to satellite-measured surface temperatures at specific boundary conditions to generate spatial ET maps for daily, monthly and/or seasonal time periods. These models are better suited to agricultural areas where large fields of relative uniform vegetation exist. The spatial resolution of the thermal infrared pixels complicates the application of these models to narrow and heterogeneous riparian zones.

Batelaan et al. (2004) used hyperspectral imagery from CASI-ATM sensor and ground measurements like air, surface, and soil temperatures, and vegetation height to estimate vegetation ET in the Doode Bemde wetland, Belgium. Coonrood et al. (2006) highlighted procedures to translate and compare ET estimates from different computational methods in to ArcGRID format to enable the use of ArcGIS for calculations of difference grids thus enabling further refinement of ET estimation methods.

Samani et al. (2007) presented a regional ET estimation model (REEM) that uses energy balance at the top of the canopy to estimate corresponding plant ET. ASTER images are used to estimate surface temperatures, albedo, and NDVI to determine net radiation, ground heat flux, and sensible heat flux. REEM generates estimates of ET in riparian areas which can be used to evaluate the impact of removing and managing undesirable riparian vegetation that is affecting middle Rio Grande river basin hydrology.

All the above studies used satellite multi-spectral remote sensing with medium (30 to 120 m) to low spatial resolution (250 m to 1 km pixels). The medium resolution proved to be inadequate in delineating the fine distinctions existing within the riparian and wetland zones (Harvey and Hill, 2001; Kalliola and Syrjanen, 1991). Chapter 2 showed that the inability of medium resolution satellite remote sensing imagery to properly map different riparian vegetation species types in detail: whether or not they were invasive or native may be the reason for many studies not being able to accurately estimate riparian vegetation ET separately by species. In this regard, the use of high resolution airborne multi-spectral imagery has a major role. Airborne remote sensing techniques, by virtue of their very high spatial resolution and flexible revisit capability, are considered as the most reliable tool to extrapolate ground based flux station reference data to large riparian zones (Carleer and Wolff, 2004; Chapter 2).

This research will take advantage of high resolution airborne multi-spectral imagery and the resulting detailed riparian vegetation map obtained from its classification to estimate the spatially distributed water consumptive use of riparian vegetation taking into consideration the advection processes that occurs at MRGR (Hattori, 2004).

Modified Penman Monteith Method and Stomatal Conductance Model

The modified Penman Monteith has been validated (Hattori, 2004) for the Bosque del Apache in the MRGR. The main issue for applying this model is estimating the stomatal conductance for the different riparian vegetation species. The spatial application of the model and the utilization of spatially distributed depth to the water table as an input will allow for modeling the spatial variability in the stomatal conductance among Tamarisk which will result in ET variability.

Stomata connect the internal region of leaves to the air. Stomata allow CO₂ to enter the leaves and oxygen and water vapor to exit as transpiration. Therefore, understanding stomatal behavior is central to understanding and describing the response of riparian vegetation to changes in environmental conditions.

A major problem in dealing with stomata is that stomatal conductance (g_s) tends to vary widely through any plant canopy, at any time. There has been a large amount of research aimed at identifying the mechanisms of stomatal response, some of which was summarized by Jarvis (1976), who produced a phenomenological model that has been widely used. A semi-empirical model for stomatal conductance developed by Leuning (1995) now provides, in a single equation, a general description of stomatal response. This includes humidity deficit at the leaf surface, which requires energy balance calculations.

Jarvis (1976) studied the stomata in relation to five variables and built a model that relates leaf water potential to the flow of water through the plant. Those variables were photon flux density (incoming radiation), leaf temperature, leaf water potential, saturated vapor deficit, and CO₂ concentration. Hattori (2004) applied the Ball-Berry

model with great success to model Tamarisk canopy conductance. This model will be discussed in more details in the methodology section.

Groundwater Modeling

Not much effort has been pursued in the past to understand the hydrologic cycle and the hydrological connectivity between river and the riparian system due to their low economic value (Hewitt, 1990; Tabacchi et al., 1998). The increasing world population is exerting pressure on water resources through the increasing demand on fresh water to the extent that is exceeding the ability of water resources to meet demand (Perkins and Sophocleous, 1999). Competition over how and where to use water resources is becoming the main issue that needs to be resolved among different countries and within the countries them selves.

In the United States water sharing and distribution among different states are always ongoing issues that needs to be resolved (Homer-Dixon, 1999; Postel and Wolf, 2001). In the Middle Rio Grande river where most of the surrounding areas are arid to semi arid, water resources management is the most important issue (Chapter 2). The decision makers in MRGR are always faced with critical management question, which is, how much water should be released from the dams to sustain sound river ecosystem, maintain fishery habitat and support human activities? To answer this question it is important to know the riparian vegetation water use (Goodrich et al., 1998) and study its interaction with the river flows.

Any changes to the nature of the interaction between the river and the riparian vegetation can cause changes to both river banks and the riparian vegetation structure along the river corridors in time and space (Hynes, 1975). In the Middle Rio River,

riparian vegetations was invaded by species harmful to the river system because the relationship between the river flow and riparian zone was altered and manipulated by further human interference (Chapter 2). Therefore it is very important to understand the connection between the river and the riparian vegetation at the same time has the ability to monitor both the riparian vegetation and groundwater. A relationship between the river flow and its direct effect on both the groundwater and riparian vegetation will very a very useful tool in the process of decision making (Goodrich et al., 1998).

METHODOLOGY

Study Area

The study area consisted of four different sections of the Middle Rio Grande River (MRGR) that represents the river from Cochiti Dam down to Elephant Butte Dam, New Mexico (NM). Forty percent of New Mexico's population lives along this 286 km long stretch of river.

The river flow is controlled by Cochiti Dam, from which water is released for municipal use, irrigation diversions, and to keep a sound river ecosystem (ideally) by maintaining river base flows. The river floodplain is bordered by two drains on each side. These drains serve the adjacent agricultural areas by collecting irrigation runoff water. Beyond the drains there is either irrigated agriculture or arid areas with natural vegetation which occupy most of New Mexico.

The main vegetation species along the riparian corridor are Cottonwood (*Populus deltoids*), Tamarisk (*Tamarix ramosissima*), Russian Olives (*Elaeagnus angustifolia*), and Coyote Willow (*Salix exigua*).

Forty-six borehole wells were distributed among the eddy covariance evapotranspiration flux tower sites and logged to measuring water table depth every half an hour. Figure 3.1 shows the reach of the MRGR that was studied and the location of the river flow gages and flux towers.



Figure 3.1 Analyzed river section of the MRGR, showing the location of river flow gages and flux towers

Water Table Modeling

Riparian vegetation depends on different sources of water. These sources are direct precipitation, river flooding, and subsurface water, subject to the depth to the water table. Weather data will be obtained from the towers distributed along four different section of the river. The water table modeling will be based on field data collected by the USGS, Middle Rio Grande Conservancy district (MRGCD), and Middle Rio Grande Bureau of Reclamation (MRGBOR). These data include soil maps, topography, river water levels, river flows, water diversions, return flows, water table measurements, and soil moisture.

Modeling water table along the riverbanks will be based on two cases. In the first case, the assumption is that the stream banks are not receiving any significant recharge from rain. The second case is for cases where rainfall occurs that has a significant recharging effect on the river and water table of both banks.

Water table modeling along the river in the riparian zone is based on the Dupuit-Forchheimer equation. Figures 3.2 and 3.3 show the equations and the parameters used in the equations with recharge, withdrawal, and no recharge cases. The Dupuit-Forchheimer equation is derived from Darcy's law as follows:

Darcy's law explains one-dimensional flow per unit width as:

$$q = -Kh(dh/dx) \quad (3.1)$$

where

q : Water Flux (m/hr)

Kh: Horizontal Hydraulic Conductivity (m/hr)

dh: Head difference (m)

dx: Distance (m)

At steady state, the rate of change of q with distance is zero, or

$$\frac{d}{dx} \left(-Kh \times \frac{dh}{dx} \right) = 0 \quad \text{OR} \quad \left(\frac{-Kh}{2} \right) \times \frac{d^2 h^2}{dx^2} = 0 \quad (3.2)$$

This implies that,

$$\frac{d^2 h^2}{dx^2} = 0$$

(3.3)

$$\int \frac{d^2 h^2}{dx^2} \Rightarrow h^2 = ax + b \quad (3.4)$$

where a and b are constants. Setting the boundary condition $h = h_0$ at $x = 0$, we can solve for b

$$b = h_0^2 \quad (3.5)$$

Differentiation of $h^2 = ax + b$ allows us to solve for a ,

$$a = 2h \frac{dh}{dx} \quad (3.6)$$

And from Darcy's law,

$$h \frac{dh}{dx} = -\frac{q}{K} \quad \text{By substitution} \quad (3.7)$$

$$h^2 = ho^2 - \frac{2qx}{K} \Rightarrow h = hl^2 - \frac{2ql}{K} \quad (3.8)$$

Rearranging the equation above results in:

$$q = \frac{K}{2l} (ho^2 - hl^2) \quad \text{Dupuit-Forchheimer Equation} \quad (3.9)$$

The general equation for the shape of the parabola is

$$h^2 = ho^2 - \frac{x}{l} (ho^2 - hl^2) \quad \text{Dupuit-Forchheimer Parabola} \quad (3.10)$$

where

h: water table level (m)

ho: Drain water level (m)

hl: River water level (m)

K: hydraulic Conductivity (m/hr)

l: distance between river and drain (m)

In order to use the Dupuit-Forchheimer equation, certain conditions should be met and assumptions must be made. The Dupuit-Forchheimer flow equation works with unconfined aquifers under steady state conditions. The assumptions made are:

- 1) The water table or free water surface is only slightly inclined
- 2) Streamlines may be considered horizontal and equipotential lines, vertical
- 3) Slopes of the free water surface and hydraulic gradient are equal

The steady state condition was assumed to prevail, because the hourly ET rate of Tamarisk or Cottonwood will not reach a level that could affect the steady state assumptions. In addition, the water flux is recharging the water table while the vegetation is using water for transpiration, maintaining similar water table levels or resulting in slow decreases.

The parameters necessary for the above equation will be either measured or calculated. Saturated hydraulic conductivity of the riparian zone will be obtained from the soil map available at 10 meter spatial resolution from the USGS.

The river will be divided into reaches according to data availability. The model calculations using the required inputs result in water table elevation along cross-sections between the river and the drains. These cross-sections are used to create a contour map of water table elevation for the river reach modeled. The accuracy of this contour map depends on how many water table depth readings from wells are used to produce it and the scale of spatial variables. The surface elevation used in the estimation of the depth to the water table is obtained from the DEM layer considering a standard reference level (mean sea level).

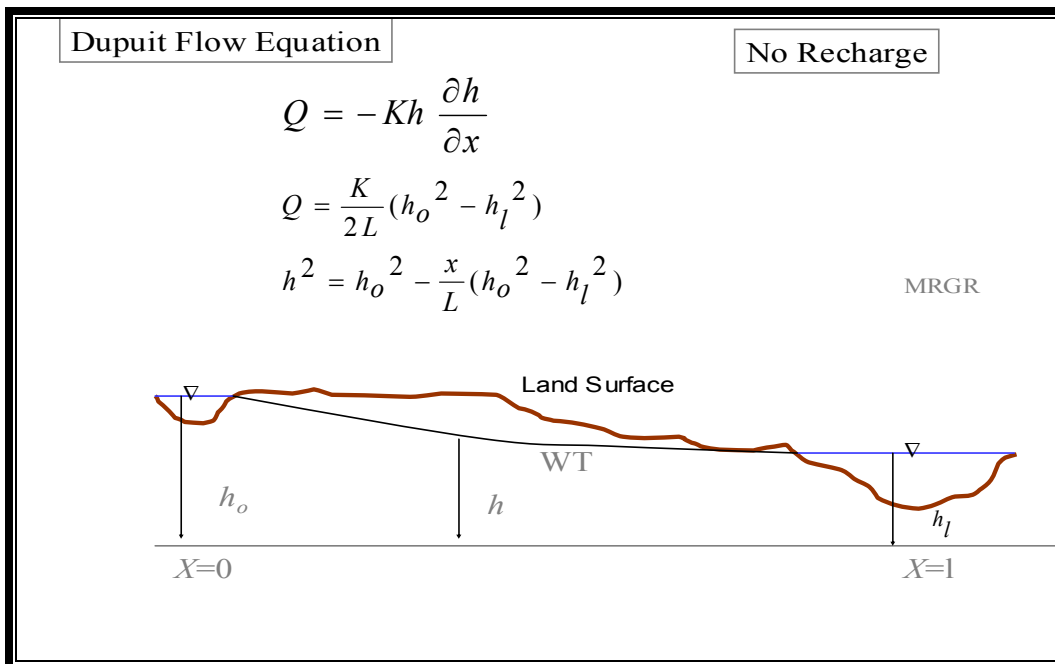


Figure 3.2 Dupuit-Forchheimer scheme and equation with no recharge

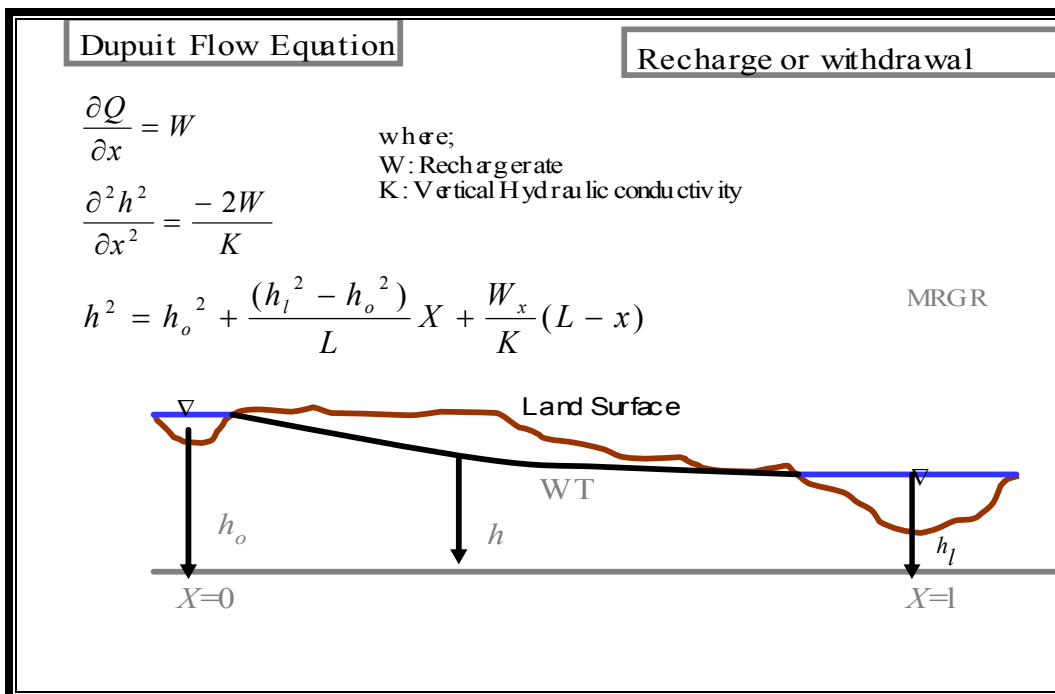


Figure 3.3 Dupuit-Forchheimer scheme and equation with recharge

Drain and River Water Levels

Water table readings from wells were used to estimate the water levels in both the drain and river using the Dupuit-Forchheimer equations applied to the cross-sections. A minimum of two water table readings at each cross-section location are required. The water levels can be achieved by substituting one unknown by another in the Dupuit-Forchheimer equation, which becomes:

$$h_1 = \left(h_o^2 - \frac{x_1}{l} \times (h_o^2 - h_l^2) \right)^{0.5} \quad (3.11)$$

$$h_2 = \left(h_o^2 - \frac{x_2}{l} \times (h_o^2 - h_l^2) \right)^{0.5} \quad (3.12)$$

Substitute h_l by h_0 , where h_0 is the drain water level and h_l is the river water level

$$h_l = \left(h_o^2 - (h_o^2 - h_l^2) \times \frac{l}{x_1} \right)^{0.5} \quad (3.13)$$

$$h_o = \left(\frac{h_2^2 + \frac{x_2}{x_1} \times h_1^2}{1 + \frac{x_2}{x_1}} \right)^{0.5} \quad (3.14)$$

where

h_1 : water table reading 1 (m)

h_2 : water table reading 2 (m)

h_l : river water level (m)

h_o : drain water level (m)

Stream flows and the geomorphology of the river are well connected; the stream width is an indication of frequent flooding and flow variation. The increased river width along with low flows creates a critical situation for fisheries and wild life. Therefore, the river course and water levels and flows in the river are very important factors.

The river flow for the different study sections on certain dates will be studied and compared with modeled water depths in the river and the water table status in the river banks.

Water Flux and Transmissivity

Groundwater recharge in the riparian corridor of the MRGR occurs through incoming water from either or both the river and parallel drains. Water flux occurs whenever head potential exist in a porous media. Head is the main factor that determines the flux quantity and direction. Figure 3.4 shows a top view describing possible flux flow directions in a section of the riparian zone. Other factors that determine flux magnitude are soil transmissivity (T) and distance.

Water flux is very hard to determine spatially because of the thousands of grids involved and the relationship among them vis-à-vis the variability in soil physical properties. Detailed soil properties are not usually known in such remote areas. Some properties necessary for flux estimation can be obtained from soil maps but do not satisfy the data quality required for the model. The method used in this paper was to estimate those properties by using monitored water table readings during night time when riparian vegetation ET is minimal. Water flux is represented by:

$$q = KD \frac{dh}{dx} \quad 3.15$$

where

q : Water flux (m^2/hr)

KD (T): Transmissivity (m^2/hr)

K : Horizontal Hydraulic conductivity (m/hr)

D : Aquifer depth (m)

To derive T (KD) from temporal water table readings

$$q = 2KD * \left[\frac{d(ho - h)}{x1} + \frac{d(hl - h)}{x2} \right] \quad (3.16)$$

$$KD = \frac{q}{2 * \left[\frac{d(ho - h)}{x1} + \frac{d(hl - h)}{x2} \right]} \quad (3.17)$$

where

$x1$: Distance between the drain to water table reading borehole (m)

$x2$: Distance between the river to water table reading borehole (m)

The above equations will be solved for both the aquifer depth and horizontal hydraulic conductivity and applied to different areas along the river using the night time water table variation to estimate the water flux or recharge during the period when the riparian vegetation has minimum ET. The water head at the drain and/or river will be estimated at the beginning of the night and during early morning (while ET is near zero) to isolate the water flux and estimate the aquifer transmissivity.

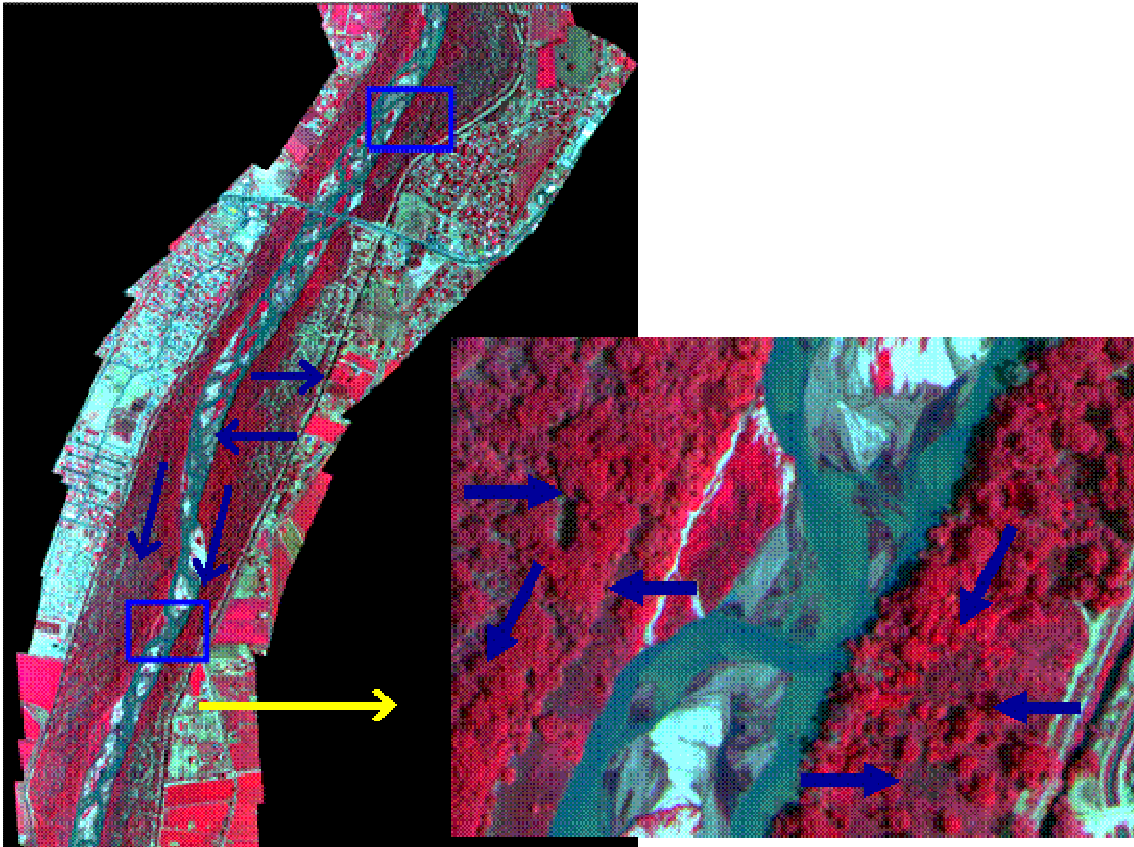


Figure 3.4 Multi-spectral image of a section of the Rio Grande river showing possible flux directions

Depth to Water Table

The groundwater table model will provide the estimated water table values to a standard reference from mean sea level. For the estimation of riparian vegetation ET, the depth to the water table is a more important variable in order to determine how close the plants roots are to the saturated zone or water source. The depth to water table will be obtained by subtracting the water elevation layer from the surface elevation using a digital elevation model (DEM) for the study areas with a 10 meter grid size resampled from 30 meter grids. The depth to water table will be used to estimate the soil water

potential and soil water content above the saturated zone and in the riparian vegetation root zone.

Soil Moisture Profile above the Saturated Zone

Soil moisture availability in the root zone is an influencing factor in the ET process. The soil water content is the main parameter used in the stomatal conductance model for estimating plant transpiration. The soil moisture above the saturated zone can be estimated if there is no surface recharge or when the recharge (infiltration) has ceased and a sufficient amount of time is allowed for water drainage and redistribution. As a result, water flow inside the soil profile will reduce to insignificant levels due to rapid reduction of hydraulic conductivity. The profile in this case is said to be in hydrostatic equilibrium. Figure 3.5 shows the equations and soil moisture profile that can be estimated under hydrostatic equilibrium. The soil water potential can be estimated from:

$$\frac{\partial \phi}{\partial z} = \frac{\partial \Psi}{\partial z} + 1 = 0 \quad (3.18)$$

Van Genuchten (1980) developed a method to obtain volumetric soil water content from soil water potential estimated from equation 3.18 as:

$$\theta = \theta_r + \frac{(\theta_s - \theta_r)}{(1 + (\alpha \psi_s)^n)^m} \quad (3.19)$$

where

α , n & m : Soil fitting parameters, where, $m = 1 - (1/n)$

θ : Soil water content

θ_r, θ_s Residual and Saturated soil water content respectively

Depth to water table is essential for estimating the soil water potential above the saturated zone and in the root zone. Soil surface water potential is an input in Van Genuchten (1980) soil moisture estimation above the saturated zone.

Evapotranspiration Estimation

Five flux towers were installed along the river at four different locations along the MRGR. The flux towers consisted of Campbell Scientific Inc. eddy covariance systems

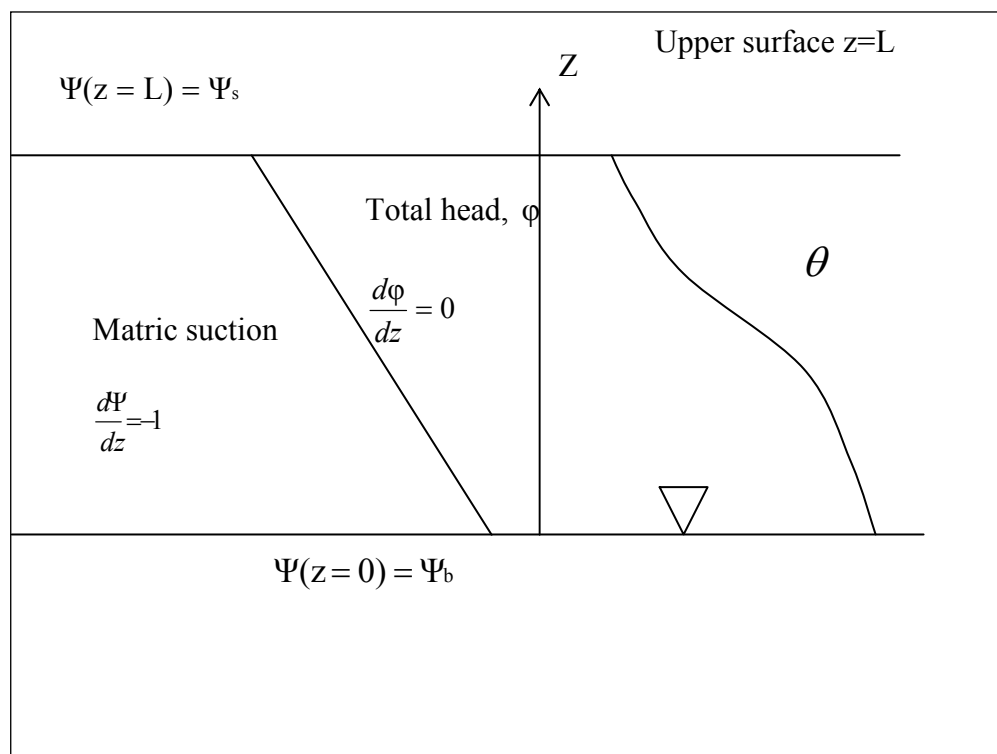


Figure 3.5 Soil moisture distribution above the saturated zone under hydrostatic equilibrium where ψ is matric suction, ϕ is total head and θ is the soil moisture content

with a 3D-sonic anemometer, a krypton hygrometer, net radiometer, four soil heat flux plates with soil temperature probes, and other meteorological instrumentation such as pyranometer, relative humidity probe, thermal infrared radiometers, etc. Two eddy covariance (EC) towers were installed at the Bosque del Apache, 600 meters apart, above a dense Tamarisk forest. The EC sensors were installed about 7.7 m above the ground. The Tamarisk trees at this location were approximately 4 m in height (Figure 3.6).

The towers were installed by the University of New Mexico except for the Bosque del Apache North tower which was installed by scientists from USDA-ARS, New Mexico State University and Utah State University. Negative values of sensible heat flux indicates advection situation. Hattori (2004) analyzed vertical profile of specific humidity and potential temperature in both Bosque del Apache and Albuquerque using radiosonde data collected over the river riparian canopy and the dry land near by the river banks. Hattori (2004) concluded that the air above the canopy is highly related to the surface in the morning and as the atmospheric boundary layer (ABL) keeps growing during the day the air above the canopy has similarity with the air above the dry land near the river banks. This observation led to the conclusion that the weather station near Bosque in the dry land is more representative to the air properties above the canopy when the ET peaks in the mid day. Therefore D_m was estimated from the humidity and air temperature values from the dry land weather station. Data collection and stations maintenance was done by researchers from University of New Mexico and Mexico State University.

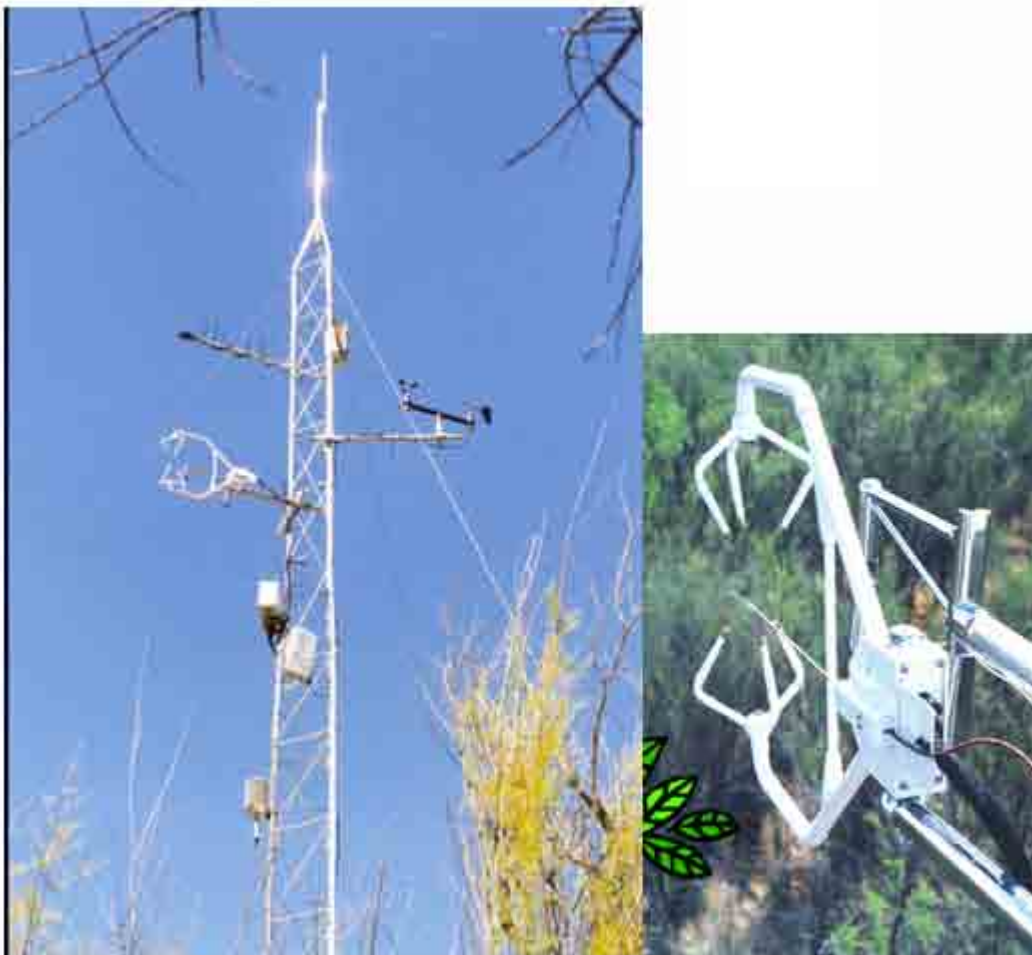


Figure 3.6 Eddy covariance flux Tower with a 3D-sonic anemometer, a krypton hygrometer, a net radiometer, and other meteorological equipment

Penman-Monteith Method

Monteith (1965) proposed modifications to the Penman equation:

$$ET = \frac{s(R_n - G)}{(s + \gamma(1 + \frac{r_c}{r_a}))} + \frac{\rho c_p (e_{sat(Ta)} - e_a)}{(s + \gamma(1 + \frac{r_c}{r_a}))r_a} \quad 3.20$$

where

R_n : Net radiation (W m^{-2})

G : Soil heat flux (W m^{-2})

s : slope of saturated vapor pressure vs. temp curve (Pa K^{-1})

γ : psychrometric constant (Pa K^{-1}) (a function of atmospheric pressure)

ρ : Density of air (kg.m^{-3})

c_p : Specific heat of air at constant pressure ($\text{W m}^{-2}.\text{C}^{-1}$)

r_a : aerodynamic resistance (sm^{-1})

r_c : bulk canopy resistance (sm^{-1})

e_{sat} saturated vapor pressure at air temperature (Pa)

e_a atmospheric vapor pressure (Pa)

This equation assumes the properties of air near the canopy surface and the saturation deficit of air is connected only to the surface below. This is not always the situation in the MRGR, because of the arid environment surrounding the riparian zone on both sides. These surrounding areas will influence the surface properties above the canopy and can increase the surface saturation deficit through advection of energy enhancing the ET rate. To solve this problem, McNaughton and Jarvis (1983) introduced a modification to the Penman-Monteith equation by adding an atmospheric boundary layer (ABL) coupling factor (Ω). This factor reflects the degree of coupling between the canopy surface and the air above it. The value of Ω theoretically ranges between 0-1, but in practice ranges from 0.2-0.8. The equation becomes:

$$ET = \Omega \frac{s}{s + \gamma} (R_n - G) + (1 - \Omega) \frac{\rho \cdot c_p \cdot D_m}{\gamma \cdot r_c} \quad 3.21$$

$$\Omega = \left(1 + \frac{\gamma}{s + \gamma} \times \frac{r_c}{r_a}\right)^{-1} \quad 3.22$$

where D_m is the saturated deficit in the mixed layer of the ABL (Pa).

When Ω equals 1 then the ET approaches the so-called equilibrium rate (ET_{eq}) and when Ω equals 0 then the canopy surface is totally coupled to the air above it and the saturated deficit of air becomes the driving force of ET leading to the so-called imposed ET ($ET_{imposed}$).

Determining Ω can be done either directly from r_a and r_c by using ET measurements and inverting above equation. Hattori (2004) analyzed radiosonde data above the Tamarisk canopy at the Bosque del Apache and compared it to radiosonde data above a nearby dry area. He detected the advection effect above the Tamarisk canopy and concluded that the D_m value could be estimated from a nearby weather station (Lat. $33^{\circ}48'15''N$ Long. $106^{\circ}52'36''W$) located in a dry area south of Bosque del Apache. The data required to estimate D_m (vapor pressure saturated deficit) are the air temperature and relative humidity.

The other data required for ET estimation will be obtained from two eddy covariance flux stations installed on towers above the canopy in Bosque del Apache. Data available are wind speed, canopy temperature, net radiation, sensible heat flux and latent heat flux which can be determined from the covariance between vertical wind speed and temperature. Hattori (2004) estimated the canopy resistance above the Tamarisk canopy by inverting Penman-Monteith and built a relationship between stomatal conductance

(estimated by Ball-Berry model) and canopy resistance. This relationship is embedded in the software provided.

Stomatal Conductance Models

In the Penman-Monteith empirical equation, the term r_c (canopy resistance) is the most complicated to estimate as many variables control stomatal behavior. There are many models proposed to compute stomatal conductance (g_s) using three different approaches. The first approach uses multiplicative algorithms that adjust a reference value according to changes in environmental variables. The second approach links g_s to transpiration. The third method scales g_s to photosynthesis. One of the more popular models used by many researchers was developed by Jarvis (1976), relating the stomatal conductance to five variables. Those variables are photon flux density, leaf temperature, vapor pressure deficit, leaf water potential (turgid pressure) and ambient CO₂ concentration.

$$g_s(Q_p, T, \delta e, \Psi_l, C_a) = g_s(Q_p) \cdot g_s(T) \cdot g_s(\delta e) \cdot g_s(\Psi_l) \cdot g_s(C_a) \quad 3.23$$

where

g_s : stomatal conductance.

Q_p : Photon flux density (incoming Solar radiation)

T : Leaf temperature

δe : vapor pressure difference.

Ψ_l : leaf water potential

Hattori (2004) used the Ball-Berry model to estimate stomatal conductance specifically for Tamarisk. This model links stomatal conductance to leaf photosynthesis, humidity deficits and CO₂ concentration at the leaf's surface (C_s).

$$g_s = (m.A.rh / C_s) + g_0 \quad 3.24$$

where

m: dimensionless slope coefficient

rh: is relative humidity at the leaf surface

g₀: is zero intercept (mol.m⁻²s⁻¹)

A: leaf photosynthesis (μmol m⁻² s⁻¹)

The Ball-Berry model was modified by Leuning (1995) arguing that relative humidity is not a valid independent variable, as plants should respond to a potential that drives water loss, such as a vapor pressure difference. He modified the equation as:

$$g_s = \{(\alpha A / [C_s - \Gamma]) * (1 + D_s / D_0)\} + g_0 \quad 3.25$$

where

α and D₀: are empirical coefficients

Γ: CO₂ compensation point (μl l⁻¹)

D_s: vapor pressure deficit (kPa)

The Ball-Berry approach will be used in this modeling effort to estimate stomatal conductance for Tamarisk. The main assumptions enabling the use of the Ball-Berry model are (1) that the plants don't accumulate water inside when they are in steady state

condition; therefore the water flux from the soil through the plant and into atmosphere should match; and (2) the soil hydraulic conductivity is constant over the root surface, but as soil water content gets smaller this assumption gets violated (Caldwell, 1976).

Hattori (2004) estimated four plant physiological parameters for Tamarisk needed in Ball-Berry stomatal conductance model. Those parameters are the slope constant m , the Ball-Berry intercept constant b , the convexity parameter θ_c and the maximal carboxylation rate of the leaf per unit area at reference temperature $V_{c,max(T_{ref})}$ in estimation of net CO_2 assimilation rate.

The model written by Hattori (2004) in FORTRAN was transformed to Visual Basic 6 (VB6) and customized to work in the ArcGIS environment so it can be applied spatially. The soil water content and soil water potential will be obtained by the method described previously.

Depth to water table is very important for soil water potential estimation in the root zone. Soil water potential is one of the variables that affect stomatal conductance. In Ball Berry model the soil water potential is used to estimate the water flux from the soil through the plant and through the plants into atmosphere (J_w) which in turn determines the abscisic acid in the xylem sap. The detailed list of equations and the Ball-Berry stomatal model equations can be found in Hattori (2004).

Canopy Minus Air Temperature ($T_c - T_a$) ET Estimation Method

Nagler et al. (2003) developed relationships between sap flow rate for Tamarisk, Coyote Willow and Cottonwood with net radiation, canopy temperature and air temperature. They estimated daily ET and compared it to measured ET. These relationships were developed in Tucson, Arizona in the year 2000.

The relationships built are;

$$ET_{(Cottonwood)} = 0.819Rn - 2.77(Tc - Ta) - 7.91, \quad 3.26$$

$$ET_{(Willow)} = 0.772Rn - 1.24(Tc - Ta) - 7.96, \quad \text{and} \quad 3.27$$

$$ET_{(Tamarisk)} = 0.674Rn - 1.56(Tc - Ta) - 6.34 \quad 3.28$$

These relationships will be used to estimate daily and hourly ET along the Middle Rio Grande River for Tamarisk, Coyote Willow and Cottonwood. The ET results obtained by these relations will be compared to latent heat flux ET measurement for the four different study areas. Another comparison will be conducted between the Tamarisk ET results obtained from this method and the modified Penman-Monteith method (using the Ball-Berry stomatal conductance model). The reason for using the models by Nagler et al. (2003) is that the physiological parameters needed for the Ball-Berry approach are not available in the literature for all the main riparian vegetation species (Cottonwood, Coyote Willow and Tamarisk) in this study.

Hattori (2004) optimized those physiological parameters for Tamarisk using measured ET values from previous year (1999) in Bosque del Apache by inverting the Penman-Monteith equation and solving for canopy resistance and other physiological parameters. These data are not available in other locations where Cottonwood and Coyote Willow are dominant.

The main justification for using these simplified models is data availability. Those models can be altered and modified in the software by editing a configuration file (ini) associated with the dll. This configuration file has all the physiological variables optimized by Hattori (2004) and can be edited for Tamarisk and created for Cottonwood once those variables are available from future research. This configuration file also

contains all the canopy temperature method equations which can also be edited according to location and vegetation type.

RESULTS AND DISCUSSION

ArcGIS Groundwater Table Model General Description

The groundwater model was developed using Microsoft Visual Studio VB6 in an ArcGIS environment. Processing spatial data in ArcGIS requires special programs. For this purpose an extension to ArcGIS using Microsoft Visual Basic and ArcGIS Software Developer Kit (SDK) was created through a DLL that can be added as an extension to ArcGIS.

The model was designed to utilize water table readings (point data) with known geographical coordinates along with a spatial land use vegetation map for the area and a digital elevation model (DEM) layer. The model gives an output of water table elevation above mean sea level between the boundary conditions (riparian zone). The number of estimated water table points depends on the interval specified in the model interface. The water table output needs to be processed in ArcGIS project to create a raster layer. In ArcGIS the 3D Analyst is used to create surface raster layer. The created surface raster layer of water table elevations from mean seal level and the DEM will be used to calculate depth to water table by subtracting the water table elevation from the DEM using spatial analyst raster calculator. The depth to water table (depth of water table from land surface) is used to estimate soil water potential in the root zone of the riparian vegetation in the evapotranspiration model.

Another output from the groundwater table model is an estimation of water flux. Water moves from one grid to another and moves from an irrigation drain or the river toward or through the riparian zone. This model will quantify this movement taking into consideration the soil physical properties (soil transmissivity; horizontal hydraulic conductivity multiplied by aquifer depth) and the water head difference as the driving force. The input and output of this model will be discussed in detail in a later section.

ArcGIS Evapotranspiration Model General Description

This model estimates evapotranspiration for the riparian vegetation using the modified Penman-Monteith equation. This model is an adoption of a point based model developed by Hattori (2004). The groundwater model output is used as an input to this model, specifically the soil water potential and the depth to the water table. The water flux is used to consider the recharge that occurs during the day and night while the vegetation is drawing from the water table through the evapotranspiration process. The water flux is added to the water table as recharge through time (depending on head difference) and updates the status of the water table for a better water potential estimation while the water used by evapotranspiration is removed from soil matrix above the water table and the water table itself.

The evapotranspiration model is designed to utilize the spatial variability of both land use (mainly different riparian vegetation species) and water potential in the root zone. The model offers a framework for estimating ET for any riparian vegetation as long as some parameters are known for the stomatal conductance Ball-Berry model which is embedded inside, as described in the methodology section. The modified Penman

Monteith equation was used to address advection conditions that prevail in this part of New Mexico where the atmospheric coupling factor plays a major role in ET estimation.

Groundwater Model Interface and Inputs

The ArcGIS environment is a result of information technology advances. Spatial data associated with spatial coverage set a new limit to what we can analyze and study. This groundwater model was developed in ArcGIS environment using water table readings across the riparian zone. The goal of this model is to use measured water table data at different locations to develop a depth to water table surface layer for the riparian zone.

Figure 3.7 shows the water table model interface with all the inputs needed as well as the anticipated output. The water table model inputs are: water table reading event data base file which represents sets of at least two borehole readings on a certain date and time along with their geographical coordinates (Figure 3.8). The water table database contains the boundary conditions which in this case of this study are the river and the drain center points (Figure 3.9). The interval window allows us to specify the distance interval in which the model will estimate water table along the boundary conditions.

Horizontal hydraulic conductivity, aquifer depth and pixel or grid size are all used to estimate water flux. In order to include the downstream flux, the box assigned for the flux must be checked. In the case of limited availability of water table data, only a small water table layer section can be created, and the first cross-section upstream resulting from the model will not have any incoming water flux and the last cross-section downstream will not have an outgoing flux. Therefore it is better to assume that the

downstream flux is equal to zero (incoming flux is equal to outgoing flux from every water table cross-section resulted from the model) and not to include downstream fluxes to avoid misleading results. The reason for including this option in the modeling is to avoid errors when data is limited or noncontinuous.

In case of recharge from flooding or a significant rainfall event, the vertical recharge box can be checked to apply the Dupuit-Forchheimer equation with a recharge factor (Figure 3.3 in methodology section). In this case, both a horizontal hydraulic conductivity and recharge rate are required. In the last four windows the starting and ending date and time can be entered for the water table simulation period.

The model requires at least two well readings to be able to produce water table cross-section along the riparian zone between the river center and the drain. Figure 3.8 shows part of the input data for two wells for one day, divided into hourly time periods over 24 hours. The geographical coordinates and elevations of the wells are also shown, and the depth to water table is in negative value which when added to the land surface elevation at that point will result in the water table elevation referenced to the mean seal level. Figure 3.9 shows the well locations (yellow triangles) in the riparian zone of the Bosque del Apache site.

Water Table and ET Models

Water Table ET ET Results

Water Table

Feature Layer of Observations: Interval(m): Hor Hyd Conductivity(m/d):

Aquifer Depth(m): Pixel Size(m): Output shapefile: Reference Height:

Select Output Directory: -->

Vert Charge/Discharge Add shapefile to map's TOC
 Vert Hyd Conductivity (m/d): Discharge/Charge(m/d): Overwrite Without Warning

Starting DOY: Ending DOY: Start Time: End Time: Include Down Stream Flux

ID	Xi	Yi	WTi	FLUXi	X

Figure 3.7 Groundwater model interface

Attributes of shkall1 Events																		
OID	READING	DOY	T_OF_DAY	E	H	Z	WT1	E_1	H_1	Z_1	WT2	CAHALE	CAHALH	CAHALZ	RIVERE	RIVERH	RIVERZ	
0	SHKWC	121	100	346310	3869774	1494.74	-118	346351	3869763	1494.74	-160	346501	3869776	1494.74	346129	3869771	1492	
1	SHKWC	121	200	346310	3869774	1494.74	-117	346351	3869763	1494.74	-160	346501	3869776	1494.74	346129	3869771	1492	
2	SHKWC	121	300	346310	3869774	1494.74	-117	346351	3869763	1494.74	-160	346501	3869776	1494.74	346129	3869771	1492	
3	SHKWC	121	400	346310	3869774	1494.74	-117	346351	3869763	1494.74	-160	346501	3869776	1494.74	346129	3869771	1492	
4	SHKWC	121	500	346310	3869774	1494.74	-117	346351	3869763	1494.74	-160	346501	3869776	1494.74	346129	3869771	1492	
5	SHKWC	121	600	346310	3869774	1494.74	-117	346351	3869763	1494.74	-159	346501	3869776	1494.74	346129	3869771	1492	
6	SHKWC	121	700	346310	3869774	1494.74	-117	346351	3869763	1494.74	-159	346501	3869776	1494.74	346129	3869771	1492	
7	SHKWC	121	800	346310	3869774	1494.74	-117	346351	3869763	1494.74	-159	346501	3869776	1494.74	346129	3869771	1492	
8	SHKWC	121	900	346310	3869774	1494.74	-117	346351	3869763	1494.74	-159	346501	3869776	1494.74	346129	3869771	1492	
9	SHKWC	121	1000	346310	3869774	1494.74	-117	346351	3869763	1494.74	-160	346501	3869776	1494.74	346129	3869771	1492	
10	SHKWC	121	1100	346310	3869774	1494.74	-118	346351	3869763	1494.74	-160	346501	3869776	1494.74	346129	3869771	1492	
11	SHKWC	121	1200	346310	3869774	1494.74	-118	346351	3869763	1494.74	-161	346501	3869776	1494.74	346129	3869771	1492	
12	SHKWC	121	1300	346310	3869774	1494.74	-119	346351	3869763	1494.74	-161	346501	3869776	1494.74	346129	3869771	1492	
13	SHKWC	121	1400	346310	3869774	1494.74	-119	346351	3869763	1494.74	-162	346501	3869776	1494.74	346129	3869771	1492	
14	SHKWC	121	1500	346310	3869774	1494.74	-119	346351	3869763	1494.74	-162	346501	3869776	1494.74	346129	3869771	1492	
15	SHKWC	121	1600	346310	3869774	1494.74	-120	346351	3869763	1494.74	-162	346501	3869776	1494.74	346129	3869771	1492	
16	SHKWC	121	1700	346310	3869774	1494.74	-120	346351	3869763	1494.74	-162	346501	3869776	1494.74	346129	3869771	1492	
17	SHKWC	121	1800	346310	3869774	1494.74	-120	346351	3869763	1494.74	-162	346501	3869776	1494.74	346129	3869771	1492	
18	SHKWC	121	1900	346310	3869774	1494.74	-120	346351	3869763	1494.74	-162	346501	3869776	1494.74	346129	3869771	1492	
19	SHKWC	121	2000	346310	3869774	1494.74	-119	346351	3869763	1494.74	-162	346501	3869776	1494.74	346129	3869771	1492	
20	SHKWC	121	2100	346310	3869774	1494.74	-119	346351	3869763	1494.74	-162	346501	3869776	1494.74	346129	3869771	1492	
21	SHKWC	121	2200	346310	3869774	1494.74	-119	346351	3869763	1494.74	-162	346501	3869776	1494.74	346129	3869771	1492	
22	SHKWC	121	2300	346310	3869774	1494.74	-119	346351	3869763	1494.74	-161	346501	3869776	1494.74	346129	3869771	1492	
23	SHKWC	121	2400	346310	3869774	1494.74	-119	346351	3869763	1494.74	-161	346501	3869776	1494.74	346129	3869771	1492	

Figure 3.8 Example of the water table model input data base table

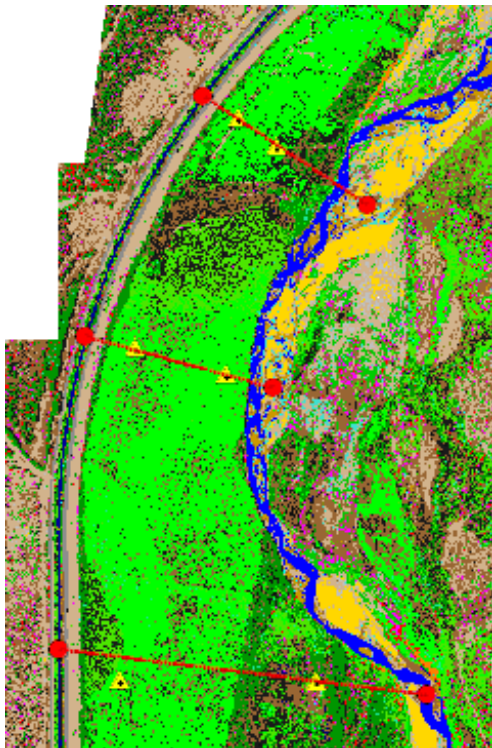


Figure 3.9 Boundary conditions (red circles), water table wells (yellow triangle) locations and groundwater model initial output (red squares) in Bosque del Apache area

Evapotranspiration Model Interface and Inputs

The spatial land use layer obtained from the multi-spectral image classification which contains estimates for Tamarisk and other riparian species is interfaced with the groundwater model through the depth to water table and flux in order to update water table elevation status after considering the evapotranspiration fluxes. The water table level is updated hourly and used as input for the estimation of ET in the next hourly time step. Figure 3.10 shows the evapotranspiration model interface with all the inputs needed as well as the anticipated output. The model inputs are; a vegetation map, climate data, soil physical properties, depth to water table and flux feature layers. The starting and ending day of year and time can be entered for the modeling period. Figure 3.11 shows a pop-up window that appears after clicking the select window on the land use code line. This allows the user to select the classes for which the ET estimation will be applied.

The model can be run with different settings, in order to produce cumulative daily ET or hourly ET values. These options can be selected by checking the appropriate boxes in the lower part of the interface (Figure 3.10). To by-pass the spatial depth to water table option in the case a DEM layer is not available, the model allows using a depth to water table reading that can be added to the climate data base input file. This will produce one value for ET for the selected land use classes and apply it spatially whenever that class exists in the land use map. Figure 3.12 shows a sample of the input data base file. Most of the variables in this table will be used in the modified Penman-Monteith equation. The water table column will be used in case there is no DEM available. The modified Penman Monteith approach can be applied on Cottonwood once the physiological parameters are determined and entered in the configuration file (ini).

Water Table and ET Models

Water Table **ET** ET Results

Land Use Shape File: Land Use Field:

Depth To Water Table: Depth To WT Field: Flux Field:

Input ET DBF File:
 -->

Select Output Directory:
 -->

Weather Station

Latitude:	Longitude:	Meridian Zone:
<input type="text" value="33.4815"/>	<input type="text" value="106.5236"/>	<input type="text" value="105"/>

Starting DOY: Ending DOY: Start Time: End Time:

Soil Bulk Density: Soil Particle Density: Output grid prefix: Point ID:

Land use code where the model applies:

Add All output to TOC Add Daily ET To TOC
 Use PM for Tamarisk Use PM for Cottonwood
 Use Water Table Reading Overwrite Without Warning

Water Table Init Value m: Flux Init Value m/hour:

Figure 3.10 Evapotranspiration model interface

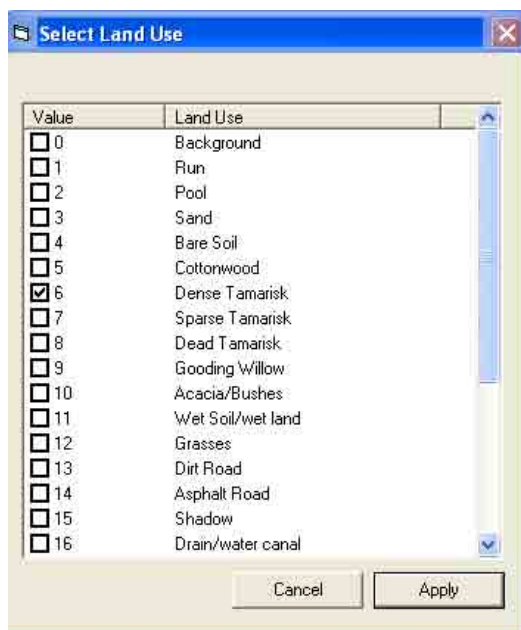


Figure 3.11 Interface for selecting land use classes for ET estimation (pops up when clicking on the select bottom adjacent to “land use code window”) (select the class by checking the small box)

	A	B	C	D	E	F	G	H	I	J	K	L	M
1	ID	DOY	T_OF_DAY	TEMP_AVG	SOL_ENG	RAIN	WIND	RH	SOIL_T	NET_RAD	TEMP_CAN	WT	FLUX
2	31	121	100	55.7	-39	0	1.93	30.5	57.4	-88	55.9	113	0.00
3	31	121	200	53.9	-35	0	3.12	34.3	57.2	-83	52.7	113	0.00
4	31	121	300	50.5	-36	0	1.94	41.6	56.7	-83	49.5	112	0.00
5	31	121	400	48.5	-30	0	2.33	43.7	56.1	-77	47.7	112	0.00
6	31	121	500	47.6	-30	0	1.17	45.5	55.9	-77	46.3	112	0.00
7	31	121	600	46.0	-32	0	2.30	57.1	55.3	-75	45.2	112	0.00
8	31	121	700	44.6	9	0	1.53	63.7	55.0	-40	44.6	112	0.00
9	31	121	800	49.4	130	0	0.67	56.3	53.7	107	49.9	112	0.00
10	31	121	900	55.7	397	0	0.90	46.1	52.2	299	56.5	112	0.00
11	31	121	1000	65.4	617	0	0.75	26.6	50.6	468	66.8	112	0.00
12	31	121	1100	71.4	818	0	1.42	17.8	50.9	623	72.4	112	0.00
13	31	121	1200	76.3	958	0	0.95	13.5	51.2	730	78.0	113	0.00
14	31	121	1300	79.8	1010	0	1.96	12.0	52.8	772	81.7	113	0.00
15	31	121	1400	82.0	1008	0	2.96	11.1	55.5	766	83.3	113	0.00
16	31	121	1500	84.1	942	0	6.53	8.7	55.7	699	85.6	113	0.00
17	31	121	1600	84.9	812	0	5.76	9.0	56.9	581	86.6	113	0.00
18	31	121	1700	85.0	610	0	5.76	8.7	58.1	415	86.9	114	0.00
19	31	121	1800	84.8	408	0	5.92	8.9	58.2	223	86.7	114	0.00
20	31	121	1900	83.6	126	0	5.15	9.2	58.3	34	85.2	113	0.00
21	31	121	2000	80.2	8	0	2.81	10.5	59.1	-107	80.5	113	0.00
22	31	121	2100	75.9	-110	0	1.48	12.2	60.2	-102	75.2	113	0.00
23	31	121	2200	70.1	-42	0	3.27	14.5	59.5	-100	70.7	112	0.00
24	31	121	2300	64.3	-39	0	3.71	21.4	58.7	-92	63.6	112	0.00
25	31	121	2400	66.9	-35	0	1.13	20.0	58.6	-90	64.7	112	0.00

Figure 3.12 Example of the ET module input data base table

GROUNDWATER MODEL OUTPUT

Groundwater Surface Creation in ArcGIS

The groundwater model produces a cross-section of water table and water fluxes estimated within the time and space interval specified. The resulting cross-sections can be used to produce a water surface raster layer in ArcGIS. A number of tools can be used to interpolate the water table points and produce a surface raster layer. In this study, the nearest neighbourhood scheme was used. The resulting water surface raster layer contains water table elevation from mean sea level. It is very important to set a reference level to standardize the data and help in further analysis.

Figure 3.9 from the previous section shows an example of cross-sections for which water table elevations were produced by the model along the boundary conditions in the Bosque del Apache area, where Tamarisk is the predominant vegetation.

Figure 3.13 shows the ArcGIS interpolated water table raster layer for the same location. The water table elevation is low if light blue and dark blue if high (referenced to mean sea level). As expected, the water head is decreasing in the downstream direction. Subtracting the water head shown in Figure 3.13 along the riparian zone from the DEM layer we can obtain the depth to water table layer which is important for soil water potential estimation.

Figure 3.14 shows the water table flux gain in the image. The head in the upper northeast corner is the highest, so water flux moves from the river (higher head) towards the drain (lower head) through the riparian zone; also moving in the downstream direction according to the head difference which is higher between the upper north part and the middle of the image. The flux movement slows down in the southern part of the

image due to a lower head difference between the middle of the image and south west part.

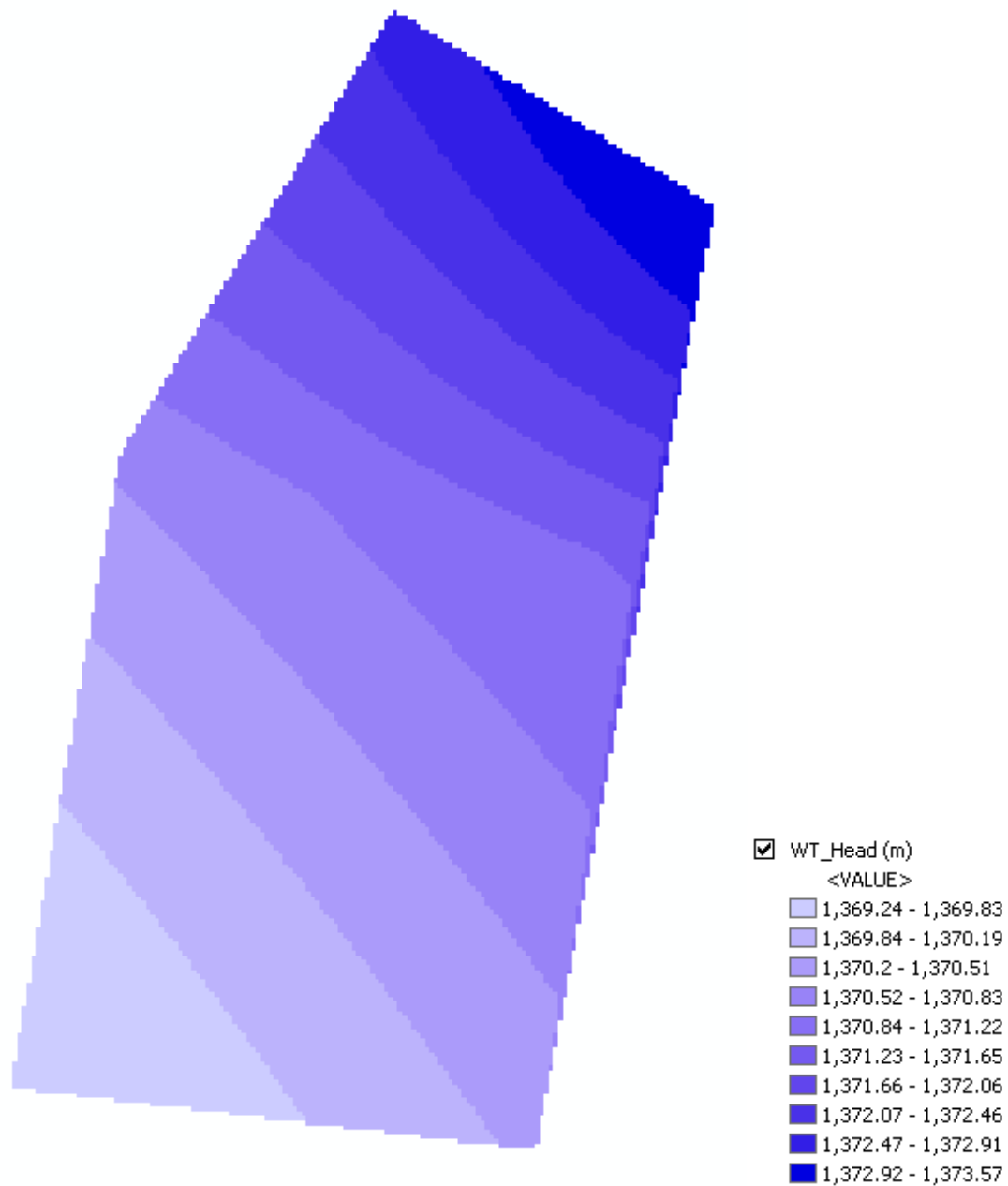


Figure 3.13 Water table raster layer created in ArcGIS for Feb. 22, 2003 at 12 pm

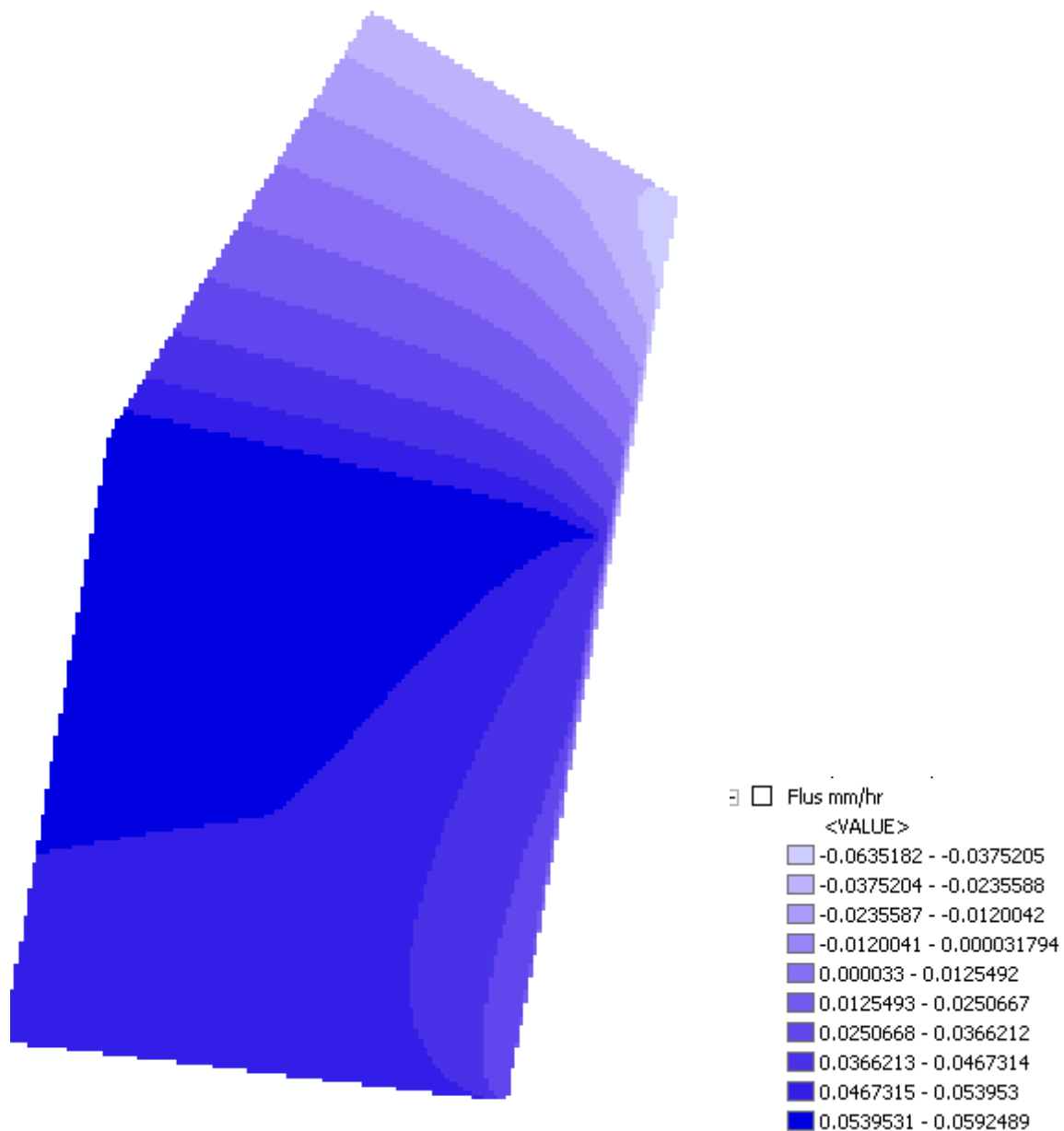


Figure 3.14 Water Flux (m/hr) including downstream flux in Bosque Del Apache area,

Feb. 22, 2003 at 12 pm

Water flux is estimated according to aquifer transmissivity and the water head at every grid, resulting from the groundwater model. The model has the ability to estimate the water flux in the downstream direction in addition to the flux that is coming from either the river or the drain or both. This model considers the head at each grid cell and determines the flow direction according to the head difference between every grid.

Figure 3.15 shows the water table cross-section above mean sea level (AMSL) along the riparian zone. This Figure shows that at Bosque del Apache, the river is losing water to the riparian zone and the drain as the water head at the river is highest. Figure 3.16 shows the depth to water table, where negative water depths mean that water level is above the land surface.

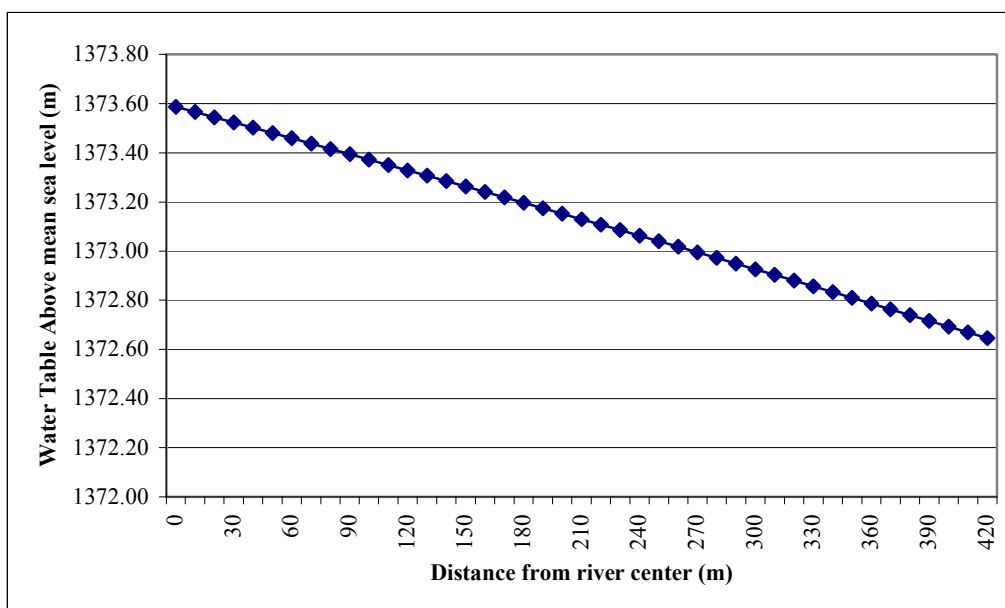


Figure 3.15 Water table cross-sections along the Bosque del Apache riparian zone, February 22, 2003

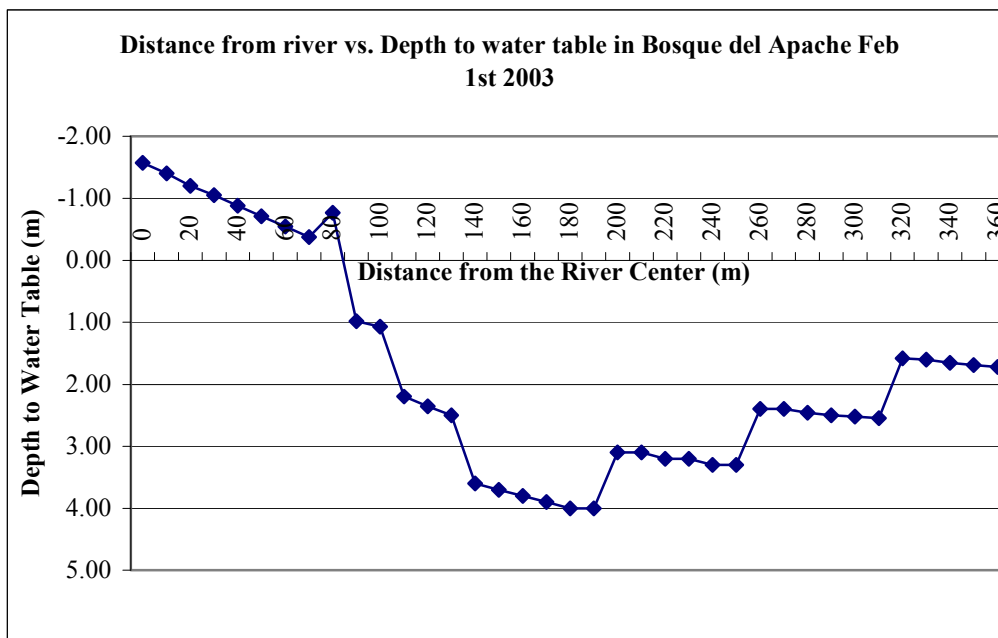


Figure 3.16 Depth to water table at the Bosque del Apache, Feb 1, 2003

The DEM was used to find the depth to water table by deducting the water table AMSL results from the land surface elevation AMSL. The drops and jumps in Figure 3.16 are the result of including the land surface terrain in DEM form as the reference to water table (depth to water table). The depth to water table varies between above surface at -2 (the river) to 4 m below the land surface in some other spots.

Depth to Water Table Estimation

The modeled water table layer is used for the estimation of the soil moisture potential in the root zone. The soil moisture potential is one of the main parameters in the Ball-Berry model used in estimating stomatal conductance for Tamarisk or other riparian vegetation. The required input for the soil water potential calculation is the depth to water table, so the digital elevation model (DEM) must be utilized in this case to arrive at this

depth. Figure 3.17 shows a DEM used in Bosque del Apache and its associated legend. The ArcGIS raster calculator was used to find the depth to water table; both DEM and water table raster input layers must be compatible with the same grid size (in this case 10 m) to perform the raster calculation. Figure 3.18 shows the resulting depth to water table at the Bosque del Apache for a modeled period in February 1, 2003. Darker colors mean that the water table is further from land surface and brighter colors describe a closer water table to the land surface.

The importance of using the DEM is clear since it helps determine how close the water table is to the vegetation on the surface and whether water is readily available for ET or not within the root zone of the vegetation. According to Figure 3.18, water appears at the surface in the river (negative values) and depth to water table increases with distance away from the river. The deep spot in the bright area is where the depth to water table is highest and is consistent with the DEM image which shows that the land surface has a high spot at that location.

If more water table readings along the river and higher resolution DEM's are available this will lead to a more accurate water table surface estimation, resulting in a better estimation of depth to water table.

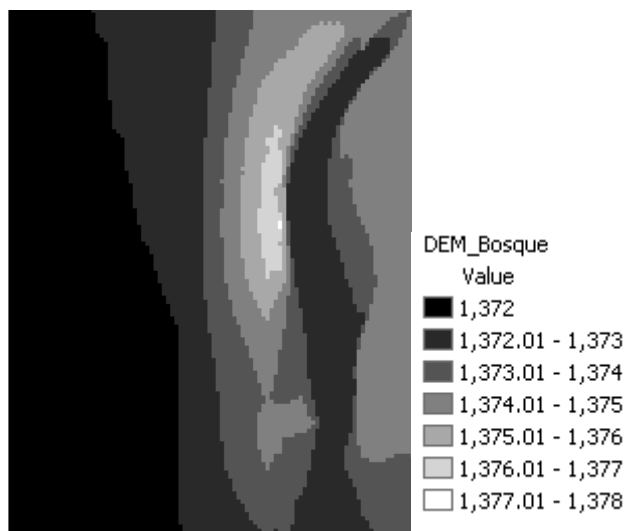


Figure 3.17 USGS 10-meter resolution DEM of the Bosque del Apache area

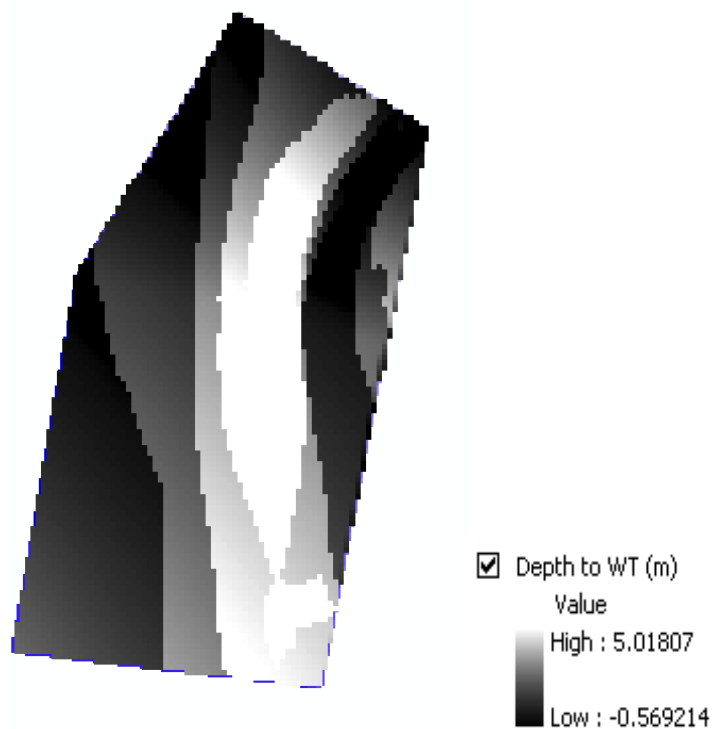


Figure 3.18 Depth to water table layer (meters) on Feb 22, 2003 at Bosque del Apache

Water Table Variation in Space and Time

Typical groundwater model calculated outputs of cross-section and depth to water table are plotted in Figures 3.19 and 3.20, 3.21, and 3.22 for two locations in the Albuquerque and Belen areas, respectively on DOY 168, 2003. Figures 3.19 and 3.21 show that in the morning, the water level is higher and closer to the surface. As the day progresses, evapotranspiration by vegetation reduces the water table levels. During the night, when ET decreases or ceases altogether, the water table level recovers due to recharge from the river and/or the drain. Figure 3.19 shows that the river is losing water to the riparian zone by a small amount due to the small water head difference about 0.32 m between the river center and the 340 meter long riparian section. Figure 3.21 shows that the drain is losing water to the river via the riparian zone. Figures 3.20 and 3.22 show the depth to water table along the riparian zone starting from the river center and ending at the drain center. The topography of the river and the riparian zone is observable in those figures as a jump occurs due to the presence of the river banks.

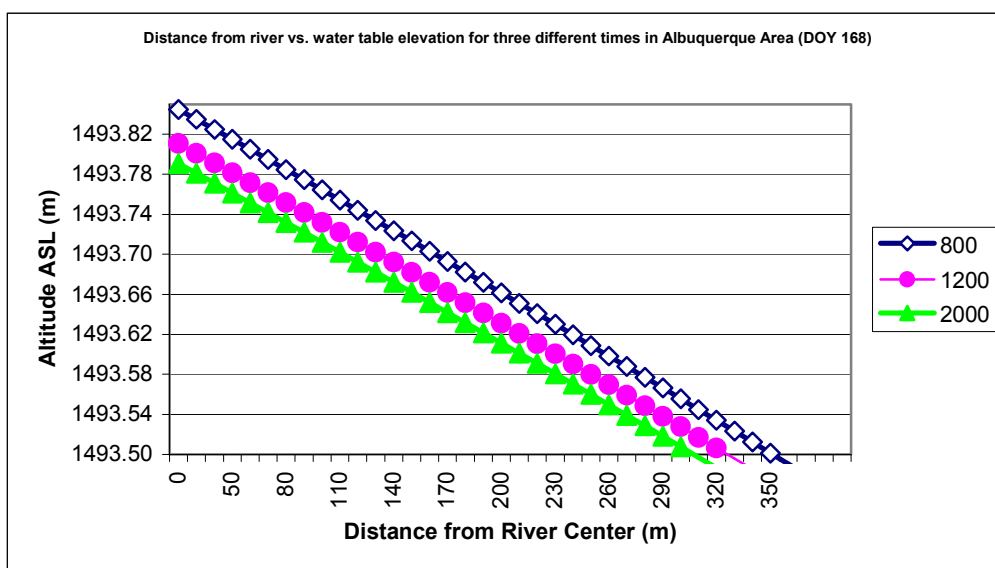


Figure 3.19 Water table elevation for a modeled cross-section in the Albuquerque area

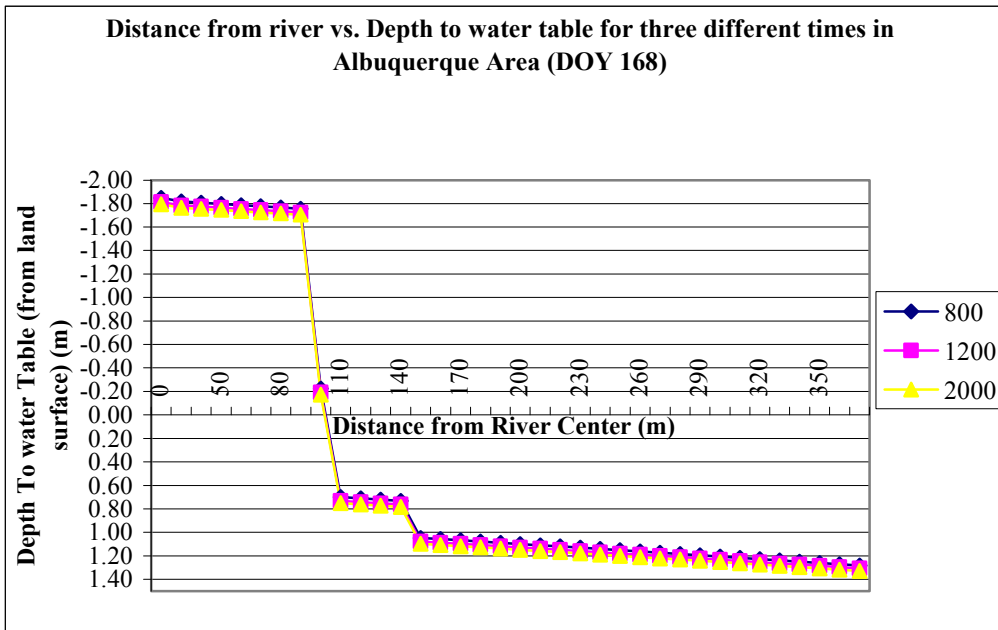


Figure 3.20 Depth to water table for a cross-section in Albuquerque area (zero distance at the river center)

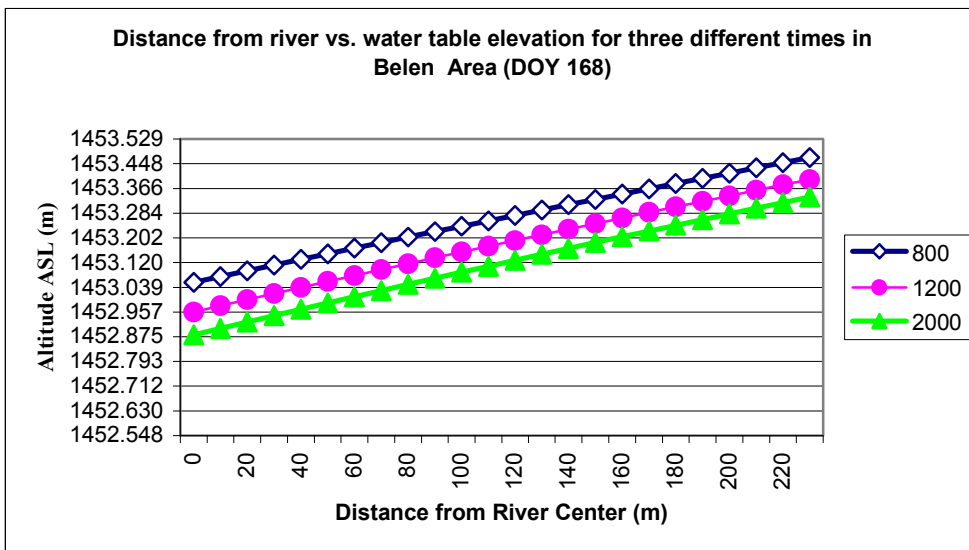


Figure 3.21 Modeled water table elevation cross-section in the Belen area

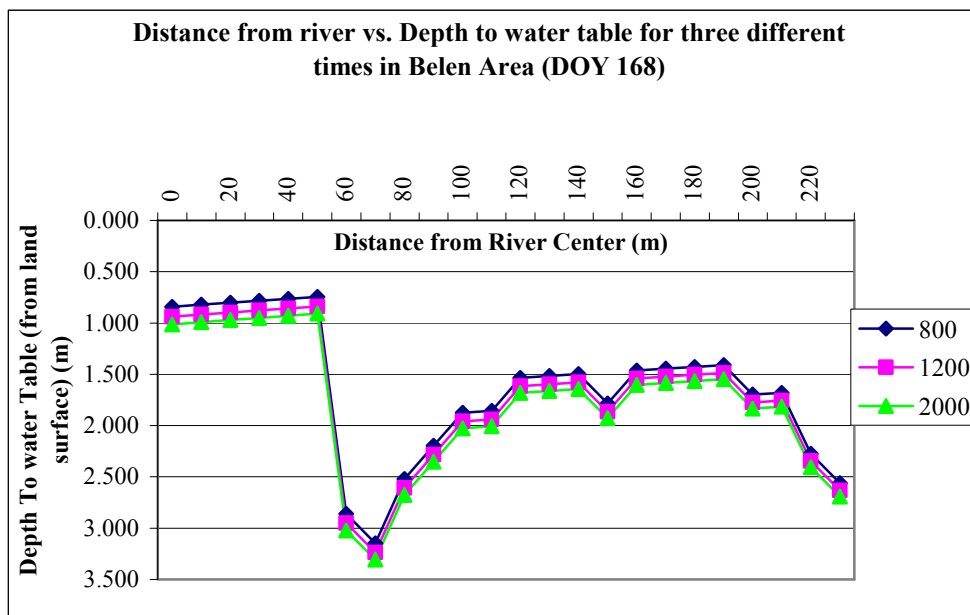


Figure 3.22 Depth to water table cross-section in the Belen area (zero distance at the river center)

Model Validation

Model outputs were checked against water table readings not used in the model as a form of validation. Model validation was done through space and time. Figure 3.23 shows the predicted values for two locations at the Albuquerque and Belen areas at different times plotted against water table readings. Six times were selected during July 1, 2001, four hours apart starting at 2:00 AM. The relationship was good with a high R^2 ; 0.98, but a consistent, systematic bias was detected that might be attributed to a reference problem. Despite the bias, this was good result in general and indicates that this model can produce estimates of water table elevation. Table 3.1 shows the geographical locations of all wells used in the validation process. Three wells are located in each area, two were used in the model and the third used for validation against the resulting values.

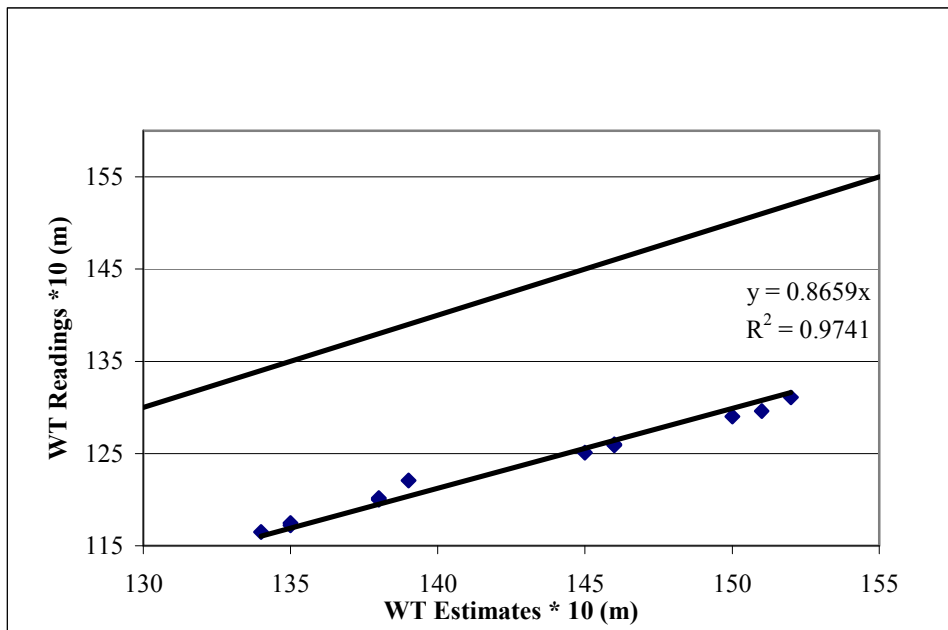


Figure 3.23 Groundwater model validations at the Albuquerque and Belen areas

Table 3.1 Well location and names used in the validation

Location	Easting	Northing	Distance (m)**
Albuquerque South*	346341	3869727	0
Albuquerque West	346310	3869774	56.3
Albuquerque Center	346351	3869763	37.4
Belen South	339570	3828945	40.5
Belen West	339543	3828988	41.3
Belen Center*	339584	3828983	0

* Reading used to validate the model estimated value

**Distance from the reading that was used in the validation

Stream Flow vs. Water Table and River Water Level

The connection between river water flow rate and water table levels in river banks help understand the hydrological connection between the river and riparian vegetation and can be important as a management tool that can be used by decision makers.

A relationship was developed between river flow rates and water table elevations for four locations: Albuquerque, Belen, Bosque del Apache, and Sevilleta. The river water level was also linked to the flow rate resulting in a strong relationship. This relationship is unique to each site and can only be applied to that specific section of the river due to variation in river geomorphology and land topography.

River water depth is very important criteria for fishery and river aquatic life. Flood control measures depend on river water depth prediction according to river water flow variation. It will be very useful to establish a relationship between river flow and river water depth and water table level along the river banks. In this study an attempt were made to create a relationship between the predicted water table cross-section along the river bank and river water flow. The river flow gages were not located at the same location as the water table reading, but somehow a good correlation was found between them, this indicates that river inflow and out flow might be stable throughout the month of July were this relationship was established in way that didn't affect this correlation. It will be best to re-establish this relationship by using values of flow gage and water table at the same location.

The geographic location of water table wells and flow gages used to build the relationships are listed in Table 3.2, which also shows the distance between the related

water table location site and the river flow gage. Figure 3.24 shows these locations along the Middle Rio Grande River.

Figures 3.25 through 3.35, present the relationship found between flow rate obtained from USGS website and water table estimated by the developed model, flow rate and river water level and river water level and water table, consecutively. USGS provided average daily flow rate, so to be consistent, the model was set to produce average daily water table elevations. The river water level and water table relationship is very strong with R^2 equal to 0.99 in all locations because the model uses one variable to estimate the other and vice versa.

The river flow rate versus the river water level and average water table for 250 m cross-section from the river were plotted for the four locations. Setting a certain distance from river center is important to standardize the relationships for comparison reasons. The relationship in all showed a similar and strong relationship. The R^2 ranges between 0.69 to 0.92 for all four locations. The distance of the water flow gage from water table wells sites did not significantly affect the strong relationship between the water flow rate and water table. The Belen and Sevilleta wells were 21.9 km and 3.2 km away from the water flow gage respectively and this did not seem to affect the flow water table relationship, though flow rates measured at the site would be more desirable. The location of the gage from the well being upstream or downstream also showed no effect on the relationship. Many sites were studied and confirmed the good relationship between the water table and flow rate and river water level and flow rate.

Figure 3.31 shows an opposite relationship between the river water level and water table because water is leaving the river since water elevation in the river is higher

at Bosque del Apache than the water table in the riparian zone as discussed earlier. In the Albuquerque section the river is also losing water but in a small amounts because the head difference between the river water head and the riparian zone water table head is very small about 0.32 m. This can easily change during higher river water flow or course (Figure 3.25). In Belen the river is gaining water from the riparian zone and the drain (Figure 3.28).

The relationships built between the river flow rate river water level and water table level (averaged for defined cross-section) can be helpful tools to predict water table and river height according to the flow rate and vice versa. This tool allows the decision

Table 3.2 Well names and location of river flow gages and distance from each other

Well Name	Geographical Location	Name & USGS No.	Geographical Location	Distance (km)
SHK	106 40 58.319 Long. 34 57 31.541 Lat.	Albuquerque No.08330000	106 40 49.084 Long. 35 05 27.273 Lat.	16.1 Upstream
BLN	106 44 56.191 Long. 34 35 21.626 Lat.	Bernardo No.08332010	106 48 2.103 Long. 34 25 1.246 Lat.	21.9 Downstream
SEV	106 52 3.969 Long. 34 15 56.153 Lat.	Bernardo No.08332010	106 48 2.103 Long. 34 25 1.246 Lat.	20.8 Upstream
SEV	106 52 3.969 Long. 34 15 56.153 Lat.	San Acacia No.08354900	106 53 20.099 Long. 34 15 23.24 Lat.	3.2 Downstream
BOSQ	106 52 48.094 Long. 33 46 56.262 Lat.	San Marcial No.08358400	106 59 32.097 Long 33 40 50.242 Lat.	17.7 Downstream

maker to predict the amount of water that should be released from the dams in to the river to maintain certain water table level in the riparian zone and supply water demand for irrigation and domestic use.

The water table raster layer resulting from the groundwater model was used to obtain the depth to water table leading to the estimation of water potential above the water table. The soil water potential layer is one of the inputs needed in the Ball-Berry stomatal conductance model which will be used in the modified Penman-Monteith to estimate spatial ET of the Tamarisk vegetation.

The role of groundwater modeling, ArcGIS and spatial layers like DEM and vegetation maps extend the ability of point data to determine the water availability status at different locations and produce spatial riparian vegetation ET estimates.

Model results could be used to monitor native vegetation water stress (invasive species are not desirable) that might occur due to extensive river water diversions that cause significant drops in the water table. Fire hazard areas could be outlined where the DEM can pin point higher elevation spots areas and water availability for riparian vegetation is likely to be less. This also will help to determine river safe flows required to maintain fishery habitat and target water table levels that result in no stress to riparian vegetation and allow fair share to water resources among different regions especially for the native vegetation like Cottonwood (Tamarisk is an invasive vegetation and not desirable in the US river systems). In this context, it is important to find a relationship between both the water table depth and the river flows at any point in time.



Figure 3.24 Locations of wells and gages along the Middle Rio Grande River, New Mexico

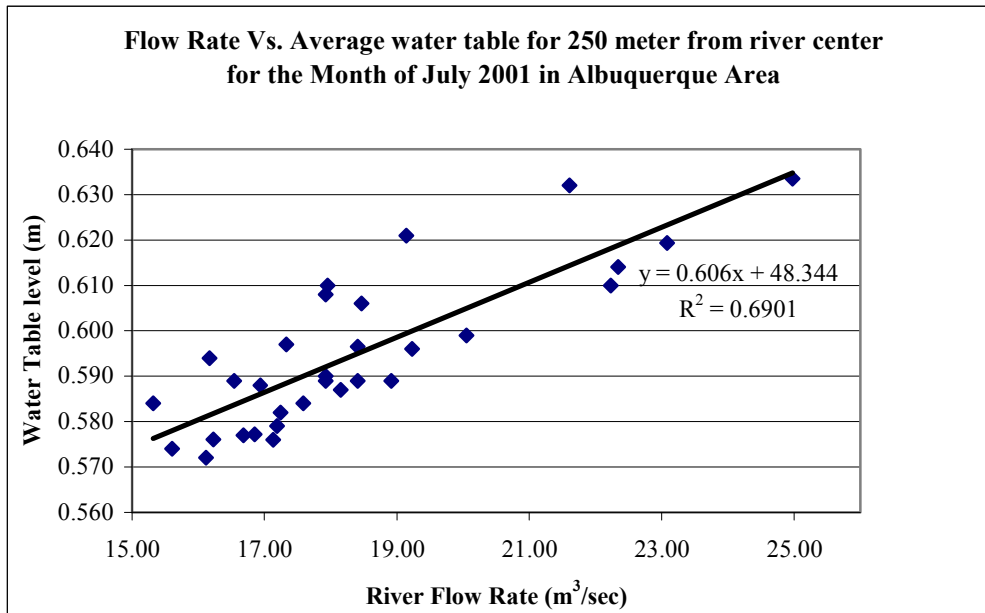


Figure 3.25 Flow rate vs. average daily water table for a 250 meter riparian section from the river center for the month of July 2001 (reference used 1490 m AMSL)

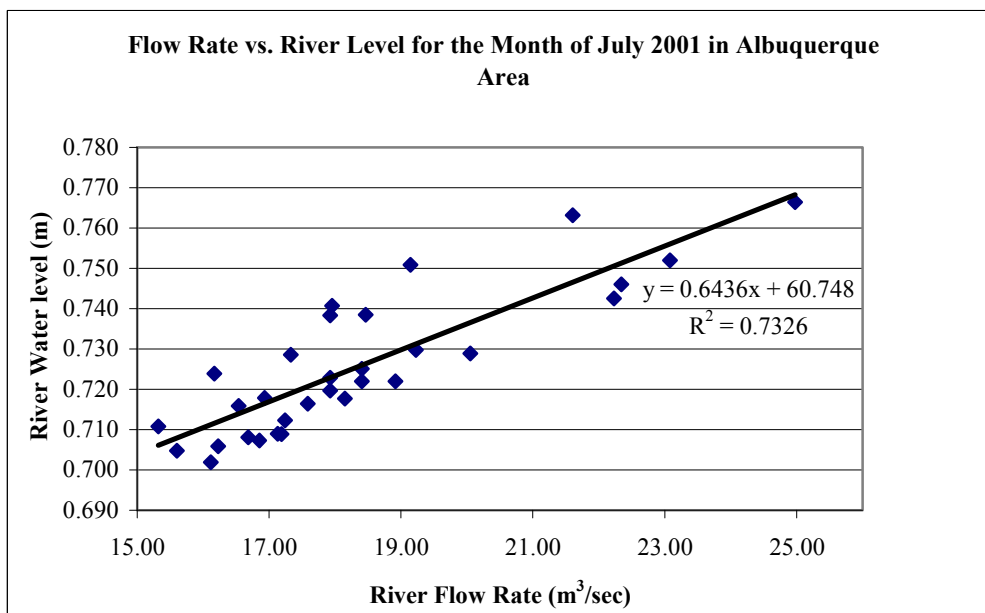


Figure 3.26 Flow rate vs. river water level for the month of July 2001 for the Albuquerque area (reference used: 1490 m AMSL)

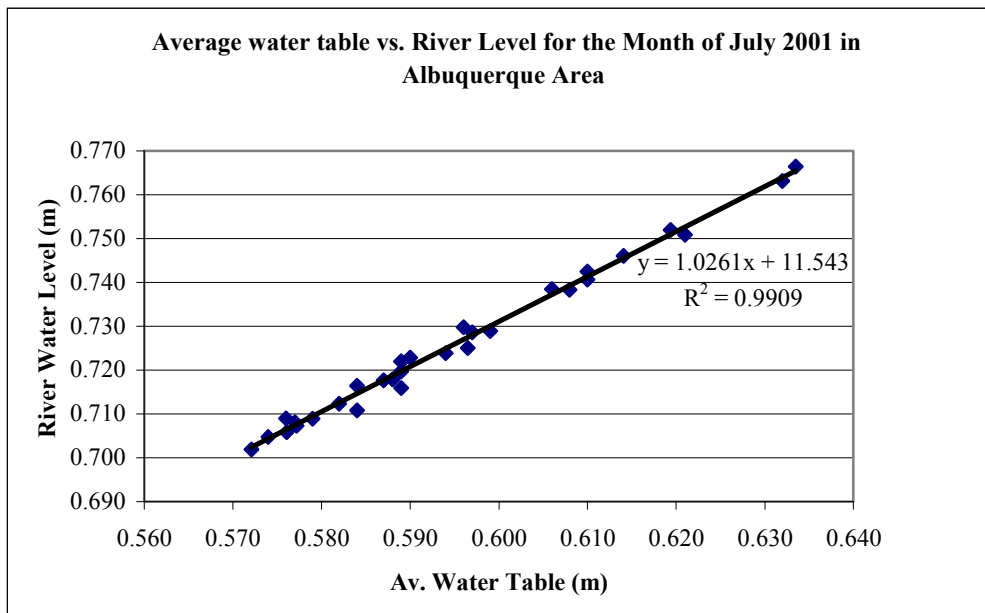


Figure 3.27 Average daily water tables for 250 meter riparian section from river center vs. river water level for the month of July 2001 (reference used: 1490 m AMSL)

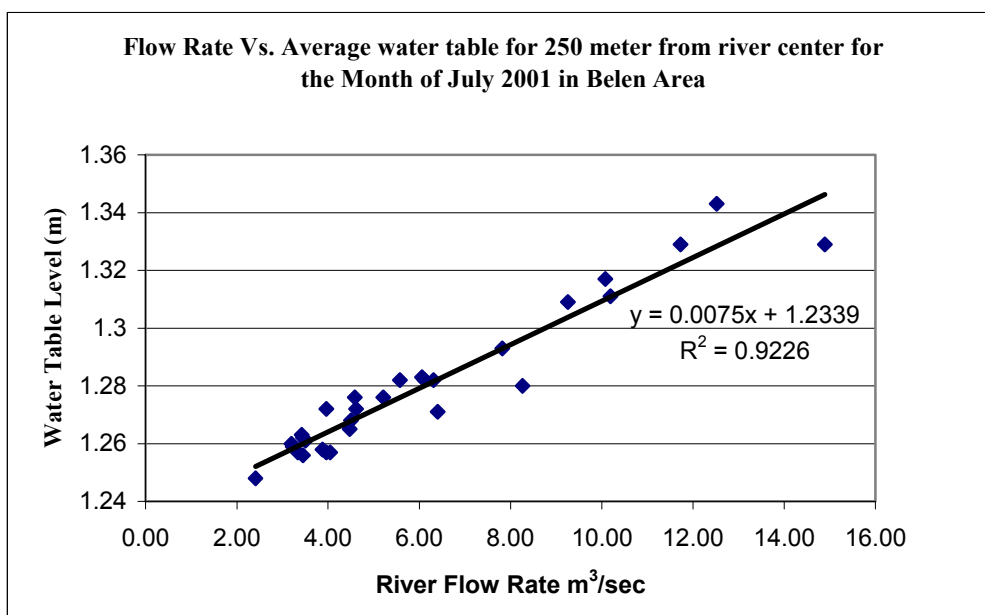


Figure 3.28 Flow rate vs. average daily water table for 250 meter riparian section from river center for the month of July 2001 (reference used: 1455 m AMSL)

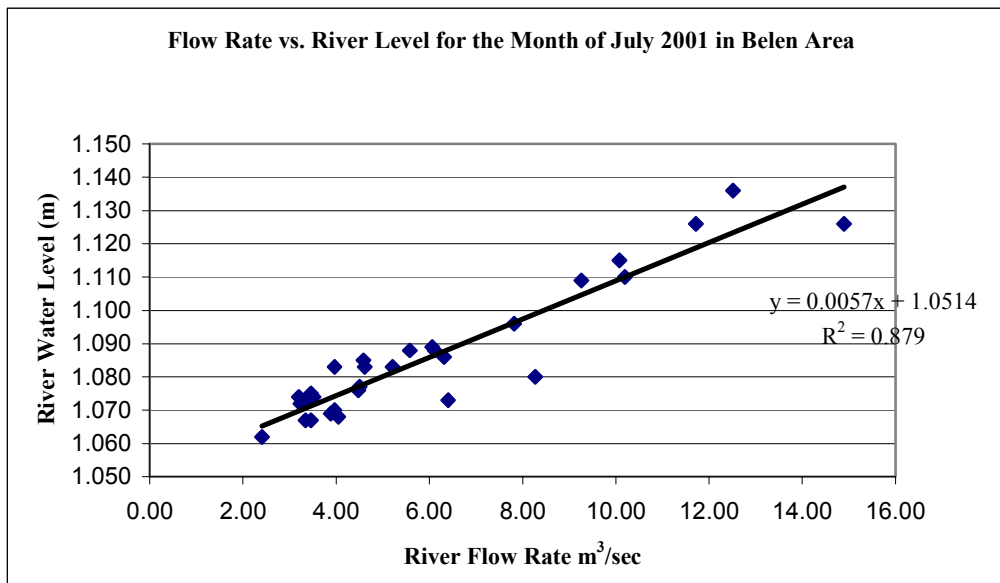


Figure 3.29 Flow rate vs. river water level for the month of July 2001 (reference used 1455 m AMSL)

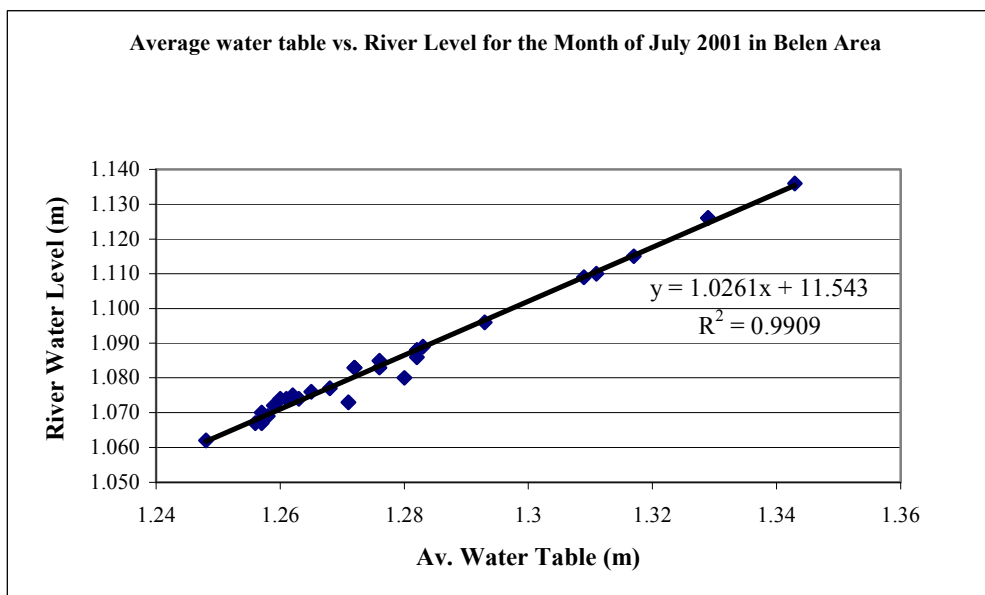


Figure 3.30 Average daily water tables for 250 meter riparian section from river center vs. river water level for the month of July 2001 (reference used: 1455 m AMSL)

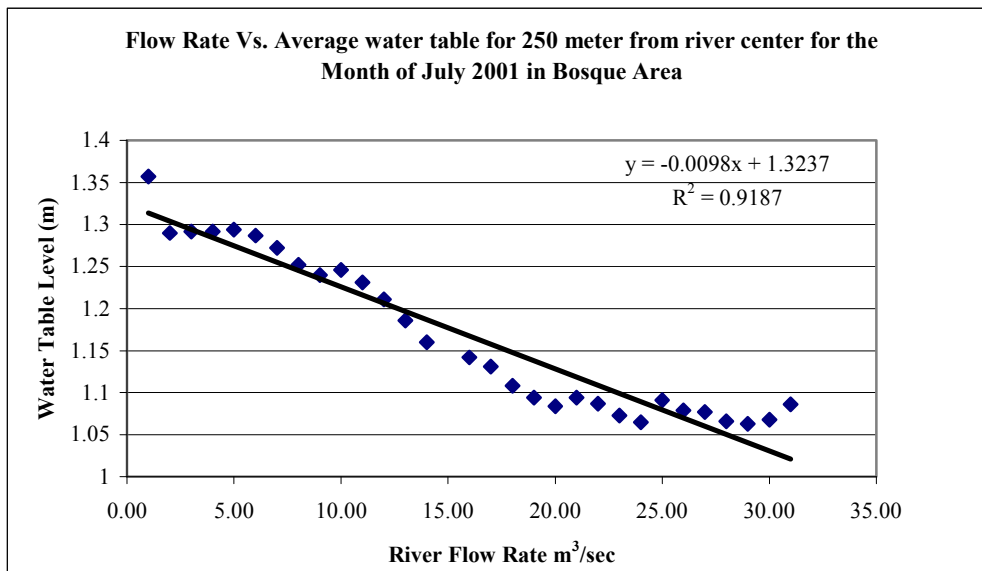


Figure 3.31 Flow rate vs. average daily water table for 250 meter riparian section from river center for the month of July 2001 (reference used: 1365 m AMSL)

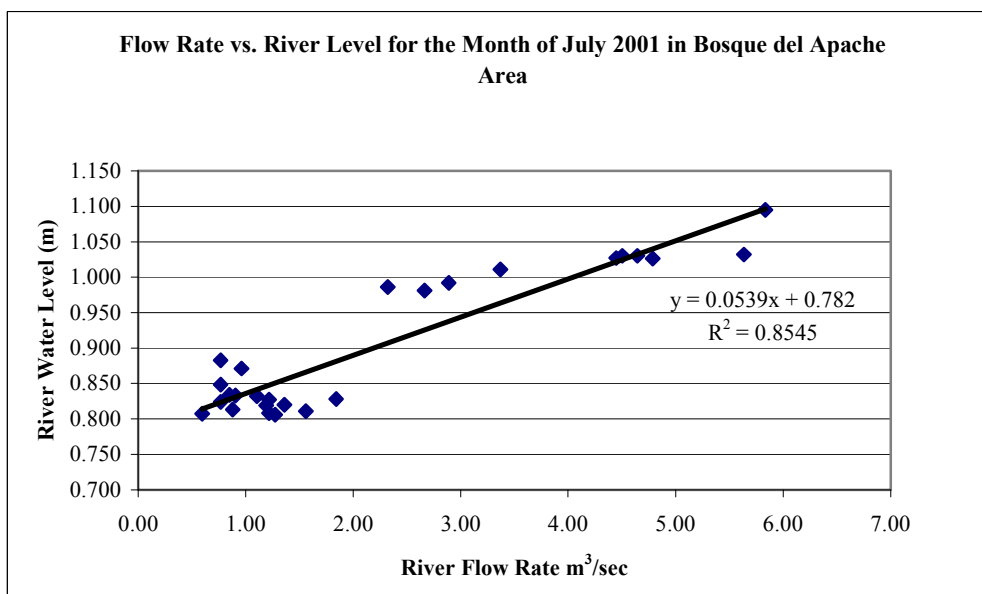


Figure 3.32 Flow rate vs. river water level for the month of July 2001 (reference used 1365 m AMSL)

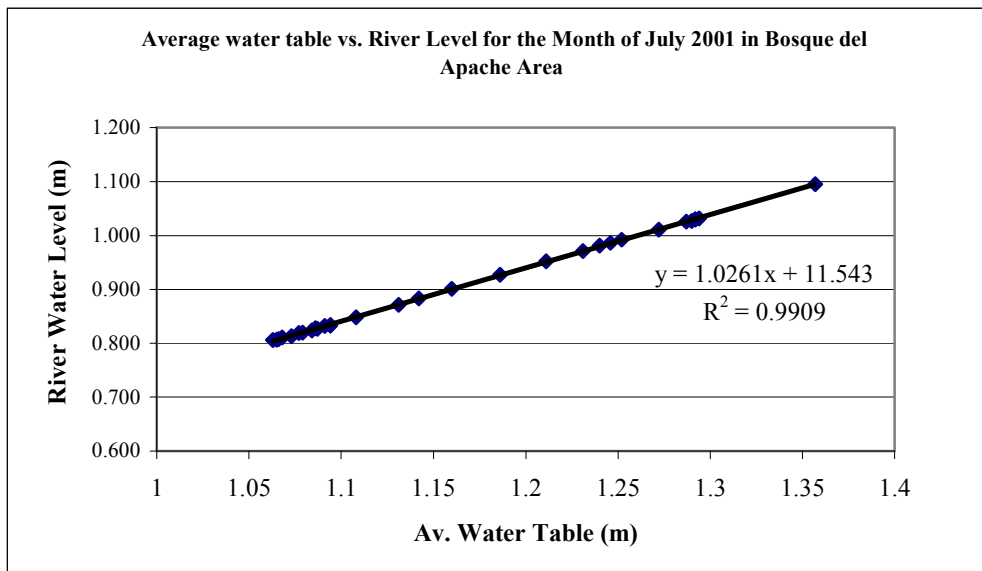


Figure 3.33 Average daily water tables for 250 meter riparian section from river center vs. river water level for the month of July 2001 (reference used: 1365 m AMSL)

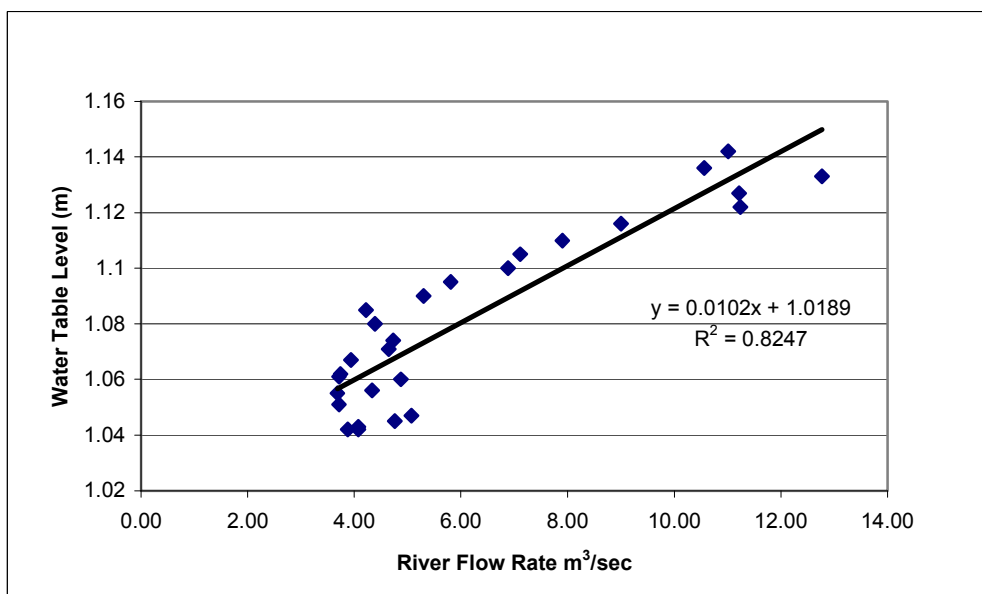


Figure 3.34 Flow rate vs. average daily water table for 250 meter riparian section from river center for the month of July 2001 at Sevilleta (reference used: 1420 m AMSL)

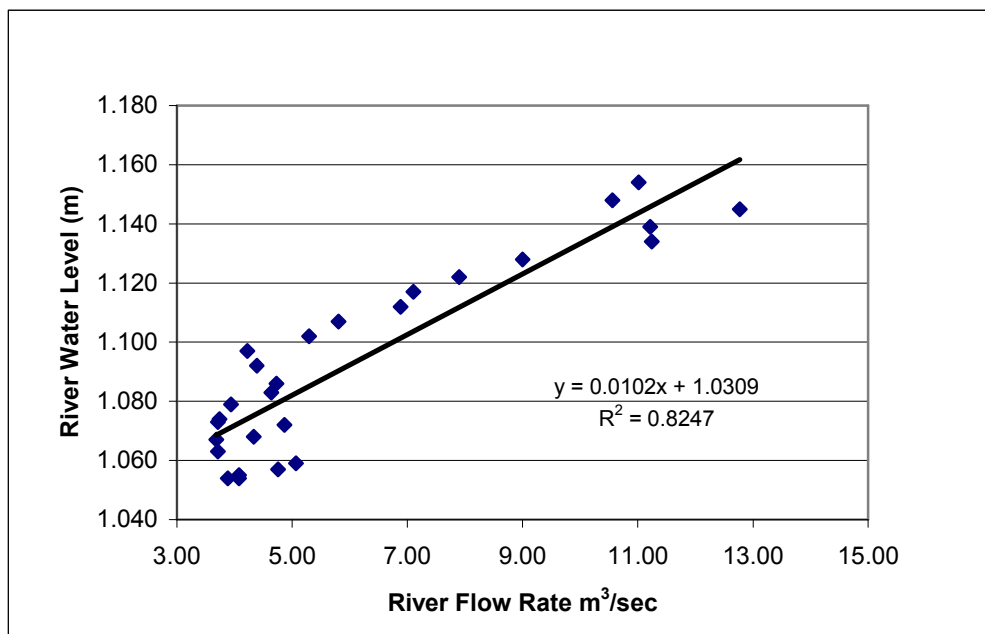


Figure 3.35 Flow rate vs. river water level for the month of July 2001 at Sevilleta
(reference used: 1420 m AMSL)

EVAPOTRANSPIRATION MODEL OUTPUTS

Evapotranspiration of Riparian Vegetation

The evapotranspiration model has the ability to read all the land use map classes separately, allowing the user to isolate and ignore irrelevant classes like roads and human made structures when running the model. The model allows for options on how to estimate the evapotranspiration. Tamarisk evapotranspiration can be estimated using either the modified Penman-Monteith with Ball-Berry stomatal conductance model or using canopy and air temperature difference method. This model also can estimate the ET for Cottonwood and Coyote Willow (assuming Coyote Willow canopy's temperature equal to the measured one by the tower) was estimated using Tc-Ta method. The model

was applied to four different areas: Albuquerque, Belen, Sevilleta, and Bosque del Apache. The daily ET was estimated for twenty days using Tc-Ta for Cottonwood and Coyote Willow and Tamarisk. ET was also estimated for Tamarisk using Penman-Monteith with Ball-Berry stomatal conductance model in all the sites. The outputs for those days were compared to latent heat flux data gathered on the same days using the EC towers.

The model can produce hourly and/or daily ET. Figures 3.36 and 3.37 show measured hourly and cumulative ET, respectively, for Tamarisk for DOY 121, 168, and 242 in 2001 season. Figure 3.36 shows that the ET is small in the morning and increases during the day until it peaks between 12 pm and 2 pm (highest available energy). The ET on May 1st (DOY 121) (5.3 mm/day) was less than June 17th and August 30th (7.4 mm/day). Figure 3.38 and 3.39 show that the drop in ET between 12 pm and 2:00 pm is resulting from a drop in the net and solar radiation during the same period. The hourly ET curve followed the same trends as the solar and net radiation curves as net radiation represents the available energy available for the ET process.

Spatial Evapotranspiration Mapping

The model can estimate spatial ET for Tamarisk and Cottonwood and was run for fourteen days at four different locations. The Bosque and Sevilleta areas have a weather station and eddy covariance system installed on towers above the Tamarisk canopy. The other two locations, Albuquerque (Shirk) and Belen have similar towers installed in Cottonwood forests.

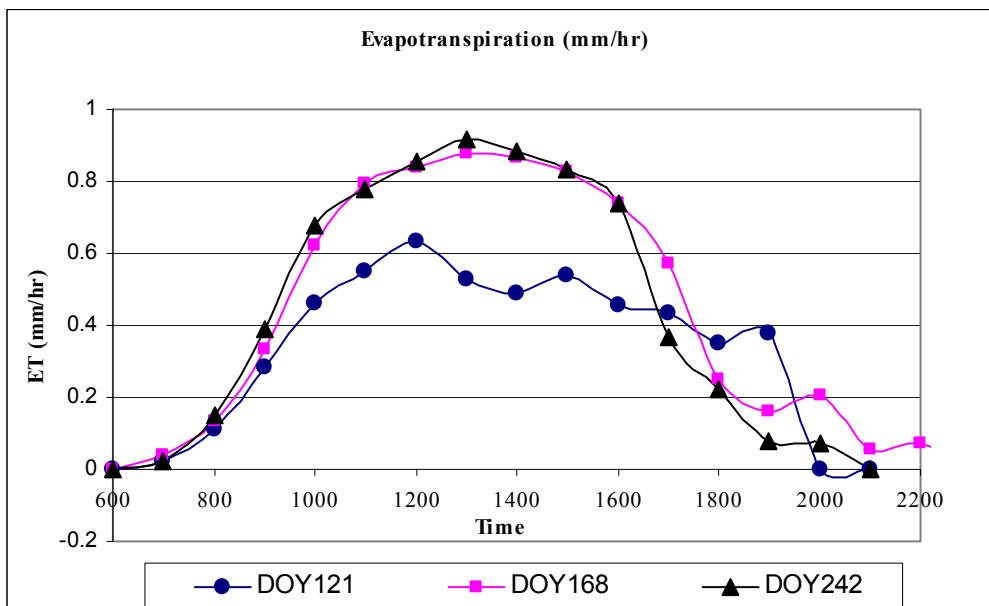


Figure 3.36 Measured Tamarisk evapotranspiration on DOY 121, 168, and 242 (mm/hr)

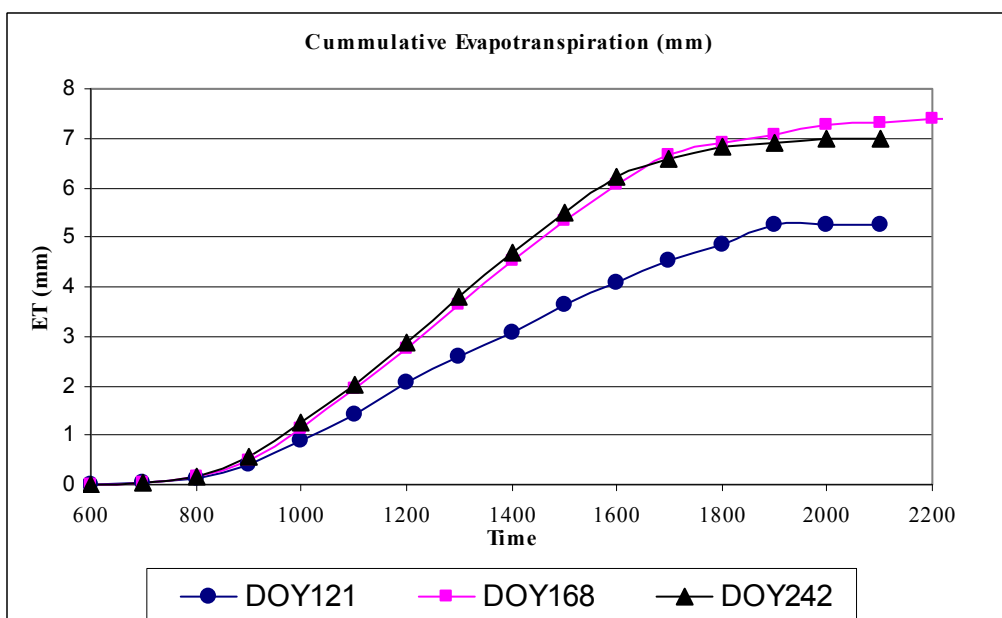


Figure 3.37 Cumulative measured evapotranspiration for Tamarisk on DOY 121, 168, and 242

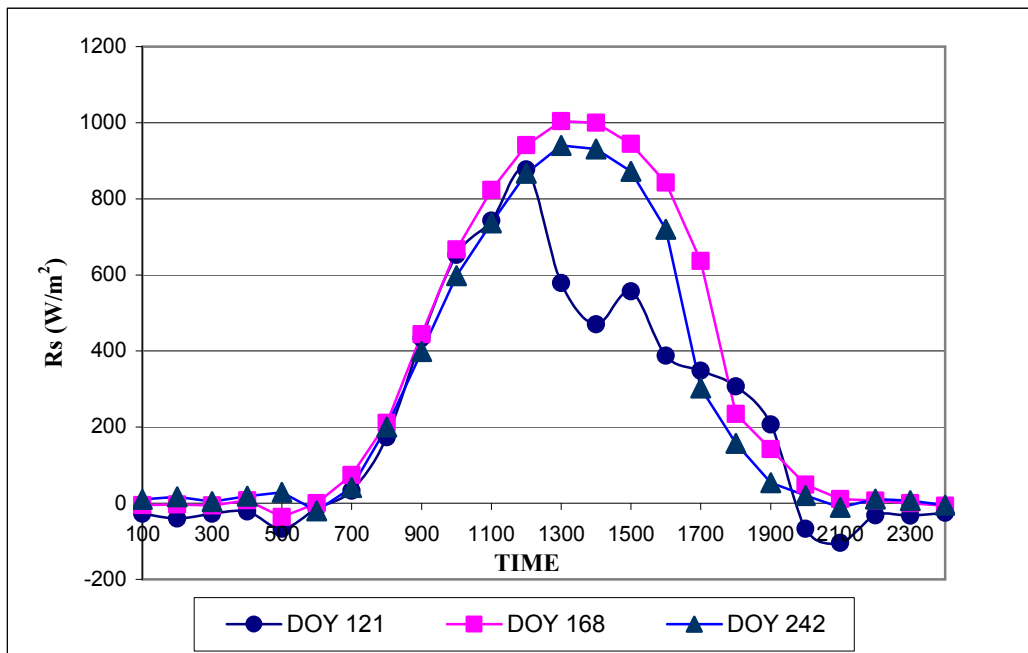


Figure 3.38 Net radiation (W/m^2) on DOY 121, 168, and 242

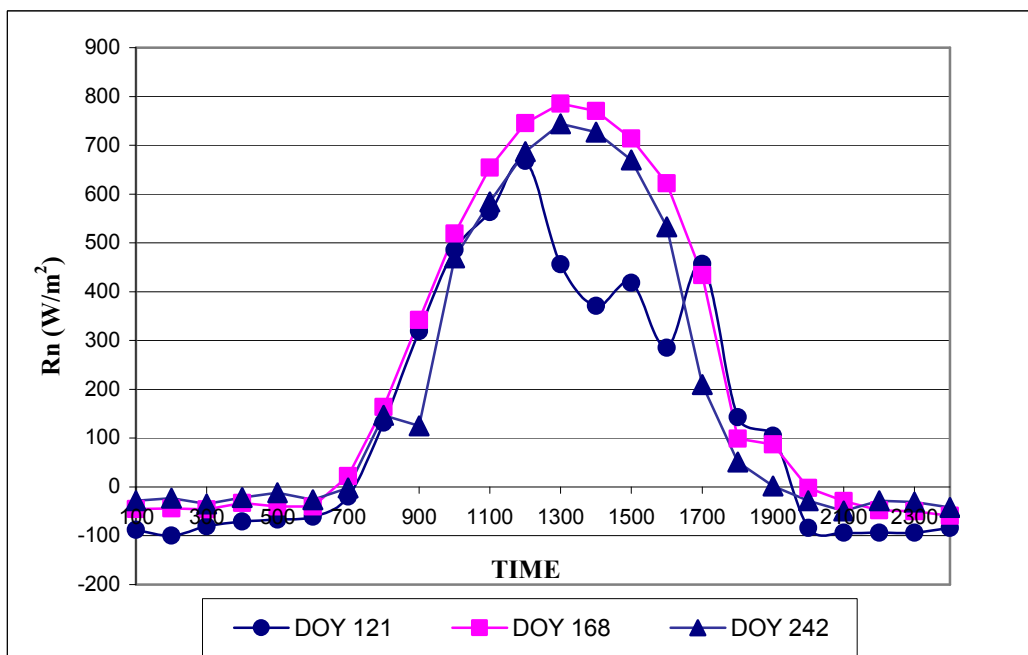


Figure 3.39 Solar radiation (W/m^2) on DOY 121, 168, and 242

When selecting Tamarisk from the land use list through the model input options, the model will run on every pixel in the image that has Tamarisk and estimate its ET using the weather data and the soil moisture potential resulting from the depth to the water table layer.

Figure 3.40 represents a snap shot of vegetation map from the Albuquerque area, this figure is followed by Figure 3.41 which shows the locations of Tamarisk trees among the dense Cottonwood cover after being selected in the model input window. Figure 3.42 shows a slice of the depth to water table coverage across the riparian zone overlaid by ET points estimated for Tamarisk for day 121. A deeper water table (dark blue) is found away from the river and surfaces closer to river (light blue, negative numbers).

Figure 3.43 shows the spatial ET output for DOY 242 in 2001 for three vegetation types, Tamarisk, Cottonwood, and Coyote Willow. The yellow color in the legend represents mostly Coyote Willow locations with the lowest ET values while the green is indicate mostly the Cottonwood locations with ET ranges between 5.68-5.99mm/day, and the blue color represent highest ET values which is mostly Tamarisk. Even though the model has the capability of predicting spatial variability in ET if there is any, this image shows relatively uniform ET values due to the uniformity in depth to water table along this section of the river. When the river and the drain are close to each other it will be harder for big changes in the depth to water table to occur, especially under uniform land topography. The riparian zone in Albuquerque is narrow and dominated by Cottonwood, represented by the dark green color in the vegetation maps. The ET values were lowest for Coyote Willow, higher for Cottonwood and the highest for Tamarisk. The ET can be different under stressed conditions (Nagler et al., 2003) when depth to

water table is deeper than the capacity of the root zone to reach readily available water. Tamarisk tends to survive harsh conditions like water stress or salinity better than Cottonwood and Coyote Willow (Glenn et al., 1998; Vandersande et al., 2001). This gives a comparative advantage to Tamarisk over the other native vegetation in situations where the river is de-watered, which is definitely the case in the southern reaches of the MRGR.

The ET outputs for fourteen selected days for Tamarisk (at two locations; Bosque and Sevilleta using Tc-Ta and Penman-Monteith methods) and for Cottonwood (in Albuquerque and Belen using Tc-Ta method) were compared with the latent heat flux measured at the towers (eddy covariance) adjusted for closure using the Bowen Ratio method described by Twine (2000). The ET was estimated for vegetation in the area around the towers. The comparisons between the estimated and the measured ET are presented in Figures 3.44 through 3.50. These figures show in general, a good agreement between the estimated and the measured ET.

Cottonwood ET was estimated using the net radiation (R_n) and temperature differential method. Figure 3.44 shows good agreement between estimated and measured ET with less than 10% error. The 1:1 line shows that the model tends to underestimate ET values but within an acceptable range. Averages of daily measured and estimated ET were 6.6 mm and 6.4 mm, respectively, with an RMSE of 0.54. Figure 3.45 also shows Cottonwood ET modeled in a different area called Belen. The root mean squared error was 0.66 which represent around 12% error if compared to both estimated and measured ET averages. Averages of daily ET measured and the ET estimated were 5.7 mm and 5.3

mm, respectively with an RMSE of 0.66 mm. In this case, the model tends to overestimate ET values which might be attributed to a model estimation error.

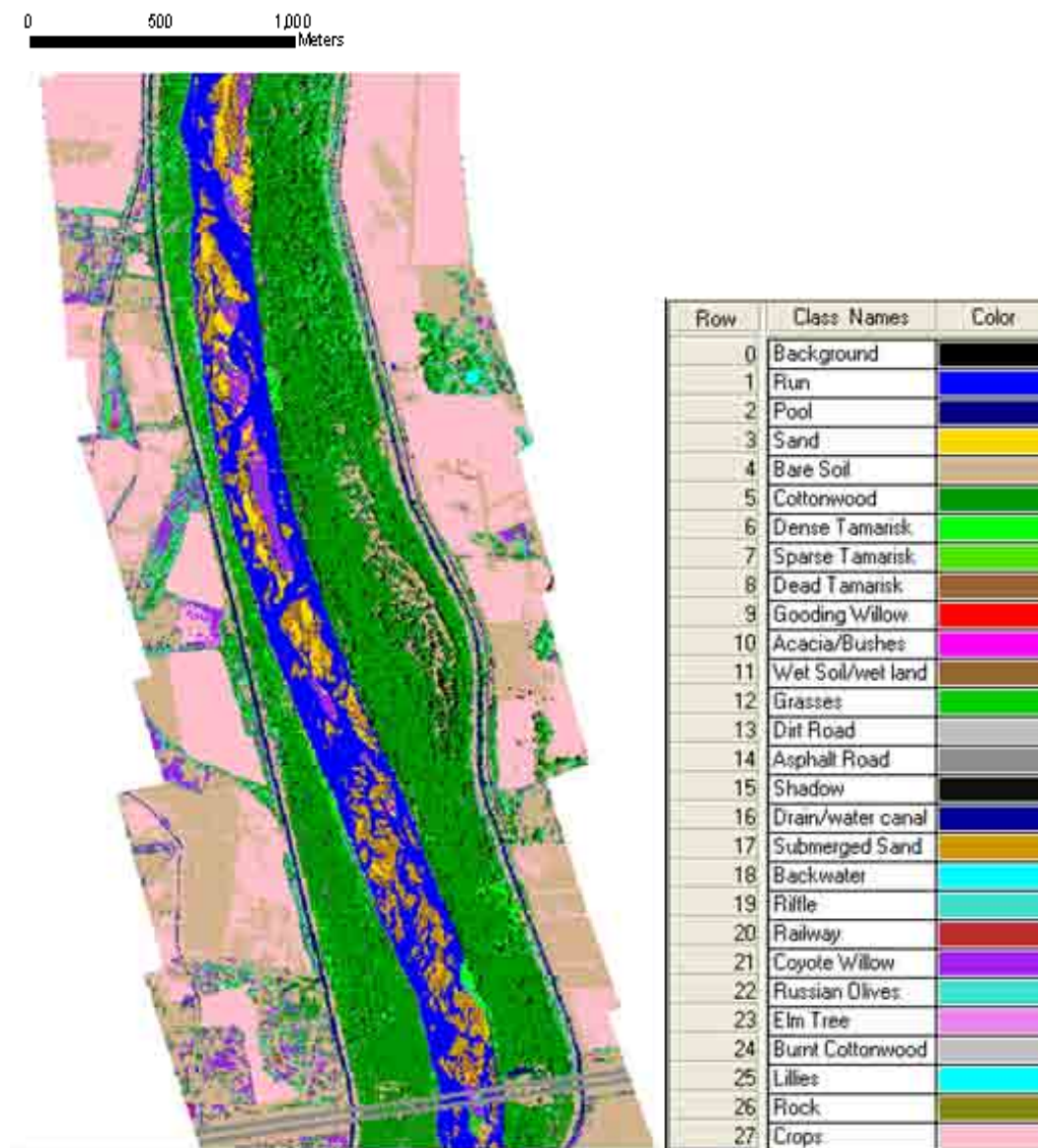


Figure 3.40 Albuquerque area vegetation map

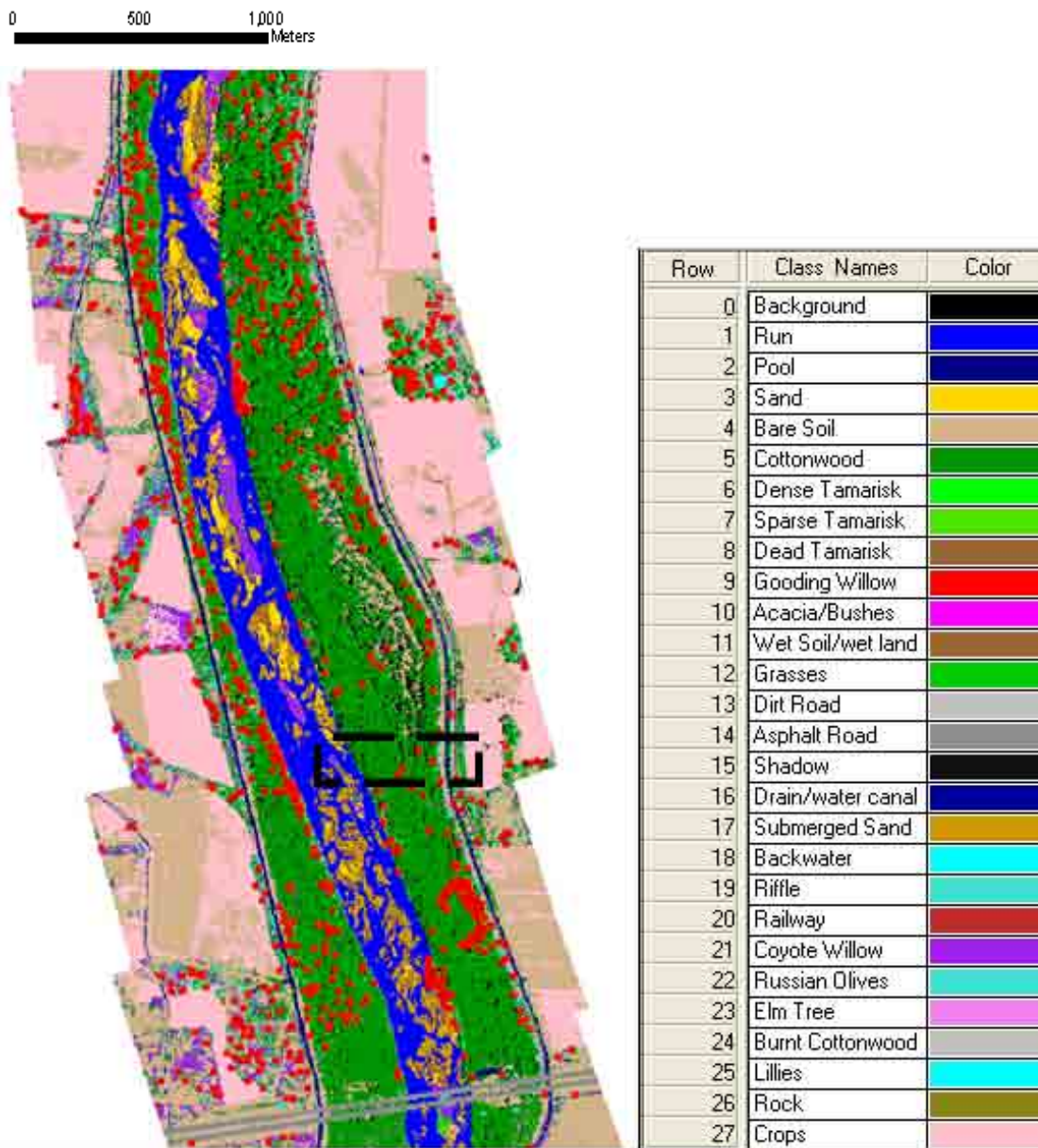


Figure 3.41 Tamarisk ET estimation locations (Red dots). The dashed box is shown in the next figure

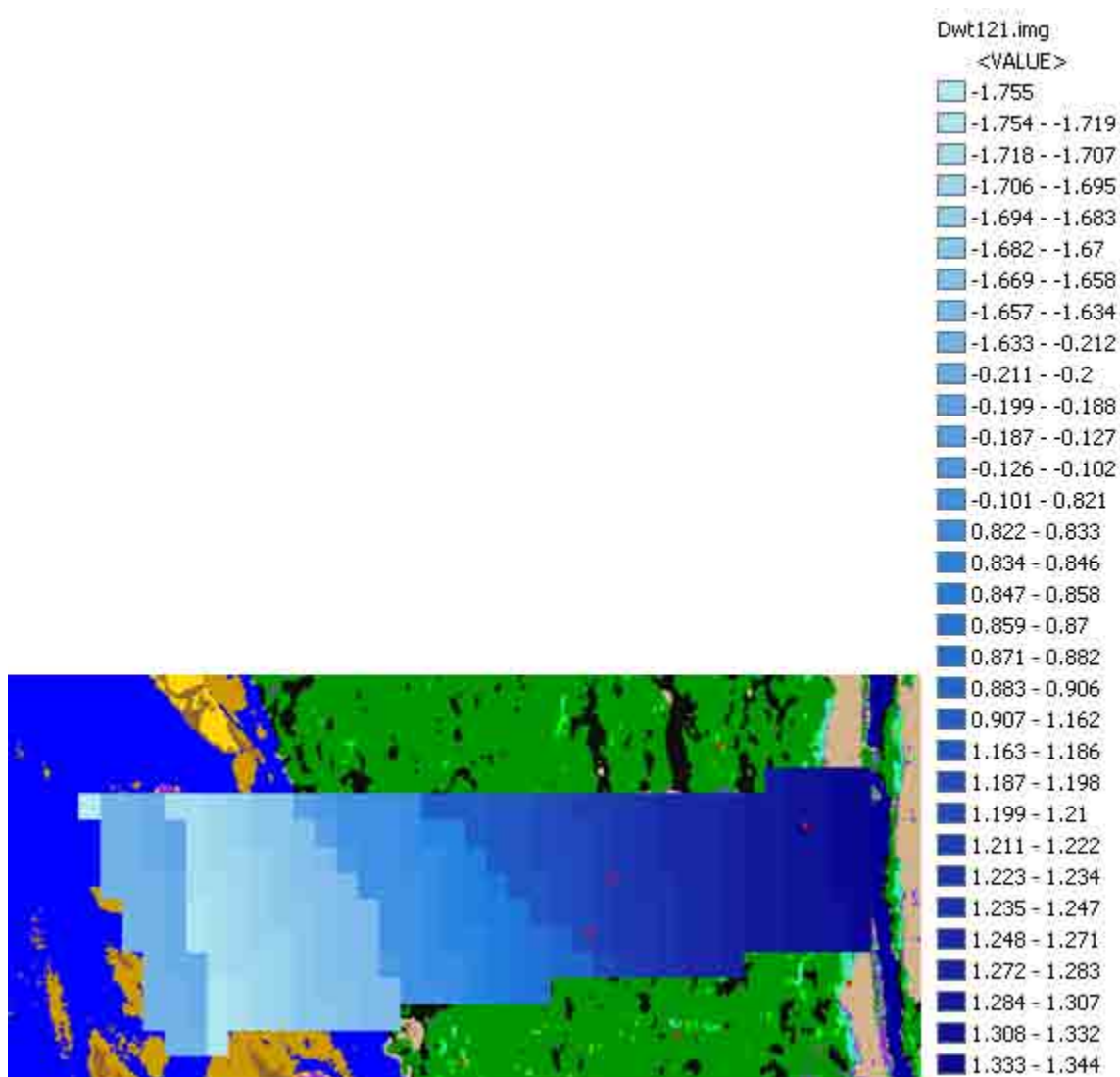


Figure 3.42 Close-up of the dashed box indicated in the previous figure showing the depth to water table coverage in that area

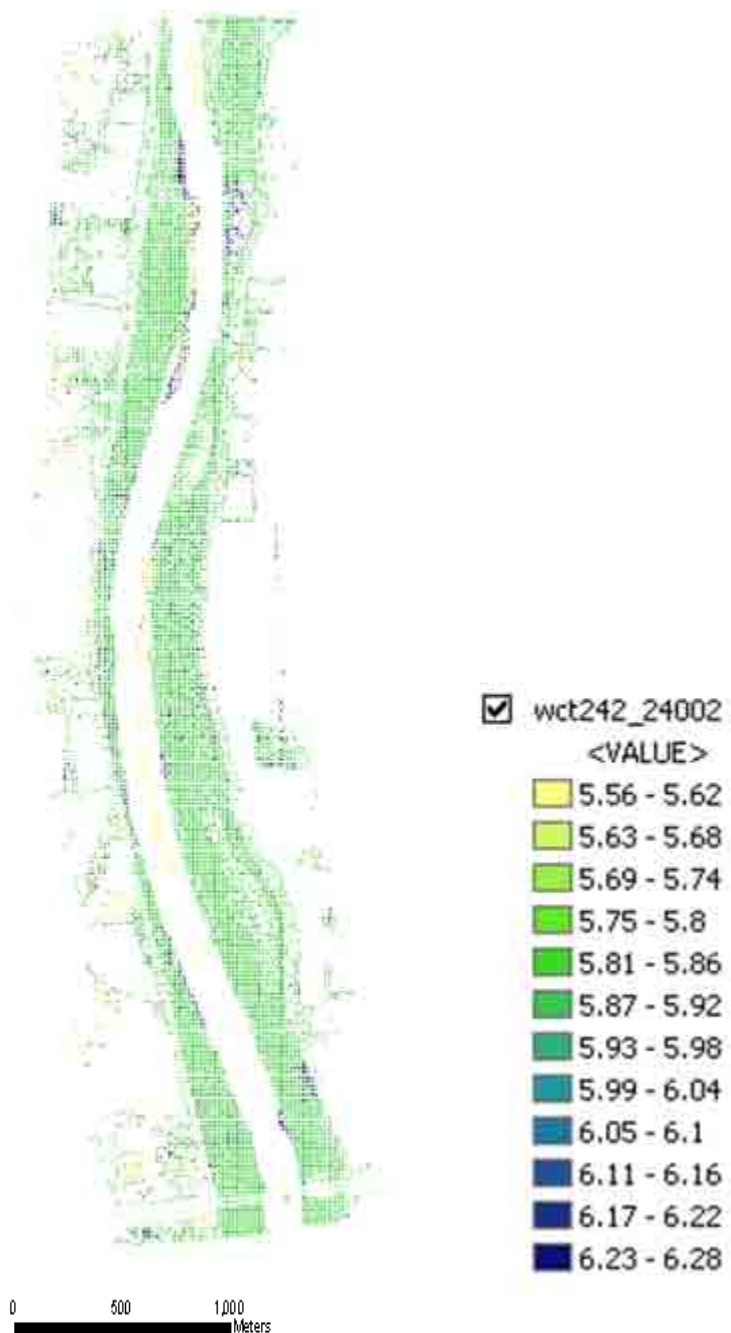


Figure 3.43 Evapotranspiration estimates (mm/day) for the riparian vegetation (Coyote Willow, Cottonwood, and Tamarisk) in the Albuquerque section for DOY 242, 2001

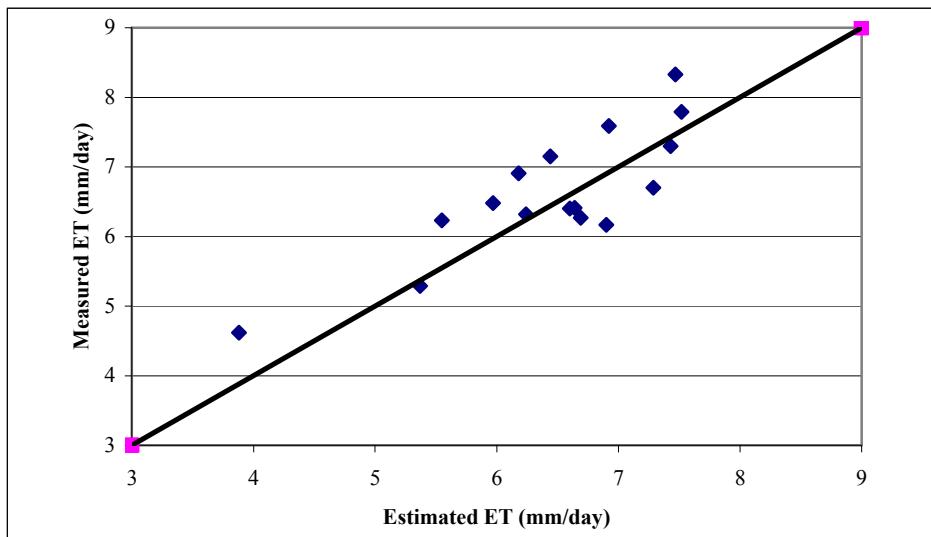


Figure 3.44 Cottonwood evapotranspiration model estimates (mm/day) (using Tc-Ta method) compared to measured ET at Albuquerque. Averages of daily measured and estimated ET were 6.6 mm and 6.4 mm, respectively, with an RMSE of 0.54 mm

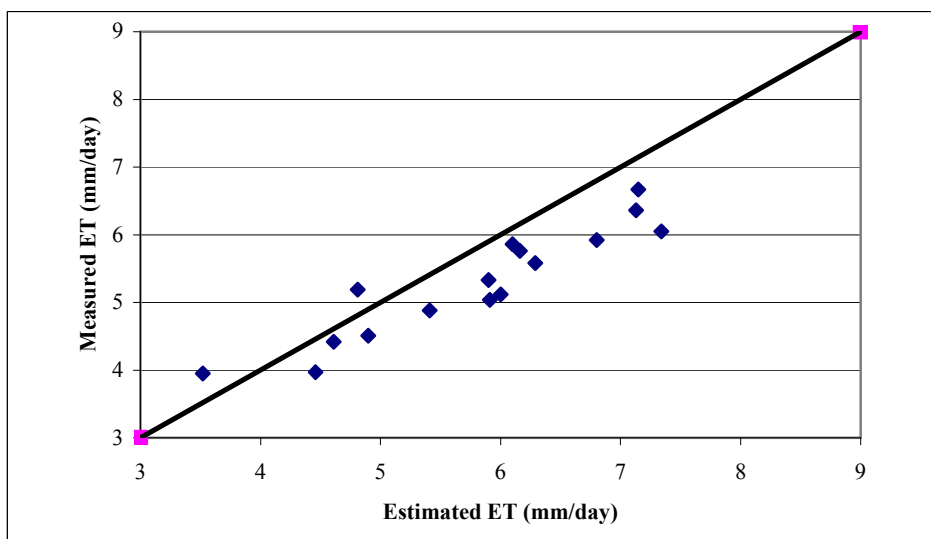


Figure 3.45 Cottonwood evapotranspiration model estimates (mm/day) (using Tc-Ta method) validation with eddy covariance ET at Belen. Averages of daily ET measured and the ET estimated were 5.7 mm and 5.3 mm, respectively, with an RMSE of 0.66 mm

Figures 3.46 and 3.47 are ET results from the two towers in the Bosque del Apache area, dominated by Tamarisk vegetation. The results from both towers compared to the model result also showed good agreement when comparing them with the latent heat flux ET results. The estimated error for the south tower was 9-9.5% when comparing the error to estimated and measured value averages. The ET was higher in the south tower location because the depth to water table was smaller in this section of the river (Figure 3.13).

Figure 3.48 shows the comparison using ET estimates obtained using the temperature differential method. The model considerably underestimated ET with a high percentage error of 30%. One of the possible reasons that contributed to this error might be attributed to the occurrence of high advection rates and heterogeneous vegetation cover. This might be an indication that the temperature differential method can not cope with these atmospheric conditions. Figure 3.49 and 3.50 show two ET results in Sevilleta area using the temperature differential method and modified Penman-Monteith method. The temperature differential method produced a reasonable agreement between estimates and measured ET with an error of 9%, while the modified Penman-Monteith method over-estimated the ET. The Tamarisk cover at the Sevilleta area is sparse unlike the Tamarisk cover at Bosque which is very dense. These conditions enhance ET process leading to larger values. In addition, the Penman-Monteith method is a one-layer big-leaf model, better suited for full cover, dense canopies. The temperature differential method might be more appropriate to use in Sevilleta than the Modified Penman-Monteith, because of the non-uniform surface cover. If the surface is not fully covered with Tamarisk, ET is expected to be lower than what Penman-Monteith method estimates.

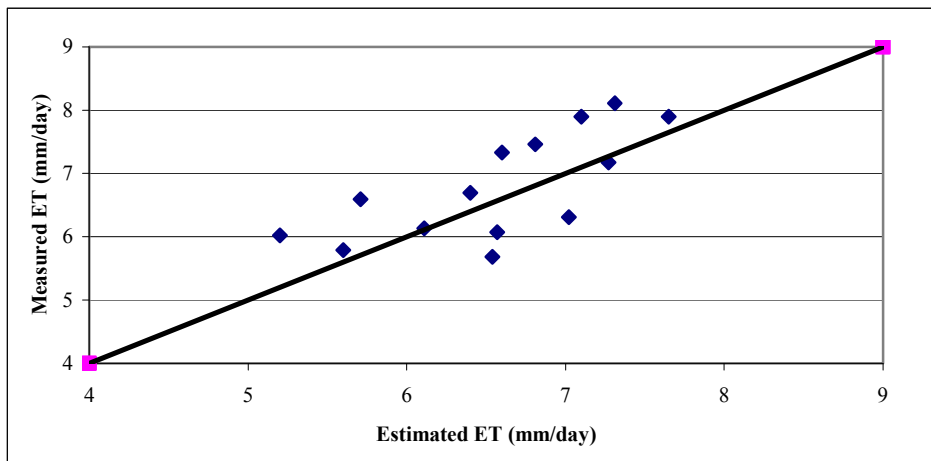


Figure 3.46 Tamarisk evapotranspiration model estimates (mm/day) using Modified Penman-Monteith compared to eddy covariance ET in the Bosque area (South tower). Averages of daily ET measured and the ET estimated were 7.0 mm and 6.5 mm, respectively. RMSE was 0.62 mm for the year 2001

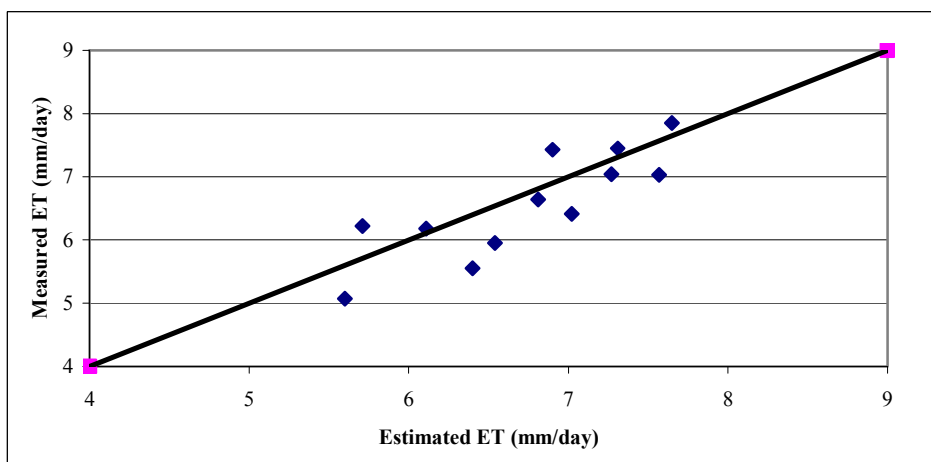


Figure 3.47 Tamarisk evapotranspiration model estimates (mm/day) using Modified Penman-Monteith compared to Eddy Covariance ET in Bosque area (North tower). Averages of daily ET measured and the ET estimated were 6.1 mm and 6.5 mm, respectively. RMSE was 0.47 mm for the year 2001

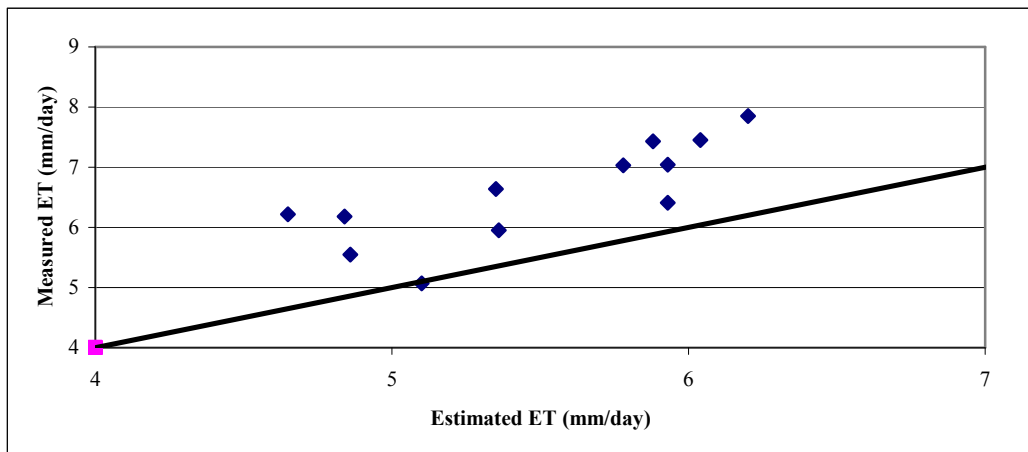


Figure 3.48 Tamarisk evapotranspiration model estimates (mm/day) by temperature differential method comparison with Eddy Covariance ET in Bosque area (North tower). Averages of daily ET measured and the ET estimated were 6.1 mm and 5.5 mm, respectively. RMSE was 1.8 mm for the year 2001

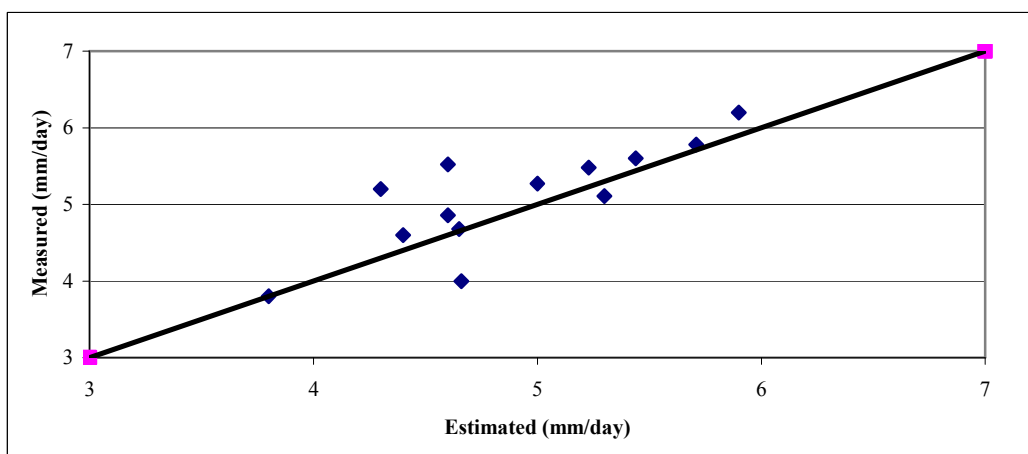


Figure 3.49 Tamarisk evapotranspiration model estimates (mm/day) using temperature differential method compared to Eddy Covariance ET in Sevilleta area. Averages of daily ET measured and the ET estimated were 5 mm and 4.7 mm, respectively. RMSE was 0.46 mm for the year 2001

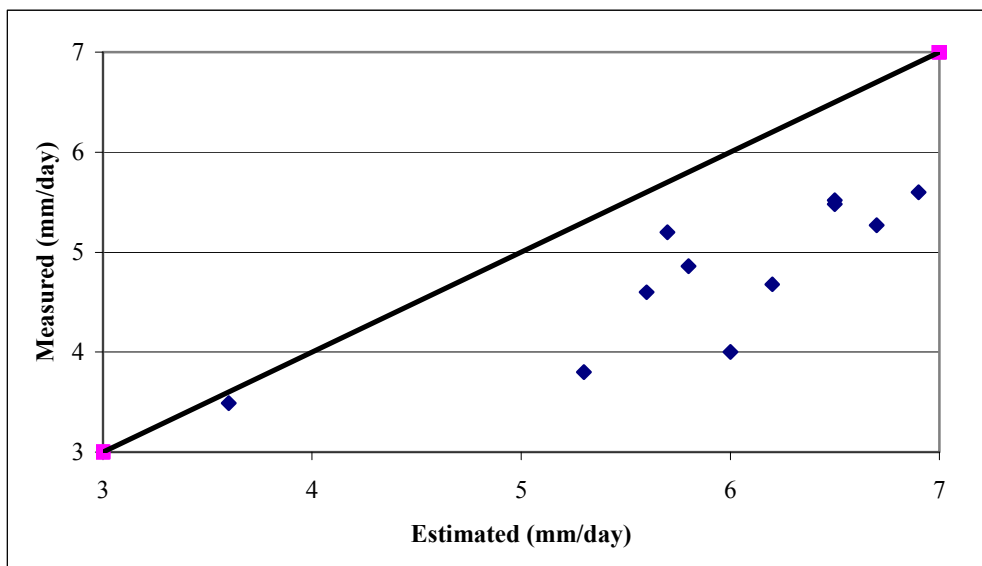


Figure 3.50 Tamarisk evapotranspiration model estimates (mm/day) using Modified Penman-Monteith compared to Eddy Covariance ET in Sevilleta area. Averages of daily ET measured and the ET estimated were 5 mm and 6.2 mm, respectively. RMSE was 1.2 mm for the year 2001

Figures 3.51 through 3.56 show the daily estimated and measured ET for all the locations and different vegetation types using T_c-T_a for Cottonwood ET estimation. Both, Penman-Monteith and T_c-T_a methods was used for Tamarisk ET estimation. Figure 3.51 and 3.52 show the daily ET for Cottonwood in Albuquerque and Belen and similar trends. The variability is mainly due to the plants response to the environmental conditions. The measured and estimated ET curves show when the model overestimates or underestimates ET values. Both curves followed the same trend with acceptable margin of error as discussed earlier. The good agreement between estimated and measured Cottonwood ET results, justify using the simpler approach for estimating ET

by using available solar energy and canopy air temperature difference. Canopy temperature can be obtained spatially from satellite or airborne platforms using the thermal infrared spectral band (8-12 μm), though satellite thermal imagery is usually coarse in pixel size and not so useful for riparian applications.

Figures 3.53, 3.54 and 3.55 show the daily ET for Tamarisk in Bosque del Apache and Sevilleta. As expected similar curves were obtained at the Bosque south and north towers and different ET curve was obtained at the Sevilleta site. The lower values of ET in Sevilleta area can be attributed to the fact that Tamarisk is not as dense as in Bosque del Apache area which may explain why the Penman-Monteith method is over estimating ET at Sevilleta.

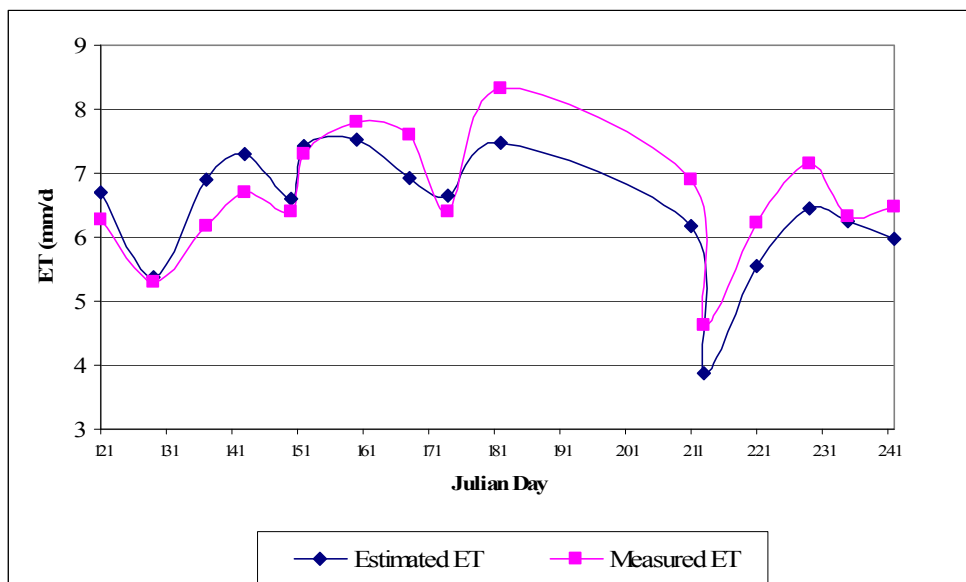


Figure 3.51 Cottonwood evapotranspiration estimates and measured values (mm/day) for 16 days in Albuquerque area using Tc-Ta method

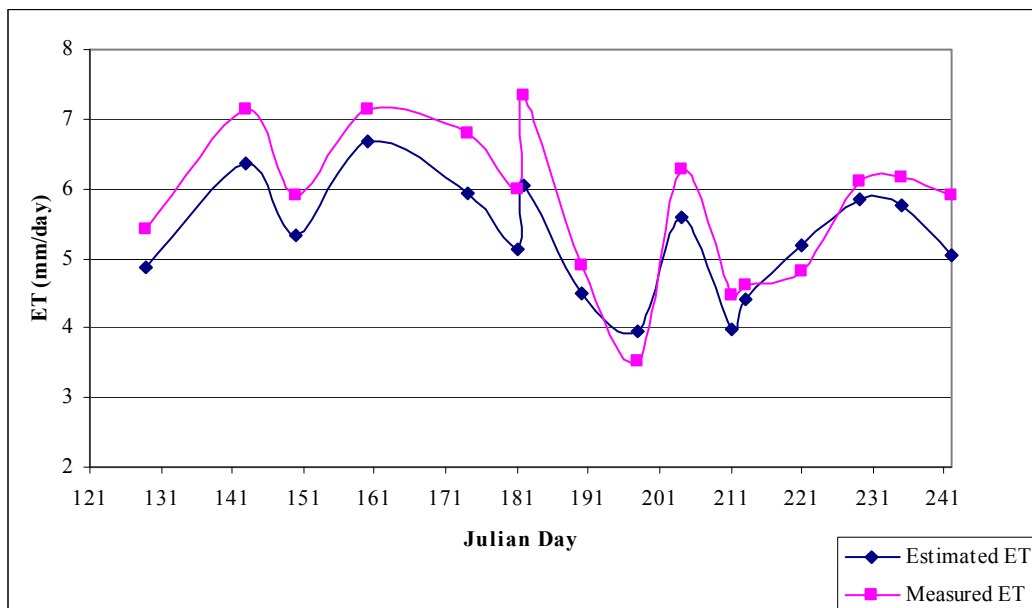


Figure 3.52 Cottonwood evapotranspiration estimates and measured values (mm/day) for 16 days in Belen area using Tc-Ta method

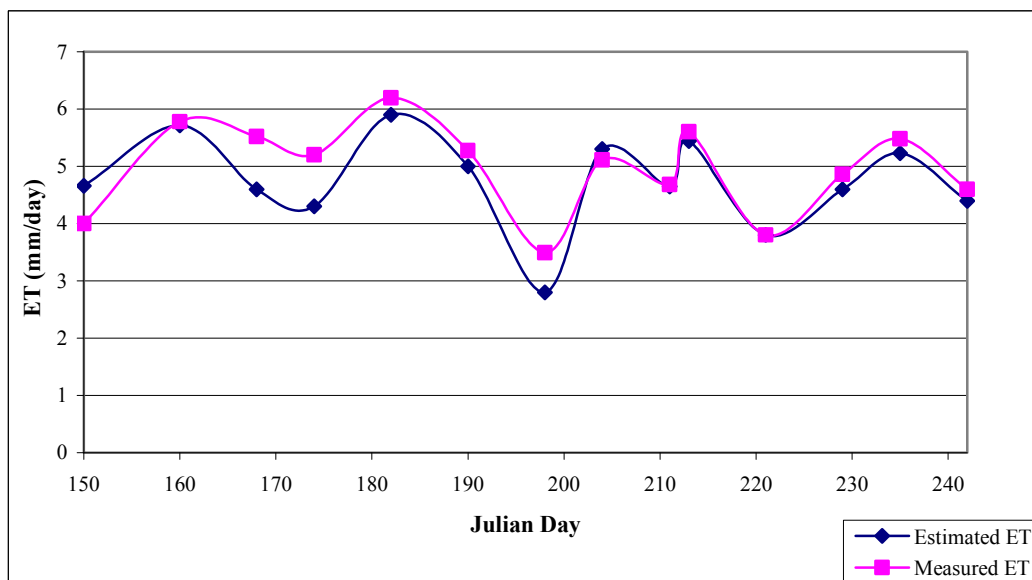


Figure 3.53 Tamarisk evapotranspiration model estimates (canopy temperature method) (mm/day) for 14 days in Sevilleta area using Tc-Ta method

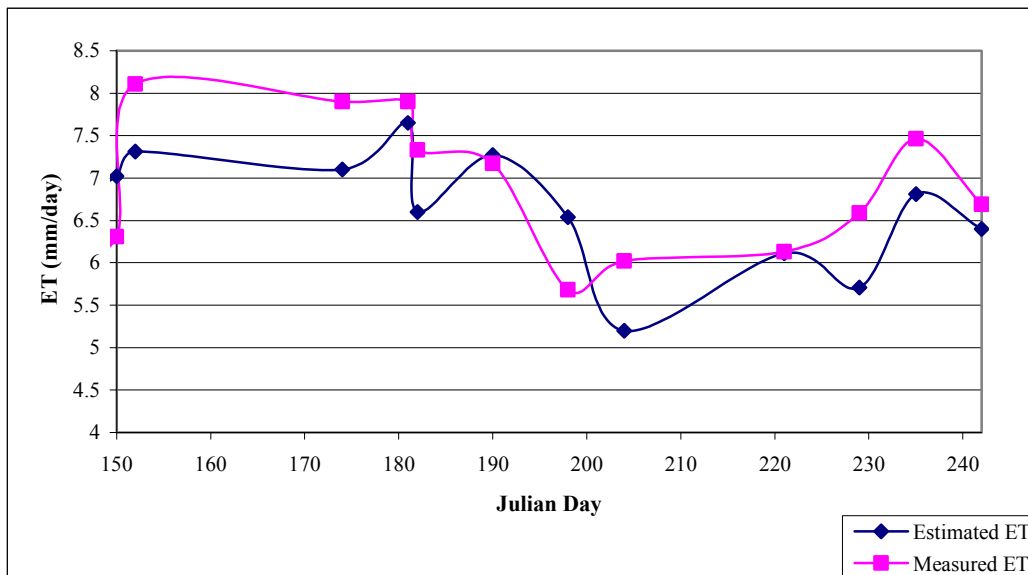


Figure 3.54 Tamarisk evapotranspiration model estimates (Penman Monteith Method) (mm/day) for 14 days in Bosque area (south tower)

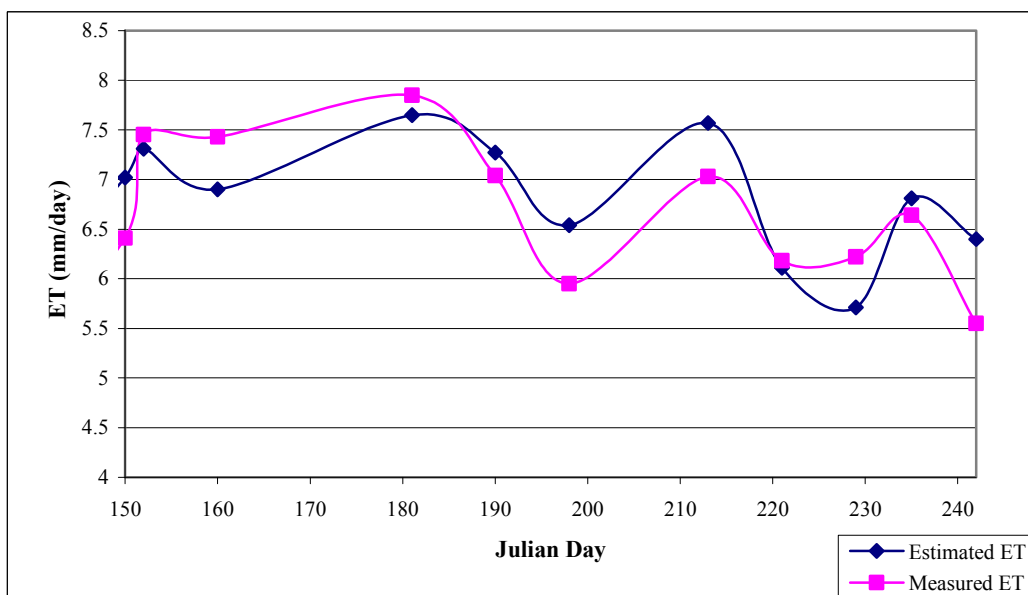


Figure 3.55 Tamarisk evapotranspiration model estimates (Penman Monteith Method) (mm/day) for 12 days in Bosque area (north tower)

Figure 3.56 shows the vegetation distribution map at the Bosque del Apache area. The ET values are very close in value and the difference among them is not significant. The highest ET was 7.48 mm/day and lowest 7.32 indicating that the depth to the water table was not large enough to result in significant differences in water potential in the root zone. The river water surface area shown is from an image acquired on a later date than day 168 and is not related to the depth to water table pattern.

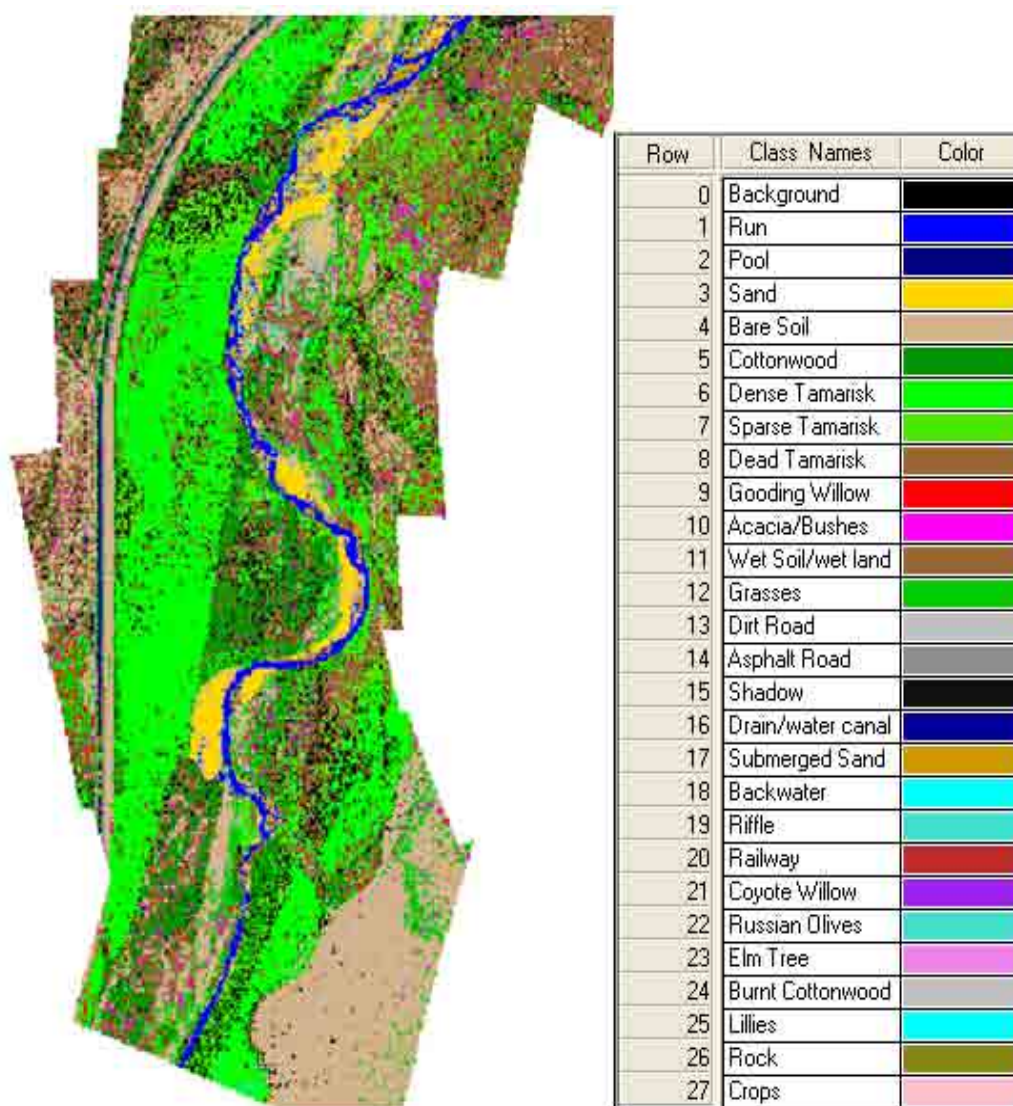


Figure 3.56 A section from Bosque del Apache area vegetation map

Canopy Resistance

Figure 3.57 shows that the modeled canopy resistance (r_c) increases as the day progresses. This is because the stomata react to vapor pressure deficit (VPD) which increases during the day (Figure 3.58). The r_c response does not necessarily follow the VPD variation at the same pace, because there are other factors affecting canopy resistance. The overall observation is that r_c estimated from Ball-Berry model behaved in a predictable and reasonable way when compared to saturation deficit.

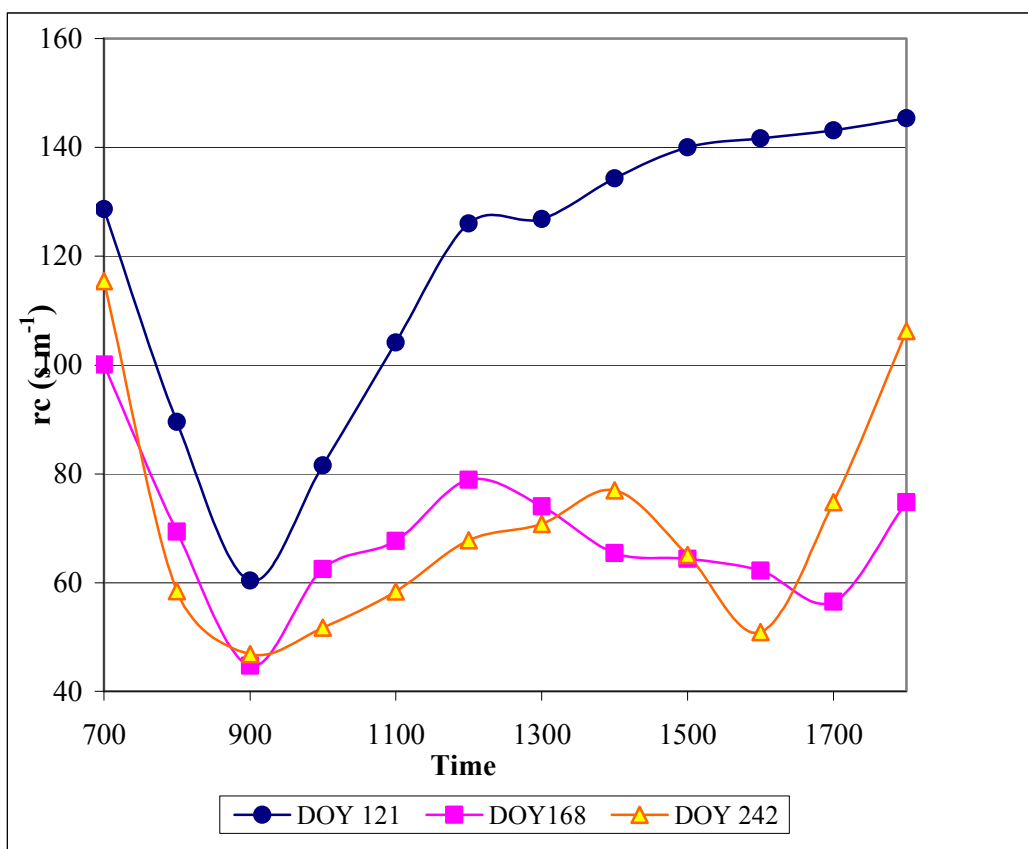


Figure 3.57 Canopy resistance for Tamarisk at the Bosque del Apache estimated using the Ball-Berry Model

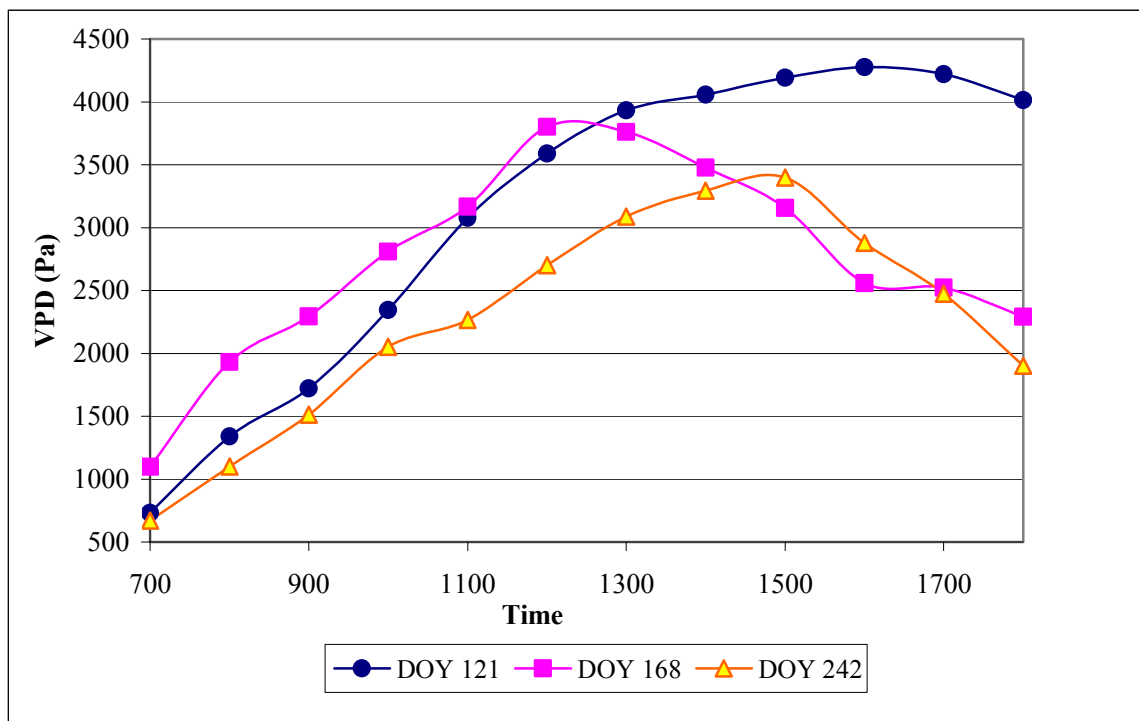


Figure 3.58 Vapor pressure deficits (Pa)

Water Potential Output

Soil water potential is an essential input to the Ball-Berry model for estimating stomatal conductance. Tamarisk is rarely stressed since it has deep roots. It is expected that other native riparian trees will experience stress far before Tamarisk does. The water table was close to the surface so the soil was at field capacity or even at saturation in the different cases examined. Therefore there was no significant difference in spatial ET since the soil water is not limiting factor in the Bosque del Apache area, where the riparian zone (around 500 meter wide on each side of the river) is located in between an agricultural irrigation water drain and the river. The canopy in this area is dense with a high leaf area. Figure 3.59 shows soil water potential for the three dates, where on DOY

242 the soil was saturated while in summer and spring time it was fairly close to field capacity (0.033 MPa).

Figure 3.60 shows soil water potential cross-section along the riparian zone. The step like shape in the curve indicates surface topography variation according to the DEM used. The deeper water table will result in higher soil water potential (in negative term) in the upper soil profile.

Water Flux Output

An hourly water flux rate was estimated as discussed in the methodology section. The water flux was calibrated using night time gain or recharge to water table. Evapotranspiration decreased to zero around 10 pm so this allowed estimating the transmissivity (KD) of the soil since the head is known (discussed in Methodology section). The water table updates take into consideration the hourly flux; deducting ET and adding recharge. Soil porosity is needed in this case to add ET and flux values to water table (in soil media). The model is capable of this process of updating and recharging the water table. Figures 3.61, 3.62, and 3.63 show the water flux along the riparian zone bordered by the drain and the river. The water flux was averaged throughout the day on an hourly basis and given hourly fixed values to maintain steady state conditions.

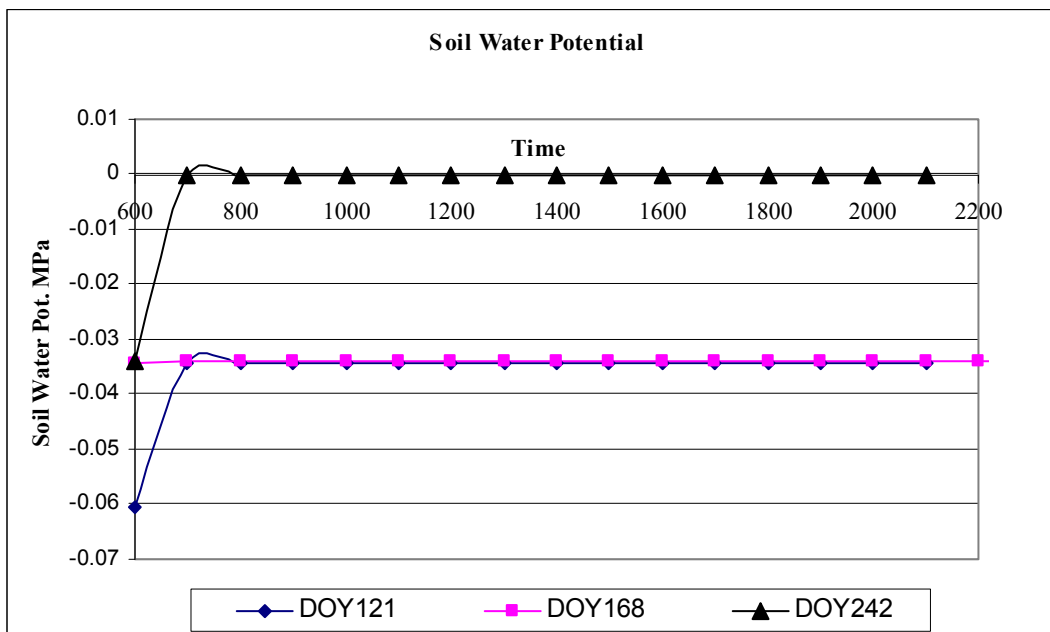


Figure 3.59 Soil water potential in Bosque del Apache

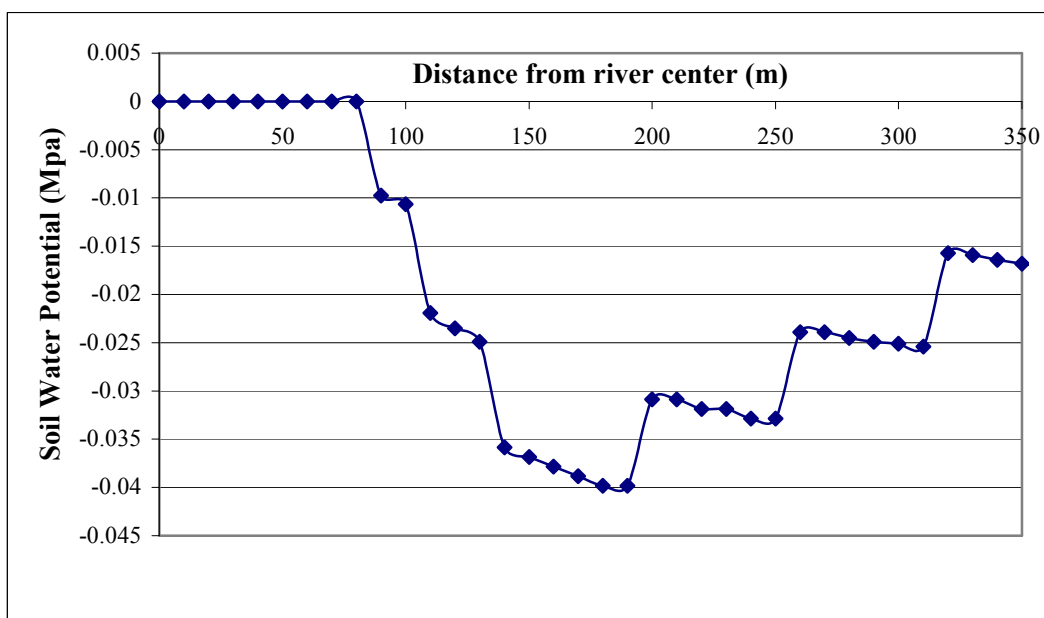


Figure 3.60 Soil water potential along a cross-section in Bosque del Apache Feb 1st 2003 (DOY 121)

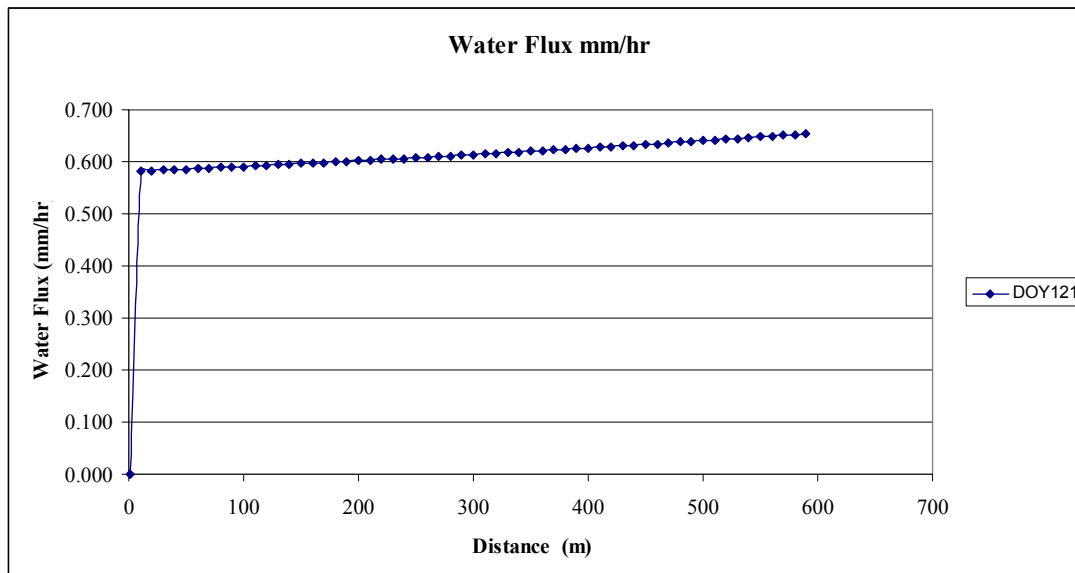


Figure 3.61 Water flux across the riparian zone between the river and the drain on DOY

121

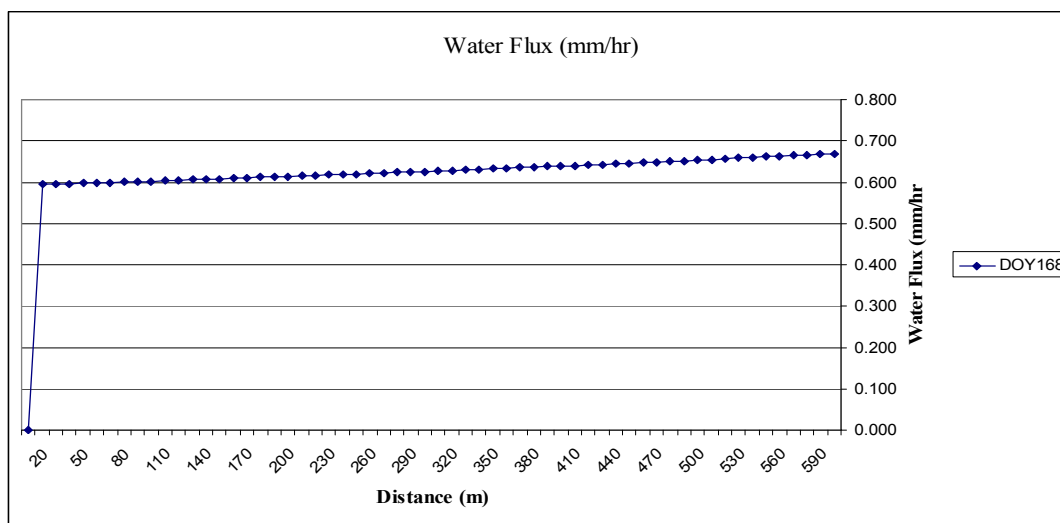


Figure 3.62 Water flux across the riparian zone between the river and the drain on DOY

168

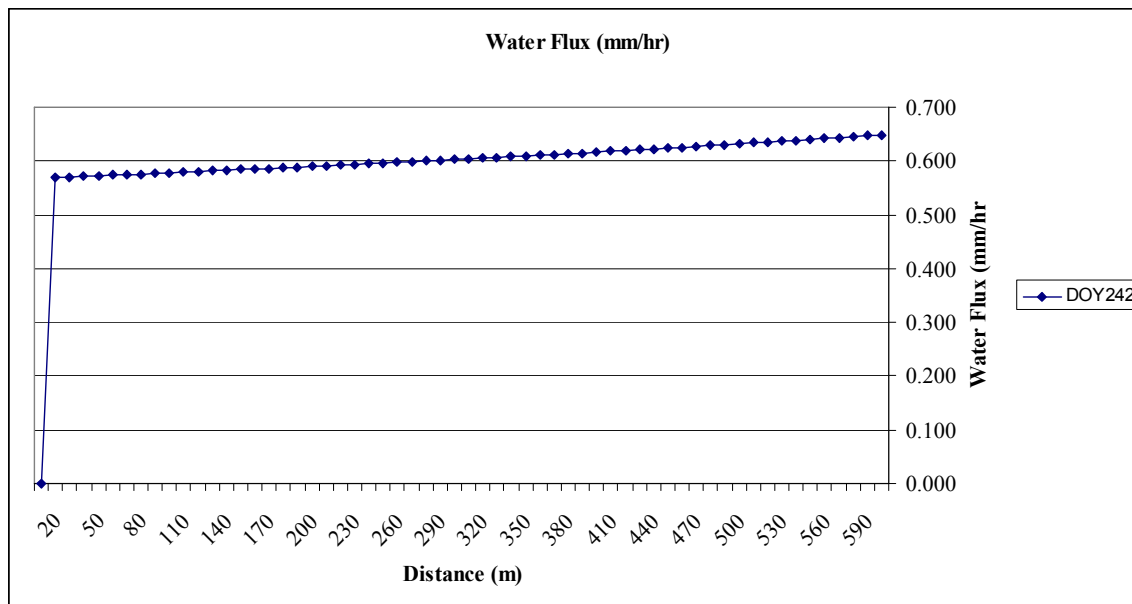


Figure 3.63 Water flux across the riparian zone between the river and the drain on DOY 242

Riparian Vegetation Water Use along the River

The major riparian vegetations in the Middle Rio Grande are Tamarisk and Cottonwood (see Chapter 2). The area occupied by each class was estimated from the vegetation map produced by Akasheh et al. (see Chapter 2). Vegetation classes areas multiplied by ET for each class result in the water use per linear km of river reach. Table 3.3 shows the estimated volume of water used per km of river reach at the four different study areas. This type of information is very important for river managers as it will help them know how much water (by volume) is required to be released from the Cochiti Dam to support the aquatic life as well as the riparian vegetation and irrigation use. The water use was highest in the Shirk area where the Cottonwood population dominates and is very dense. The second highest is at the Bosque area where Tamarisk is the main vegetation

type. The Tamarisk is also dense at this location which explains the high water use. This does not mean that the water is more available than the other locations, but because Tamarisk has the ability to transpire and survive even under stressful conditions (Cleverly et al., 1997).

SUMMARY

This research provided a comprehensive way to estimate the spatial evapotranspiration for the riparian vegetation in the Middle Rio Grande River, New Mexico. Two spatial layers were developed to prepare the base for ET estimation and water use by the riparian vegetation along the river. The first layer is the water table layer produced by the groundwater table model. The water table is the main source of moisture for the riparian vegetation. The other layer is the vegetation map which was produced to cover the whole Middle Rio Grande river reach at 0.5 meter resolution. This map is the first in the history of middle Rio Grande River at this detailed scale. These two layers along with the meteorological data obtained from the four different towers along the river were used to produce spatially distributed ET estimates. The negative sensible heat flux indicate an advection condition where the prevailing arid conditions in New Mexico affected the river microenvironment by adding more energy (hot dry air) above the riparian canopy enhancing the ET process. Therefore, the modified Penman-Monteith with atmospheric coupling factor was adopted to estimate ET. The estimated ET was validated with eddy covariance latent heat flux and found to be in a very good agreement under dense canopy conditions.

Table 3.3 Total water used by major riparian vegetation in (m³/day/km)

DOY	Bosque del Apache			Sevilleta			Belen			Isleta		
	T	CW	TOTAL	T	CW	TOTAL	T	CW	TOTAL	T	CW	TOTAL
121	775	511	1286	597	826	1422	394	1271	1664	283	1710	1993
129	1043	561	1604	392	550	943	349	1021	1370	234	1373	1607
137	1892	621	2512	597	615	1211	388	1310	1698	340	1764	2103
143	1632	721	2353	648	930	1577	404	1346	1750	287	1863	2150
150	2017	721	2737	515	658	1172	394	1114	1508	361	1687	2048
152	2429	731	3159	652	771	1423	442	1352	1794	313	1899	2212
160	2371	721	3091	631	887	1518	462	1350	1812	325	1922	2247
168	2542	721	3262	508	581	1089	462	1269	1731	426	1769	2195
174	2813	691	3504	475	612	1087	419	1284	1703	326	1697	2023
181	2883	761	3644	539	772	1311	422	1133	1555	311	1457	1768
182	2703	601	3304	652	907	1559	518	1386	1904	268	1909	2177
190	2282	721	3003	553	754	1306	375	925	1300	270	1048	1318
198	2273	661	2934	309	511	820	323	665	988	408	1810	2217
204	2349	451	2800	586	806	1392	476	1188	1663	390	1580	1969
211	2737	621	3357	514	624	1138	363	842	1205	190	992	1182
213	2230	701	2931	601	783	1384	334	870	1205	314	1419	1733
221	2117	591	2708	420	680	1100	404	908	1312	307	1646	1954
229	1989	561	2550	508	760	1268	417	1152	1568	276	1595	1871
235	2063	651	2713	578	835	1413	397	1163	1560	328	1526	1854
242	1843	591	2433	486	748	1234	388	1116	1503	328	1820	2148

T: Tamarisk, CW: Cottonwood

Spatial variation in ET for each class was not significant. This is because water was not a limiting factor in the year of this study.

The resulting vegetation map accompanied with the evapotranspiration estimation will provide the decision makers in the Middle Rio Grande River with a very good tool to determine how much water is used by riparian vegetation along river sections and how much water needed to be released from dams to sustain healthy river system.

CONCLUSIONS AND RECOMMENDATIONS.

Spatial ET mapping is a powerful tool in understanding the effect of spatial variability of different parameters like water table and soil water potential. A digital elevation model proved to be an important layer for rivers system management and riparian vegetation ET estimation. Both the water table surface layer and depth to the water table created in this model help in determining the water availability to riparian vegetation.

This model can serve in many aspects concerning rivers and riparian forests management. The spatial coverage of depth to the water table can be an indicator of potential water stress especially in areas with desirable vegetation coverage (native vegetation) by detecting high spots where the plants are more vulnerable to water stress. A good relationship was found between river water flow rate and water table levels. This relationship can be used to determine the amount of water that should flow in the river to sustain a healthy in-stream river system.

The ET spatial variation was not significant for the year of study 2001. It is recommended to apply this data on a dry year to detect ET variation due to increasing depth to water table.

The physiological parameters needed for Ball-Berry model are not known for the riparian vegetation, therefore it is recommended to study and determine those parameters for better ET estimation.

Riparian vegetation water use is very useful for decision makers in the Middle Rio Grande River to determine the amount of water needed to be released from Cochiti Dam to supply the water demand for different uses.

It is recommended that higher resolution DEM's be used to improve the depth to water table estimates. Digital elevation models are an essential input and better spatial resolution will improve the model results. The ideal scenario for better river management is to have systematic water table reading distributed along the river spaced at reasonable distances. The model requires a minimum of two wells at each location, for its application. This will help creating a continuous and more accurate water table surface layer.

REFERENCES

- Allen, R. G., Tasumi, M., Trezza, R., 2007. Satellite-Based energy balance for mapping evapotranspiration with internalized calibration METRIC model. *Journal of Irrigation and Drainage Engineering*, ASCE 133, 380-394.
- Bastiaanssen, W. G. M., Noordman, E. J. M., Pelgrum, H., Davids, G., Thoreson, B. P., Allen, R.G., 2005. SEBAL model with remotely sensed data to improve water resources management under actual field conditions. *Journal of Irrigation and Drainage Engineering*, ASCE 131(1), 85-93.
- Batelaan, O. L., Hung, L. Q., Verbeiren, B., 2004. Water and energy fluxes in a riparian wetland. In: *Workshop on Airborne Imaging Spectroscopy*, Bruges, 8 October 2004.

- Brinson, M. M., 1990. Riverine forest. In: Lugo, A. E., Brinson, M. M., Brown, S. (Eds.), *Forested Wetlands*, Amsterdam, pp. 87-141.
- Brotherson, J. D., Carman, J. G., Szyska, L. A., 1984. Stem-diameter age relationships of *Tamarix ramosissima* in central Utah. *Journal of Range Management*, 37, 362-364.
- Brown, G. W., Krygier, J. T., 1970. Effects of clear-cutting on stream temperature. *Water Resources Research* 6, 1133-1139.
- Caldwell, M. M., 1976. Root extension and water absorption. In: Lange, O. L., Kappen, L., Schulze, E. D. (Eds.), *Water and plant life: Problems and modern approaches*, Springer, Berlin-Heidelberg, New York, pp. 63-85.
- Carleer, E., Wolff, E., 2004. Exploitation of very high resolution satellite data for tree species identification. *Photogrammetric Engineering and Remote Sensing* 70, 135-140.
- Chescheir, C. M., Gilliam, J. M., Skaggs, R. W., Broadhead, R. G., 1991. Nutrient and sediment removal in forested wetlands receiving pumped agricultural drainage water. *Wetlands* 11, 87-103.
- Cleverly, J. R., Smith, S. D., Sala, A., Devitt, D. A., 1997. Invasive capacity of *Tamarix ramosissima* in a Mojave Desert floodplain: the role of drought. *Oecologia* 111, 12-18.
- Coonrod, J., Etlanus, A., Vanderbilt, K., 2006. Using grid to evaluate different methods to estimate evapotranspiration. In: 26th Annual ESRI International User Conference, 7-11 August 2006, San Diego, CA.
- DeLoach, C. J., Carruthers, R. I., Lovich, J. E., Dudley, T. L., Smith, S. D., 2000. Ecological Interactions in the Biological Control of Saltcedar (*Tamarix* spp.) in the United States: Toward a New Understanding. In: *Proceedings of International Symposium on Biological Control of Weeds*, 4-14 July 1999, Bozeman, MT.
- Glenn, E., Tanner, R., Mendez, S., Kehret, T., Moore, D., Garcia, J., Valdes, C., 1998. Growth rates, salt tolerance and water use characteristics of native and invasive riparian plants from the delta of the Colorado River, Mexico. *Journal of Arid Environment* 40, 281-294.
- Goodrich, D. C., Moran, M. S., Scott, R., Williams, J. Q. D., Schaeffer, S., MacNish, R., Maddock, T., Goff, B. F., Toth, J., Hipps, L., Cooper, D., Schieldge, J., Chehbouni, A., Watts, C., Shuttleworth, W. J., Hartogensis, O., De Bruin, H., Kerr, Y., Unkrich, C. L., Marsett, R., Ni, W., 1998. Seasonal estimates of riparian evapotranspiration (consumptive water use) using remote and in-situ measurements. *American Meteorological Society, special symposium on hydrology*, 11-16 Jan 1998, Phoenix, AZ.
- Gurnell, A. M., 1995. Vegetation along river corridors: hydrogeomorphological interactions. In Gurnell, A.M. and Petts, G.E. (Eds.), *Changing River Channels*, Wiley, Chichester, pp. 237-260.
- Harvey, K. R., Hill, G. J. E., 2001. Vegetation mapping of a tropical freshwater swamp in the Northern Territory, Australia: A comparison of aerial photography, Landsat TM and SPOT satellite imagery. *International Journal of Remote Sensing* 22, 2911-2925.

- Hattori, K., 2004. The transpiration rate of tamarisk riparian vegetation. Thesis (M.S.) Utah State University, Dept. of Plants, Soils, and Biometeorology, 74pp.
- Hewitt, M. J., 1990. Synoptic inventory of riparian ecosystems: The utility of Landsat Thematic Mapper data. *Forest Ecology and Management*, 33-34, 605-620.
- Homer-Dixon, T., 1999. *Environment, Scarcity, and Violence*. Princeton University Press, NJ. 272pp.
- Huete, A., Didan, K., Miura, T., Rodriguez, E., 2002. Overview of the Radiometric and Biophysical Performance of the MODIS Vegetation Indices. *Remote Sensing of Environment*, 83, 195-213.
- Hughes, F. M. R., Richards, K. S., El-hames, A. S., Harris, T., Peiry, J. L., Pautou, G., Girel, J., 1997. Investigations into hydrological influences on the establishment of riparian tree species. In Large, A.R.G. (Eds.), *Floodplain Rivers: Hydrological Processes and Ecological Significance*. British Hydrological Society Occasional Paper 8, 17-29.
- Hynes, H. B. N., 1975. The stream and its valley. *Verhandlungen der Internationale Vereinigung für Theoretische und Angewandte Limnologie* 19, 1-15.
- Jarvis, P. G., 1976. The interpretation of variations in leaf water potential and stomatal conductance found in canopies in the field. *Philosophical Transactions of the Royal Society of London, Series B, Biological Sciences* 273, 593-610.
- Kalliola, R., Syrjanen, K., 1991. To what extent are vegetation types visible in satellite imagery. *Annales Botanici Fennici*, 28, 45-57.
- Knopf, F. L., Johnson, R. R., Rich, T., Samson, F. B., Szaro, R. C., 1988. Conservation of riparian ecosystems in the United States. *Wilson Bulletin* 100, 272-284.
- Large, A. R. G., 1997. Linking floodplain hydrology and ecology – the scientific basis for management. In Large, A.R.G., editor, *Floodplain rivers: hydrological processes and ecological significance*. British Hydrological Society Occasional Paper 8, pp. 1-5.
- Leuning, R., 1995. A critical-appraisal of a combined stomatal-photosynthesis model for C-3 plants. *Plant Cell and Environment* 18, 339-355.
- McNaughton, K.G., Jarvis, P. G., 1983. Predicting effects of vegetation changes on transpiration and evaporation. In: Kozlowski, T. T. (Ed.), *Water Deficit and Plant Growth*. Academic Press, New York 7, pp. 2-47.
- Monteith, J. L., 1965. Evaporation and environment. In: Lugo, A.E., Brinson, M.M., Brown, S. (Eds.), *Proceedings of the 19th Symposium of the Society for Experimental Biology*. Cambridge University Press, New York, pp. 205-233.
- Nagler, P., Glenn, E., Thompson, T. L., 2003. Comparison of transpiration rates among saltcedar, cottonwood and willow trees by sap flow and canopy temperature methods. *Agricultural and Forest Meteorology* 116, 73-89.

- Nagler, P., Scott, R., Westerberg, C., Cleverly, C., Glenn, E., Huete, A. E., 2005. Evapotranspiration on U.S Rivers estimated using enhanced vegetation index from MODIS and data from eddy covariance and Bowen ratio flux towers. *Remote Sensing of Environment* 97, 337-351.
- National Research Council, 1992. Restoration of aquatic ecosystem. Science, Technology and Public Policy. National Academy Press, Washington, DC. 576pp.
- Nichols, J., Eichinger, W., Cooper, D. I., Prueger, J. H., Hipps, L. E., Neale, C. M. U., Bawazir, A. S., 2004. Comparison of evaporation estimation methods for a riparian area. United States Bureau of Reclamation, Technical Report, 46pp.
- Perkins, S. P., Sophocleous, M., 1999. Development of a comprehensive watershed model applied to study stream yield under drought conditions. *Ground Water* 37(3), 418-426.
- Peterjohn, W. T., Correll, D. L., 1984. Nutrient dynamics in an agricultural watershed: observation on the role of a riparian forest. *Ecology* 65, 1466-1475.
- Poff, N. L., Allan, J. D., Bain, M. B., Karr, J. R., Prestegard, K. L., Richter, B. D., Sparks, R.E., 1997. The natural flow regime: A paradigm for river conservation and restoration. *Bioscience* 47, 769-784.
- Postel, S. L., Wolf, A. T., 2001. Dehydrating conflict. *Foreign Policy* 126, 60-67.
- Rana, G., Katerji, N., 2000. Measurement and estimation of actual evapotranspiration in the field under Mediterranean climate. *European Journal of Agronomy* 13, 125-153.
- Samani Z., Bawazir, A. S., Skaggs, R. K., Bleweiss, M. P., Tran, V., 2007. Water use by agricultural crops and riparian vegetation: An application of remote sensing technology. *Journal of Contemporary Water Resources and Research* 137, 8-13.
- Sinokrot, B. A., Stefan, H. G., 1993. Stream temperature dynamics: measurements and modeling. *Water Resources Research* 29, 2299-2312.
- Tabacchi, E., Correll, D. L., Hauer, R., Pinay, G., Tabacchi, A. M., Wissmar, R. C., 1998. Development, maintenance and role of riparian vegetation in the river landscape. *Freshwater Biology* 40, 497-516.
- Twine, T. E., Kustas, W. P., Norman, J. M., Cook, D. R., Houser, P. R., Meyers, T. P., Prueger, J. H., Starks, P. J., Wesely, M. L., 2000. Correcting eddy covariance flux underestimates over a grassland. *Agricultural and Forest Meteorology* 103, 279-300.
- Van Genuchten, M.T., 1980. A closed-form equation for predicting the hydraulic conductivity of unsaturation soils. *Soil Science Society of America Journal* 44, 892-896.
- Vandersande, M., Glenn, E., Walworth, J., 2001. Tolerance of five riparian plants from the lower Colorado River to salinity, drought and inundation. *Journal of Arid Environment* 49, 147-160.
- Ward, J. V. 1989. The four-dimensional nature of the lotic ecosystem. *Journal of the North American Benthological Society* 8, 2-8.

Wylie, B. K., Johnson, D. A., Laca, E., Saliendra, N. Z., Gilmanov, T. G., Reed, B. C., Tieszen, L. L., Worstell, B. B., 2003. Calibration of remotely sensed, coarse resolution NDVI to CO₂ fluxes in a sagebrush-steppe ecosystem. *Remote Sensing of Environment* 85, 243–255.

CHAPTER 4

GENERAL CONCLUSIONS AND RECOMMENDATIONS

The Middle Rio Grande River is facing a critical management question. That is, how much water to release from Cochiti Dam upstream to meet all the water requirements for different land uses and the New Mexico domestic population and industrial needs?. This study tried to answer this question by mapping the riparian vegetation and estimate their water use.

The results of this research showed deterioration in the native vegetation and increase in the invasive harmful vegetation like Tamarisk. This is very clear when looking into the vegetation distribution analysis where Tamarisk occupies more areas than any other type of vegetation, including Cottonwood, in the downstream direction of the river riparian zone.

The vegetation evapotranspiration was found to be uniform for certain type of vegetation along the riparian zone because water was not a limiting factor in the root zone in the year of this study (2001).

Future monitoring of riparian and wetland ecosystems using high-resolution airborne RS will aid in the detection of escalating problems due to water quantity and quality in the riverine habitats. High-resolution RS can aid in detecting changes in vegetation due to natural causes or control practices on introduced or invasive species such as Tamarisk. The effectiveness of new Tamarisk control methods, such as using a beetle imported from Asia, could also be assessed with a future over flight of the river and similar analysis of the imagery.

It is recommended to study a dry year in the future to detect any variability in the vegetation evapotranspiration along the riparian zone and with respect to vegetation proximity to the river. Also better digital elevation model resolution is recommended in future studies where depth to water table could be estimated more accurately.

APPENDICES

APPENDIX A

Three Band and Classification Images List

Quad Name	Three-Band Size (MB)	Classification Size (MB)
Albuquerque	1670	623
Isleta	1700	666
Las Lunas	1890	653
Tome	1000	363
Turn_Veguita	1290	808
Abeytas	2090	697
La Joya	1450	472
San Acacia	1320	435
Loma De Canas	1650	599
San Antonio N.	1070	345
San Antonio S.	1540	547
San Marcial	2300	1550
Paraje	1880	664

APPENDIX B

Permissions from coauthor and Journal of Arid Environments



From: Gorczyca, Marek (ELS-OXF) <M.Gorczyca@elsevier.com>

Date: Tue, Aug 19, 2008 at 5:56 AM

Subject: permission request

To: OSAMA@cc.usu.edu

Cc: "Woodham-Kay, Frankee (ELS-EXE)" <F.Woodham-Kay@elsevier.com>

Dear Osama Akasheh

We hereby grant you permission to reprint the material detailed below at no charge in your thesis subject to the following conditions:

1. If any part of the material to be used (for example, figures) has appeared in our publication with credit or acknowledgement to another source, permission must also be sought from that source. If such permission is not obtained then that material may not be included in your publication/copies.

2. Suitable acknowledgment to the source must be made, either as a footnote or in a reference list at the end of your publication, as follows:

"This article was published in Publication title, Vol number, Author(s), Title of article, Page Nos, Copyright Elsevier (or appropriate Society name) (Year)."

3. Your thesis may be submitted to your institution in either print or electronic form.

4. Reproduction of this material is confined to the purpose for which permission is hereby given.
5. This permission is granted for non-exclusive world English rights only. For other languages please reapply separately for each one required. Permission excludes use in an electronic form other than submission. Should you have a specific electronic project in mind please reapply for permission.
6. Should your thesis be published commercially, please reapply for permission.

This includes permission for UMI to supply single copies, on demand, of the complete thesis. Should your thesis be published commercially, please reapply for permission.

Kind regards,

Marek Gorczyca

Rights Assistant

Elsevier LTD

Phone number: +441865843841

Fax number: +441865853333

m.gorczyca@elsevier.com

Permission from co-author

From,

Harikishan Jayanthi

3-5-1094/3 (I Floor),

Venkateswara Colony,

Narayanguda, Hyderabad 500 029 (A.P)

India

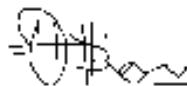
Sir/Madam,

Sub: Permission to include and reprint Paper in dissertation-Reg.

I hereby give my full consent and permission to Osama Akasheh to include and reprint the material in the following publication in his dissertation:

“Detailed mapping of riparian vegetation in the middle Rio Grande River using high resolution multi-spectral airborne remote sensing”

Yours sincerely



Harikishan Jayanthi

APPENDIX C

Bibliography

<http://ndis1.nrel.colostate.edu/riparian/Ripwetdef.htm>

http://www.tucson.ars.ag.gov/salsa/archive/documents/background/salsa_fact_sheet_apr98.html)

http://www.tucson.ars.ag.gov/salsa/archive/publications/ams_preprints/goodrich2.html

http://www.tucson.ars.ag.gov/salsa/research/research_1997/AMS_Posters/estimation_of_evaporation_rates/estimation_of_evaporation_rates.html

http://www.tucson.ars.ag.gov/salsa/research/research_1999/jafm/paperindex.html

http://www.tucson.ars.ag.gov/salsa/archive/publications/ams_preprints/goodrich2.html

http://gsa.confex.com/gsa/2002AM/finalprogram/abstract_41030.htm

<http://www.db.arm.gov/cgi-bin/IOP/selectPreProposal.pl?proposalNo=3072>

<http://www.iihr.uiowa.edu/products/pubvid/pdf%5CIIHR436.pdf>

http://aiwg.gsfc.nasa.gov/esappdocs/progplans/water_ver1-1.pdf

<http://edndoc.esri.com/arcobjects/9.2/welcome.htm>

<http://gis.utah.gov/agrc-uic-geospatial-integration/uic-editing-vba-code>

<http://support.esri.com/index.cfm?fa=homepage.homepage>

United States Bureau of Reclamation, 2005. Evaluation report for AWARDS ET toolbox and Riverware decision support tools. Hydrological Sciences Branch, Goddard Space Flight Center, Greenbelt, Madison, WI.

CURRICULUM VITAE

Osama Z. Akasheh

2008

CAREER OBJECTIVE:

Obtain a teaching position in a reputable institution.

SPECIAL AREAS OF INTEREST:

Study land-atmosphere interaction, vegetation evapotranspiration, and remote sensing applications.

EDUCATION

Ph.D. Irrigation Engineering Utah State University, (2008)

M.S. Soil and Irrigation Science University of Jordan, 1996

B.S. Soil and Irrigation Science University of Jordan, 1991

AREAS OF EXPERTISE

Irrigation Engineering

Remote Sensing Applications for Resource Planning

Geographic Information System (GIS)

Water and Land Resources management

Wastewater Reuse

Hydrology & Hydraulics

PUBLICATIONS

- Akashah, O. Z., Abu-Awwad, A. M., 1997. Irrigation and Soil Surface Management in Arid Soils with Surface Crust. *Journal of Arid Environments* 37, 243-250.
- Akashah, O. Z., Neale, C. M. U., Farag, F., 2003. Spatial Mapping of Riparian Vegetation of the Middle Rio Grande River, New Mexico. 19th Biennial workshop on color photography and videography in resource assessment.
- Akashah, O. Z., Neale, C. M. U., 2004. An Assessment of Meso-scale Hydraulic and Vegetation Characteristics of the Middle Rio Grande River Using High Resolution Multispectral Airborne Imagery. American Geophysical Union.
- Akashah, O. Z., Neale, C. M. U., 2006. A Study of Hydraulic and Hydrological Processes interaction of the Middle Rio Grande River Using High Resolution Multispectral Airborne Imagery. American Water Resources Association (AWRA).
- Akashah, O. Z., Neale, C. M. U., 2007. Modeling the Water Table in the Middle Rio Grande River Riparian Corridor. American Geophysical Union.
- Akashah, O. Z., Neale, C. M. U., Harikishan J., 2008. Detailed mapping of riparian vegetation in the Middle Rio Grande River using high resolution multi-spectral airborne remote sensing. *Journal of Arid Environments* 72, 1734-1744.

AWARDS

Dean's list 2001, USU

General Science award, Jordan.

Biological sciences award, Jordan.

Amal Cancer Treatment Center, Jordan.

GIS class of 2003 Best project award, USU.

LANGUAGES

Arabic, English, and Communicative French